



National Library
of Canada

Acquisitions and
Bibliographic Services Branch

395 Wellington Street
Ottawa, Ontario
K1A 0N4

Bibliothèque nationale
du Canada

Direction des acquisitions et
des services bibliographiques

395, rue Wellington
Ottawa (Ontario)
K1A 0N4

Your file *Votre référence*

Our file *Notre référence*

NOTICE

The quality of this microform is heavily dependent upon the quality of the original thesis submitted for microfilming. Every effort has been made to ensure the highest quality of reproduction possible.

If pages are missing, contact the university which granted the degree.

Some pages may have indistinct print especially if the original pages were typed with a poor typewriter ribbon or if the university sent us an inferior photocopy.

Reproduction in full or in part of this microform is governed by the Canadian Copyright Act, R.S.C. 1970, c. C-30, and subsequent amendments.

AVIS

La qualité de cette microforme dépend grandement de la qualité de la thèse soumise au microfilmage. Nous avons tout fait pour assurer une qualité supérieure de reproduction.

S'il manque des pages, veuillez communiquer avec l'université qui a conféré le grade.

La qualité d'impression de certaines pages peut laisser à désirer, surtout si les pages originales ont été dactylographiées à l'aide d'un ruban usé ou si l'université nous a fait parvenir une photocopie de qualité inférieure.

La reproduction, même partielle, de cette microforme est soumise à la Loi canadienne sur le droit d'auteur, SRC 1970, c. C-30, et ses amendements subséquents.

University of Alberta

**Ethylene and 1-Butene Copolymerization:
Catalytic Gas-Phase Synthesis and Characterization**

by

James Chin-Kuang Huang



A thesis submitted to the Faculty of Graduate Studies and Research in partial fulfillment of the requirements for the degree of Master of Science

Department of Chemical Engineering

Edmonton, Alberta

Fall 1995



National Library
of Canada

Acquisitions and
Bibliographic Services Branch

395 Wellington Street
Ottawa, Ontario
K1A 0N4

Bibliothèque nationale
du Canada

Direction des acquisitions et
des services bibliographiques

395, rue Wellington
Ottawa (Ontario)
K1A 0N4

Your file *Votre référence*

Our file *Notre référence*

THE AUTHOR HAS GRANTED AN IRREVOCABLE NON-EXCLUSIVE LICENCE ALLOWING THE NATIONAL LIBRARY OF CANADA TO REPRODUCE, LOAN, DISTRIBUTE OR SELL COPIES OF HIS/HER THESIS BY ANY MEANS AND IN ANY FORM OR FORMAT, MAKING THIS THESIS AVAILABLE TO INTERESTED PERSONS.

L'AUTEUR A ACCORDE UNE LICENCE IRREVOCABLE ET NON EXCLUSIVE PERMETTANT A LA BIBLIOTHEQUE NATIONALE DU CANADA DE REPRODUIRE, PRETER, DISTRIBUER OU VENDRE DES COPIES DE SA THESE DE QUELQUE MANIERE ET SOUS QUELQUE FORME QUE CE SOIT POUR METTRE DES EXEMPLAIRES DE CETTE THESE A LA DISPOSITION DES PERSONNE INTERESSEES.

THE AUTHOR RETAINS OWNERSHIP OF THE COPYRIGHT IN HIS/HER THESIS. NEITHER THE THESIS NOR SUBSTANTIAL EXTRACTS FROM IT MAY BE PRINTED OR OTHERWISE REPRODUCED WITHOUT HIS/HER PERMISSION.

L'AUTEUR CONSERVE LA PROPRIETE DU DROIT D'AUTEUR QUI PROTEGE SA THESE. NI LA THESE NI DES EXTRAITS SUBSTANTIELS DE CELLE-CI NE DOIVENT ETRE IMPRIMES OU AUTREMENT REPRODUITS SANS SON AUTORISATION.

ISBN 0-612-06483-2

Canada


University of Alberta

Library Release Form

Name of Author: James Chin-Kuang Huang
Title of Thesis: Ethylene and 1-Butene Copolymerization: Catalytic Gas-Phase Synthesis and Characterization
Degree: Master of Science
Year this Degree Granted: 1995

Permission is hereby granted to the University of Alberta Library to reproduce single copies of this thesis and to lend or sell such copies for private, scholarly, or scientific research purposes only.

The author reserves all other publication and other rights in association with the copyright in the thesis, and except as hereinbefore provided, neither the thesis nor any substantial portion thereof may be printed or otherwise reproduced in any material from whatever without the author's prior written permission.


6 Galloway Road
Sherwood Park, Alberta
Canada T3A 3K8

September 29, 1995

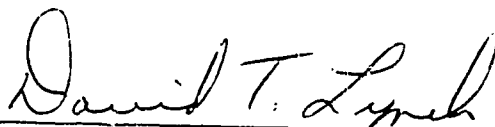
Ars Longa, Brevis Scientia

— Huangus

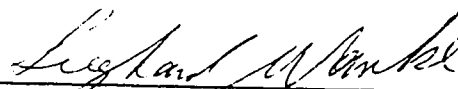
University of Alberta

Faculty of Graduate Studies and Research

The undersigned certify that they have read, and recommend to the Faculty of Graduate Studies and Research for acceptance, a thesis entitled Ethylene and 1-Butene Copolymerization: Catalytic Gas-Phase Synthesis and Characterization in partial fulfillment of the requirements for the degree of Master of Science.



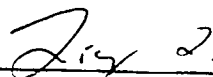
David T. Lynch (Co-Supervisor)



Sieghard E. Wanke (Co-Supervisor)



Michael C. Williams



Liang Li

August 22, 1995

To Jesus Christ, my Lord and Risen Saviour

ABSTRACT

Ethylene and 1-butene in various proportions were copolymerized over a commercial titanium-based Ziegler-Natta catalyst in a semibatch gas-phase reactor. Activity of the catalyst was found to be sensitive to the exposure to the cocatalyst. Gas chromatographic analysis of the gas mixtures showed that 1-butene incorporation was limited to the early stages of the reaction, indicating that heterogeneity of branching frequency in linear low density polyethylene (LLDPE) was largely due to the changes in oxidation states of the active sites.

LLDPE samples were characterized by gel permeation chromatography (GPC), differential scanning calorimetry (DSC), and temperature rising elution fractionation (TREF). GPC results suggested that hydrogen was a more effective chain transfer agent for one type of active site than the other and that the kinetics of termination were of mixed-order. DSC studies revealed that major differences in crystallinity, melting temperature, and miscibility existed between the nascent reactor powder and the melt recrystallized resins. DSC fractionation was found to be quantitatively equivalent to the analytical TREF.

Acknowledgements

It is my utmost duty to recognize many individuals of noble characters who have at sundry times and in divers manners contributed to the totality of the present endeavour:

Thanks be unto my thesis advisors, Dr. David T. Lynch, Dean of Engineering, and Dr. Sieghard E. Wanke, Chair of Chemical Engineering, for their ceaseless guidance in research, scholarly verve in analysis, admirable patience for progress, and thorough revisions of manuscripts;

Thanks be unto Dr. Michael C. Williams, Professor of Chemical Engineering, for the countless hours of enlightening philosophical transactions on the rheology of solution and melt and the physics of blends and glass transition, the delightful intellectual discourses on history, geography, and current events, and the provision of liquid nitrogen;

Thanks be unto Dr. Liang Li, Associate Professor of Chemistry, for his interest in my thesis work and the final scrutiny thereof;

Thanks be unto my associates at the Polymerization and Characterization Laboratory, among them are Dr. Shemin Wang, whom I was initially an apprentice under, Ms. Naiyu Bu, whom I received much help in reactor operation, GPC, TREF and FTIR characterization, and thesis correction, Mr. Yves Lacombe, whom I learned much of the prior art of TREF from, and Mr. Long Wu, whom I gained much information on, perspectives of, and understandings in catalytic polymerization from;

Thanks be unto my colleagues at the Polymers and Rheology Laboratory, among them are Dr. Leigh Wardhaugh, Dr. Tamal Ghosh, Dr. Nai-Hong Li, Mr. Robert Spaans, Ms. Apinya Duangchan, and Mr. Wei-Yan Wang, for ideas and discussions;

Thanks be unto the staff members of the Department of Chemical Engineering, among them are Ms. Cindy Heisler, Mr. Bob Barton, Mr. Walter Boddez, Mrs. Diane Reckhow, Mr. Keith Faulder, Mrs. Beverly Walker, and Mr. Henry Sit, for their generous assistance;

Thanks be unto those who knowingly or otherwise have answered my questions for, provided their opinions on, or expressed more than cursory interests in, various parts of the thesis, whether in person or over the phone: Professor Roger Porter of the University of Massachusetts at Amherst, Professor Williams Graessley of Princeton University, Professor Chris Macosko of the University of Minnesota, Professor U. T. Sundararaj of the University of Alberta, Professor Ian

Harrison of Penn State University, Professor Archie Hamilec of McMaster University, Professor Kim McAuley of Queen's University, Professor John Bercaw of California Institute of Technology, Dr. Leszek Utraki of the National Research Council of Canada, Drs. Charles Russell, Elizabeth Karbasheski, Peter Hoang, and Tim Bremner of Novacor Research and Technology Corporation, and Dr. Larry Vandegriend of AT Plastics;

Thanks be unto Novacor Chemical Ltd. and Natural Science and Engineering Research Council of Canada for the financial support to the Polymerization and Characterization Laboratory and this individual;

Thanks be unto other fellow graduate students of the Department of Chemical Engineering and members of the University of Alberta Concert Choir, for their friendship;

Thanks be unto the beloved saints of the LORD meeting in Flushing, NY, Pennington, NJ, Magnolia, NJ, Silver Spring, MD, Richmond, VA, Arden Hill, MN, Toronto, ON, and Taipei, Taiwan, for the remembrance of me in their prayers to the God Almighty;

Thanks be unto my parents and my sister, for their incessant love, unfailing encouragement, and tremendous sacrifice; and

Thanks be unto Norman and Barbara Law and their children, Nathanael and Joanna, for their exceeding abundant love in Christ towards me which made the completion of my studies at the University of Alberta possible.

TABLE OF CONTENTS

CHAPTER 1	INTRODUCTION	1
CHAPTER 2	LITERATURE SURVEY	5
2.1	Activity of Polymerization	6
2.1.1	Effect of Comonomer on Activity	6
2.1.2	Effect of Hydrogen on Activity	8
2.1.3	Effect of Cocatalyst on Activity	8
2.1.4	Effect of Support on Activity	10
2.1.5	Effect of Temperature on Activity	11
2.2	Molar Mass Distribution	12
2.2.1	Diffusion versus Multiplicity of Site on the Molar Mass Distribution	12
2.2.2	Control of Molar Mass and Molar Mass Distribution	14
CHAPTER 3	EXPERIMENTAL	17
3.1	Polymerization Equipment and Materials	17
3.2	Cocatalyst and Cocatalyst Handling	20
3.3	Polymerization Procedure	21
3.4	Gas Chromatography (GC)	23
3.5	Gel Permeation Chromatography (GPC)	24
3.6	Temperature Rising Elution Fractionation (TREF)	25
3.7	Melt Index (MI)	25
3.8	Differential Scanning Calorimetry (DSC)	26
CHAPTER 4	REACTOR OPERATION	28
4.1	Reactor Pretreatment	28
4.2	Catalyst Injection	33
4.3	Choice of Seedbed	37

CHAPTER 5	PROPAGATION KINETICS	39
5.1	Effects of Hydrogen and Temperature on Copolymerization Rates	39
5.2	Effect of Ti Oxidation States on Copolymerization	42
5.3	Fractional Conversion of 1-Butene to n-Butane	45
5.4	Effect of Comonomer Precharge on Copolymerization	47
CHAPTER 6	CHARACTERIZATION OF POLYETHYLENE	52
	Part 1: Molar Mass Distribution, Molar Mass, and Melt Index	
6.1	Molar Mass Distribution	52
6.2	Hydrogen Termination Rate Order	60
6.3	Melt Index	67
CHAPTER 7	CHARACTERIZATION OF POLYETHYLENE	72
	Part 2: Crystallinity, Melting Temperature, Density, and Miscibility	
7.1	Effect of Molar Mass on Crystallinity and Melting Temperature in Ethylene Homopolymer	74
7.2	Effect of Branching on Crystallinity and Melting Temperature in Ethylene/1-Butene Copolymer	79
7.3	Effect of Molar Mass on Crystallinity and Melting Temperature in Ethylene/1-Butene Copolymer	83
7.4	Density	87
7.5	Linear-Low Density Polyethylene: A Blending Perspective	89
CHAPTER 8	CHARACTERIZATION OF POLYETHYLENE	98
	Part 3: DSC Fractionation of Linear-Low Density Polyethylene	

CHAPTER 9	CONSIDERATIONS FOR FUTURE STUDIES	106
9.1	Kinetics of Comonomer Incorporation	106
9.2	Kinetics of Termination by Hydrogen	108
9.3	Gel Permeation Chromatography (GPC)	109
9.4	Differential Scanning Calorimetry (DSC)	110
9.5	Temperature Rising Elution Fractionation (TREF)	110
9.6	Matrix-Assisted Laser Desorption Ionization Mass Spectroscopy (MALDI-MS)	111
9.7	Modelling of Crystallization in Dilute Solution	112
9.8	Polyethylene Blends	114
CHAPTER 10	REFERENCES	116
APPENDIX	SUMMARY TO ALL POLYMERIZATION RUNS	129

LIST OF TABLES

Table 3.1	DSC programme for polyethylene analysis	27
Table 4.1	Pretreatment procedure used in Run 128	33
Table 4.2	Composition of the gas mixtures into which catalyst was injected	34
Table 4.3	Viscosities of catalyst suspending media	35
Table 4.4	Thermophysical properties of selected seedbeds	38
Table 6.1	Effect of hydrogen on M_n , M_w , and melt index of linear low density polyethylene	58
Table 6.2	Effect of precharged 1-butene on M_n , M_w , and melt index of linear low density polyethylene	58
Table 7.1	Percent crystallinities and melting temperatures of HDPEs produced at 50°C under constant ethylene pressure	75
Table 7.2	Percent crystallinities and melting temperature of LLDPEs produced at 70°C under constant hydrogen pressure and 1-butene comonomer	80
Table 7.3	Percent crystallinities and melting temperatures of LLDPEs produced at 70°C under constant precharged 1-butene with varying molar mass	84
Table 7.4	Density of polyethylene according to dilatometry equation	88
Table 8.1	Temperature programme used for DSC fractionation	99

LIST OF FIGURES

Figure 3.1	Schematic diagram of the reactor system	18
Figure 4.1	A comparison of two pretreatment methods	31
Figure 4.2	Effect of catalyst suspending medium on the activity profile	36
Figure 5.1	Effect of hydrogen pressure on the instantaneous ethylene consumption rate of ethylene/1-butene copolymerization	40
Figure 5.2	Effect of hydrogen pressure on the reaction temperature	41
Figure 5.3	Mole fraction of ethylene and 1-butene versus time at different hydrogen pressures	43
Figure 5.4	Mole fraction of ethylene and 1-butene versus time under different 1-butene feed patterns	44
Figure 5.5	Fractional conversion of 1-butene to n-butane as a function of reaction time	46
Figure 5.6	TREF profiles of LLDPEs produced with various 1-butene precharges	48
Figure 5.7	Integrated TREF profiles of LLDPEs	49
Figure 5.8	TREF profile of LLDPE produced without comonomer precharge	51
Figure 6.1	Effect of hydrogen on molar mass distribution	53
Figure 6.2	Effect of 1-butene on molar mass distribution	54
Figure 6.3	Effect of hydrogen on M_n and M_w	56
Figure 6.4	Effect of 1-butene on M_n and M_w	57
Figure 6.5	Effect of hydrogen on polydispersity	59
Figure 6.6	Effect of hydrogen on M_n	63
Figure 6.7	Fractional order dependence of M_n on hydrogen pressure	65

Figure 6.8	M_n versus hydrogen, mixed-order curve-fitting	66
Figure 6.9	Melt index dependence on hydrogen pressure	68
Figure 6.10	Relationship between melt index and M_w	69
Figure 6.11	Shear viscosity versus shear rate for a typical polymer	71
Figure 7.1	Percent crystallinity versus M_w for ethylene homopolymers	76
Figure 7.2	Melting temperature versus M_w for ethylene homopolymers	77
Figure 7.3	Percent crystallinity versus M_w for LLDPE: effect of branching	81
Figure 7.4	Melting temperature versus M_w for LLDPE: effect of branching	82
Figure 7.5	Percent crystallinity versus M_w for LLDPE: effect of M_w	85
Figure 7.6	Melting temperature versus M_w for LLDPE: effect of M_w	86
Figure 7.7	Endotherms of samples examined in Section 7.1	90
Figure 7.8	Endotherms of samples examined in Section 7.2	92
Figure 7.9	Endotherms of samples examined in Section 7.3	95
Figure 8.1	Endotherms of thermally fractionated LLDPE	100
Figure 8.2	Percentage of fractionated molecules versus temperature	102
Figure 8.3	Integrated fractional DSC profile	103
Figure 8.4	Elution temperature versus annealing temperature	104

NOMENCLATURE

ΔH	enthalpy of fusion of the sample polyethylene
ΔH_c	enthalpy of fusion of 100% crystalline polyethylene
ΔT_m	change of peak melting temperature upon melt recrystallization
ΔX_c	change of crystallinity upon melt recrystallization
η	shear viscosity
η_0	zero-shear viscosity
θ_f	Flory's theta temperature
π	degree of polymerization
ρ_a	density of 100% amorphous polyethylene
ρ_c	density of 100% crystalline polyethylene
σ_e	lamella surface energy
Φ	universal constant for dilute polymer solutions
A-TREF	analytical temperature rising elution fractionation
ASTM	American Society of Testing and Materials
cMSL	characteristic methylene sequence length
Cp	cyclopentene
CRYSTAF	crystallization analysis fractionation
DEAC	diethylene aluminium chloride
DSC	differential scanning calorimetry
DTA	differential thermal analysis
F-DSC	fractional differential scanning calorimetry
FTIR	Fourier-transform infrared spectroscopy
GC	gas chromatography
GPC	gel permeation chromatography
HDPE	high-density polyethylene
HDV	hydrodynamic volume
ICI	Imperial Chemical Industries
IPRAL	isoprenyl aluminium

l_{avg}	average lamella thickness
LDPE	low-density polyethylene
LLDPE	linear low-density polyethylene
M_n	number-average molar mass
M_v	viscosity-average molar mass
M_w	weight-average molar mass
MALDI	matrix-assisted laser desorption ionization
MDSC™	modulated differential scanning calorimetry
MI	melt index
MMD	molar mass distribution
MSL	methylene sequence length
MSLD	methylene sequence length distribution
MSL_n	number-average methylene sequence length
MSL_w	weight-average methylene sequence length
NIST	National Institute of Science and Technology, U.S. Dept. of Commerce
NMR	nuclear magnetic resonance
PE	polyethylene
P_{H_2}	hydrogen partial pressure
Q	polydispersity
Q_E	ethylene volumetric flowrate
r_1, r_2	reactivity constants for copolymerization kinetics
R_p	rate of propagation
R_t	rate of termination
SALS	small-angle light scattering
SANS	small-angle neutron scattering
SAXS	small-angle x-ray spectroscopy
sccm	standard cubic centemeter per minute
SEM	scanning electron microscopy
SMST	silica/butyl magnesium/silica tetrachloride/titanium tetrachloride
SMT	silica/butyl magnesium/titanium tetrachloride
SRM	Standard Reference Material

SSXS	synchrotron-sourced x-ray scattering
T_A	annealing temperature
T_E	elution temperature
T_{eq}	equilibrium melting temperature of 100% crystalline polyethylene
TEAL	triethyl aluminium
TEM	transmission electron microscopy
TIBAL	tri-isobutyl aluminium
TNHAL	tri-n-hexyl aluminium
TNOAL	tri-n-octyl aluminium
TREF	temperature rising elution fractionation
WAXS	wide-angle x-ray spectroscopy
x	mass fraction
X_c	percent crystallinity
XRD	x-ray diffraction

1. INTRODUCTION

Polyethylene is the largest commodity polymer worldwide. As a direct consequence of its low cost, physical versatility, and chemical inertness, polyethylene has been screw-extruded, injection-moulded, and film-blown into more end-use products than any other thermoplastic material in the world.

Despite its structural simplicity, polyethylene was not synthesized until 1897 when E. Hinderman decomposed diazomethane to produce polymethylene, the precursor of modern polyethylene (Sailors and Hogan, 1982). Industrial production of polyethylene did not start until 1936, when Imperial Chemical Industries (ICI) polymerized ethylene at high pressure (ca. 300 MPa) and high temperature (ca. 300°C) using free-radical technology. In early 1953, Karl Ziegler and coworkers in Mülheim, Germany discovered that polyethylene with density higher than ICI's analogue could be made catalytically with a titanium tetrachloride and triethyl aluminium complex at pressure just above atmospheric and temperature below 100°C. Giulio Natta and coworkers in Milan, Italy later found that the same catalyst system was capable of producing isotactic polypropylene. The explosion of research activity in laboratories around the world ensuing from the discoveries by Ziegler and Natta, who were jointly awarded the Nobel Prize in Chemistry in 1964, has subsequently produced catalysts with efficiencies several order of magnitudes higher than the ones originally discovered.

In ICI's high-pressure process, free-radical ends of growing polymer chains can, in addition to attacking the monomer units, extract hydrogen atoms from within the macromolecules to form more stable secondary radicals which will then continue to react with monomer units to form long chain branches. These branches severely limit the extent of crystallinity polymer molecules may attain. On the other hand, for the catalytic process, the only propagation mechanism possible on the catalyst surface is direct monomer insertion at the active site;

hydrogen on the saturated portion of the molecule are not susceptible to migration.

The structural dissimilarity caused by the difference between free-radical and catalytic polymerization mechanisms divides polyethylenes into low-density polyethylene (LDPE) and high-density polyethylene (HDPE). The former generally has density around 0.920 g/cm^3 and the latter, 0.960 g/cm^3 . This gap in density was not filled until the advent of linear-low density polyethylene (LLDPE) in the late 1960s.

Linear low density polyethylene is produced by catalytic polymerization of ethylene and an α -olefin such as 1-butene, 1-hexene, 4-methyl-1-pentene, or 1-octene. These copolymers retain the basic linear structure characteristic of HDPE, yet their short side branches along the backbones interfere with the crystallization process. As crystallinity is closely related to the bulk density, the extent of comonomer incorporation can be tailored to the density specifications.

Three major types of low-pressure processes exist for industrial production of HDPE: solution, slurry, and gas-phase. In all solution processes, the temperature is sufficiently high such that the polymer is in solution. While higher polymerization temperature offers considerable increase in catalytic activity, the process is restricted to the production of injection-moulding grade (lower molar mass) resins due to the increased solution viscosity associated with the higher molar mass film-blowing grade resins in the solvent. Slurry processes expand the range of molar mass through lowering the operating temperatures under which diluents and solid polymer particles remain in different phases. However, production of LLDPE in slurry reactors is discommoded by the increased solubility of low-crystallinity molecules in the diluent. These inherent viscosity and solubility restrictions associated with liquid solvent/diluent become moot in the gas-phase process. The advantage of the gas-phase process extends beyond product diversity: elimination of light hydrocarbons used in the slurry or solution reactors abolishes the necessities of solvent extraction and recovery and reduces the hazard of explosion. The UNIPOL process, the very successful LLDPE production technology developed by Union Carbide Corporation and licensed

worldwide, is gas-phase. Currently, the combined capacity of 81 UNIPOL reactors in 22 countries is sufficient to supply 25% of the global demand for polyethylene (Karol, 1995).

While gas-phase polyethylene production technology has obtained its due preeminence, industrial and academic research investigations on catalyst activity and polymerization kinetics (reviewed briefly in Chapter 2) are overwhelmingly conducted in slurry reactors for the concern over reproducibility, despite strong cautions from Lynch et al. (1991) that catalyst behaves differently under slurry and gas-phase reactors. In Chapter 3, descriptions of the gas-phase polymerization reactor along with characterization equipment used for the present study are provided, and in Chapter 4, investigations into the probable causes of irreproducibility in gas-phase reaction are presented.

In Chapter 5, the emphasis is on the results of propagation kinetics. Factors that can influence the activity and the extent of comonomer incorporation are addressed. The evidence gathered through temperature rising elution fractionation (TREF) and gas chromatography (GC) is used to support the kinetic argument.

The focus of Chapter 6 is on the kinetics of chain termination. Whether the growing polymer chains are terminated via first- or half-order kinetics is examined. The effect of hydrogen and 1-butene on the molar mass distribution as determined by gel permeation chromatography (GPC) is presented.

The effects of branching distribution and molar mass on the thermophysical properties of polyethylene (melting temperature, crystallinity, etc.) as measured by differential scanning calorimetry (DSC) is discussed in Chapter 7. A novel concept of kinetic miscibility of molecules is introduced. And in Chapter 8, exploratory investigations on the prospect of fractional DSC as a potential substitute for the standard TREF technique is reported.

Finally, in Chapter 9, recommendations are made for further studies on the comonomer incorporation on the catalyst, the effect of hydrogen on the molar mass distribution, improvement on various characterization techniques (gel permeation chromatography, mass spectroscopy, temperature rising elution

fractionation, and differential scanning calorimetry), mathematical modelling of dilute solution crystallization and branching distribution, and the blending of different polyolefins.

2. LITERATURE SURVEY

The discovery of Ziegler-Natta catalytic systems ushered in an epoch of unprecedented explosive research activities on polymerization catalysts around the world. Publications produced by academic and industrial laboratories on the subject of Ziegler-Natta polymerized polyolefins encompasses catalysis¹, reactor operation², product attributes on the molecular³, microscopic⁴, and macroscopic⁵ levels, characterization techniques⁶, and processing characteristics⁷. Given the vastness of the relevant literature just outlined, the modest intent of the following sections is to provide a synopsis of the recent advances on the activity of polymerization (Section 2.1) and studies on the molar mass distribution (Section 2.2), rather than a thorough review addressing each and every facet of the research conducted worldwide; areas of research not reviewed in this section will be discussed within the context of the experimental results (Chapters 4 through 8) and the proposed future research (Chapter 9) where warranted.

¹For example, catalyst composition, preparation, and activation, reaction mechanisms and kinetics.

²For example, process design, control, and modelling.

³For example, average molar masses, molar mass distribution, and the extent of comonomer incorporation.

⁴For example, lamellae size distribution, average lamellae size, and crystallinity.

⁵For example, impact strength, shear strength, tear strength, density, and melting and crystallizing temperatures.

⁶For example, FTIR, NMR, and TREF (for branching analyses); DSC, DTA, and XRD (for crystallinity); and TREF-GPC or TREF-DSC cross fractionation.

⁷For example, miscibility, cocrystallization, and melt stability.

2.1 Activity of Polymerization

One major research emphasis of Ziegler-Natta polymerization is on the factors that influence the catalyst activity. The original recipe ($\text{TiCl}_4\text{-AlEt}_3$) discovered by Ziegler in 1953 had a very low overall efficiency, as active centres were only a small fraction of all the titanium species (Floyd et al., 1988). Titanium left in the polymer presented difficulties in sustaining colour and chemical stabilities, and the associated chloride resulted in severe corrosion problems to the processing equipment (Hsieh, 1984). During the 1960s, as the art of supporting transition metal on carriers began to mature, materials such as magnesium chloride, silica, or to a lesser extent, alumina were used as supports for titanium trichloride or tetrachloride. Supported catalysts are more desirable than their non-supported predecessor as the active species may be used more efficiently if it is dispersed upon the surface of a carrier particle. In addition, the quantity of residual transition metal left in the polymer product is reduced, for MgCl_2 is inert to polyethylene. Furthermore, the activity or stereoregularity of the final product can be improved through modifications to the support, and the morphology of polymer resins can be controlled by the morphology of the support through replication processes. Due to the greatly enhanced activity, separation of <10 ppm catalyst particles from polymer product is not necessary for commercial applications. Effects of operating conditions and catalyst compositions on the polymerization activity will be reviewed in the following sections.

2.1.1 Effect of Comonomer on Activity

Enhancement of activity during the early stages of ethylene polymerization by a small quantity of α -olefins is well documented (Calabro and Lo, 1988; Chien and Nozaki, 1993; Karol et al., 1989, 1993; Kim et al., 1990; Muñoz-Escalona et al., 1987; 1990; Nowlin et al., 1988; Pasquet and Spitz, 1991; 1993; Pino et al., 1988; Soga et al., 1989; 1991; Spitz et al., 1988a; Tait et al., 1988; 1990; Xiao and Lu, 1992; Wang et al., 1993). The magnitude of the initial activity enhancement depends on

the comonomer (propylene > 1-butene > 1-hexene) and can be totally eliminated by the addition of electron donors (Karol et al., 1993). Chien and Nozaki (1993) reported that the activation (by 1-hexene) was most pronounced for the previous generation of catalyst ($\text{TiCl}_3/\text{DEAC}$) and quite moderate for the current generation of heterogeneous catalyst (SMT/TEAL or SMST/TEAL). Koivumäki and Seppälä (1993) on the other hand claimed that the consumption of ethylene increased 8-fold with MgCl_2 -supported catalyst and 2.5-fold increase with Cp_2ZrCl_2 when a small amount of 1-hexene was added. In addition, it has been reported that catalysts prepared with silica showed much higher sensitivity to comonomer (Nowlin et al, 1988; Wang et al., 1993).

There are two schools of thoughts in explaining the comonomer activation effect: one based on active site generation, the other mass-transfer limitations. By using the ^{14}CO active centre determination technique, Tait et al. (1988) showed that the enhanced rate was due to an increase in active sites. More recently, by noting a significant increase in the rate of gas-phase ethylene homopolymerization after an interlude of ethylene/1-butene copolymerization, Pasquet and Spitz (1993) also maintained that the increase in activity was due to creation of new sites by the comonomer. The same phenomenon can also be explained in terms of other irreversible transformations suggested by Tait et al. (1988) and Chien and Nozaki (1993): the activation of dormant (or potential) sites, the triggering effect by α -olefin to increase the rate of propagation, the variation of titanium oxidation state, the displacement of complexed molecules such as Lewis bases, among others.

An alternative explanation to the apparent increase in activity was offered by Soga et al. (1989; 1991) who used a correlation between a decrease in crystallinity and an increase in comonomer content in the product resins to suggest that the increased activity was a result of reduced mass-transfer resistance through the less crystalline copolymer film. These two phenomena are not necessarily exclusive: Tait et al. (1988) acknowledged the contribution of the latter while providing strong experimental evidence for the former, and Chen (1993) recognized the presence of the former while accentuated the significance of the

latter based on the good agreement between experimental data and diffusion modelling.

It should be noted that the much discussed increase in activity occurs only in the first few minutes of polymerization, and discussions on the rapid deactivation after the maximum activity are much more infrequent. Karol et al. (1993) believed that catalyst deactivation was caused by reaction of catalytic sites with deactivating Lewis bases and by a possible lowering of the oxidation state of the metal.

Lastly, it should be emphasized that excess amount of comonomer would actually decrease the rate of polymerization (Quijada and Wanderley, 1987), as α -olefins react more slowly than does ethylene.

2.1.2 Effect of Hydrogen on Activity

Polymerization rate enhancement induced by a small amount of hydrogen has been well recognized for both propylene (Chien and Hu, 1987; Chien and Nozaki, 1991; Spitz et al., 1988b; 1989) and ethylene polymerizations (Marques et al., 1993a). Keii (1987) speculated that the activity enhancement by hydrogen was due to reactivation of highly reduced Ti^{+2} or Ti^{+1} by oxidative adsorption of hydrogen, a process where titanium donates two electrons to accept hydrogen atoms as ligands (Gates et al., 1979). At higher hydrogen pressure, however, the activity would decrease (Pasquet and Spitz, 1993; Marques et al., 1993a). Marques et al. (1993a) suggested that these two opposite effects can be reconciled by allowing the following scenario: a small amount of hydrogen increases the rate by easing the access of monomer molecules to active centres through molar mass reduction, but higher hydrogen pressure causes the competitive adsorption between monomer and hydrogen and thus reduces the activity.

2.1.3 Effect of Cocatalyst on Activity

Cocatalysts are required to activate titanium tetrachloride-based catalysts by reducing the oxidation state of Ti from +4 to either +3 or +2. From a stoichiometric point of view, the choice of cocatalyst and the amount thereof

determine the distribution of the oxidation states of titanium. Typical cocatalysts are triethyl aluminium (TEAL), triisobutyl aluminium (TIBAL), tri-n-hexyl aluminium (TNHAL) and tri-n-octyl aluminium (TNOAL). Recently zirconium tetrabenzyl, a transition metal organometallic compound, has also been used as a cocatalyst (Galimberti et al., 1993).

2.1.3.1 Type of Cocatalyst

Under similar Al/Ti ratios, Lynch et al. (1991) found that while the catalytic activity for SiO₂/MgCl₂ supported Ti catalysts all approached a constant value and can be approximated by a first-order rate equation after the first two hours, the initial kinetic profiles for tri-n-hexyl aluminium (TNHAL), isoprenyl aluminium (IPRAL) and tri-n-hexyl aluminium (TEAL) differed significantly. The order of the cocatalyst effectiveness (obtained by averaging the rates for the first two hours of the reactions) obeyed the general observation that increasing the size of the alkyl group in trialkylaluminiums enhanced the activity. Similar observation in activity behaviour by Nooijen (1994) was explained in terms of the diffusional barrier experienced by the individual cocatalyst: the bulkier the side group, the greater the delay of activation.

2.1.3.2 Amount of Cocatalyst

The Al/Ti ratio influences the activity in several ways. The dissimilarities in the activity profiles due to different types of cocatalyst can be eliminated by adjusting the Al/Ti, according to Marques et al. (1993a). Lynch et al. (1991) reported that there appeared to be an optimal TEAL/Ti for the catalyst system (TiCl₄/MgCl₂/SiO₂) examined. Dusseault (1991) while studying MgCl₂-supported catalyst observed that deactivation kinetics differed above and below a critical Al/Ti. The sensitivity of activity toward Al/Ti was reportedly less for cocatalysts with higher alkyl ligands (Lynch et al., 1991). Soga et al. (1981; 1982) noted that by increasing the Al/Ti, the product of ethylene with propylene, 1-hexene or 1,3-butadiene copolymerization changed from a random copolymer to pure polyethylene. According to Soga et al. (1982), Ti⁺³ species were active for various

α -olefins and diene polymerization, whereas further reduced Ti^{+2} species are only active for ethylene polymerization.

2.1.4 Effect of Support on Activity

Magnesium chloride and silica are the most widely used $TiCl_4$ carriers for the current generation of Ziegler-Natta catalysts. The catalyst used for commercial processes such as UNIPOL is typically bisupported Ti on $MgCl_2$ and silica. Recent efforts to replace inorganic materials with polyethylene or polypropylene powders have had limited success, as the activities of polymer supported catalysts are in general lower than those of $MgCl_2$ -supported catalysts (Sun et al., 1994).

2.1.4.1 Magnesium Chloride

While silica and alumina are generally inert to titanium species, magnesium chloride is not. The desirable features of $MgCl_2$, among others, as summarized by Karol (1984) and Xie et al. (1994), are: one, $MgCl_2$ can effectively incorporate $TiCl_4$, due to the proximity of ionic radii of Mg^{+2} (68 pm) and Ti^{+4} (66 pm); two, $MgCl_2$ has a stable morphology during operational manipulation yet is sufficiently friable during polymerization; three, $MgCl_2$, with its lower electronegativity than $TiCl_3$, (6.0 vs. 10.5) increases productivity of ethylene polymerization (Soga et al., 1987) and enhances chain-transfer reactions (Karol, 1984); four, the presence of magnesium ions can stabilize active titanium centres from deactivation processes; and five, $MgCl_2$ -supported catalysts produce polyethylenes of narrower molar mass distribution.

Without any activation process, magnesium chloride has a negligibly small specific surface of less than $1 \text{ m}^2/\text{g}$ (Kinkelin, 1986). Chien et al. (1987) increased the area over a hundred-fold by ball-milling $MgCl_2$ in the presence of electron donor such as ethyl benzoate and impregnating *p*-cresol and TEAL to the surface. The primary effect of milling is to shatter the layered structure of the magnesium chloride crystals (Karol, 1984), but excessive grinding has been shown to be undesirable (Terano and Ishii, 1990) as active sites would agglomerate. This ball-milling step has been omitted in more recent techniques, where magnesium

chloride supports with high surface areas are produced by direct precipitation from saturated solutions. The process of MgCl_2 recrystallizing from a methanol-decane mixture was found capable of producing spherical particles between 10-40 microns in size and $45 \text{ m}^2/\text{g}$ in surface area (Chung et al., 1995).

2.1.4.2 Silica

Incorporation of silica into MgCl_2 -supported TiCl_4 has reportedly been able to enhance ethylene homopolymerization and ethylene/1-butene copolymerization (Wang et al., 1993). The dispersing effect of silica on MgCl_2 increased the number of effective titanium centres on the surface. In terms of resin morphology, the higher the amount of silica added into the MgCl_2 -supported catalyst, the larger and more uniform the particles produced in the ethylene/1-butene copolymerization (Wang et al., 1993). Muñoz-Escalona et al. (1990) also reported a drastic increase in activity when TiCl_4 was bisupported on silica and MgCl_2 . The condition at which silica was calcined profoundly influenced the activity for ethylene polymerization as well: the higher the temperature, the better the yield on a per gram of Ti basis (Muñoz et al., 1990; Lu and Xiao, 1993).

2.1.5 Effect of Temperature on Activity

In studying the temperature effect from the very stable kinetic behaviour of $\text{SiO}_2/\text{MgCl}_2$ supported Ti catalyst activated by tri-n-octyl aluminium (TNOAL), Bu et al. (1995) observed that the reaction orders were highly dependent on temperature for gas-phase ethylene polymerization: as the temperature was increased from 30 to 70°C, the order of the reaction increased from as low as 0.9 to about 1.5. Discussion on the significance of this work will be deferred until Section 2.2.1.

2.2 Molar Mass Distribution

Molar mass distribution (MMD), an important property of polymers, is of great research interest not only because it is intimately linked to the nature of the catalytic systems but also because it has profound influence on polymer melt processing and solid state properties. Generally MMD is more succinctly expressed in terms of number average molar mass (M_n) and weight average molar mass (M_w). The former is the first moment of the molar mass distribution and the latter, the ratio of the second moment to the first. The ratio between M_w and M_n is known as polydispersity (Q). The following summary will focus on the publications with an experimental flavour.

2.2.1 Diffusion versus Multiplicity of Sites on the Molar Mass Distribution

One characteristic feature of polyolefins produced by Ziegler-Natta catalysts is their unusually broad MMD. While M_w controls the mechanical properties of a polymer, both Q and M_w exert relevance in the rheological properties. Again, there are two schools of thoughts on the origin of the broad distribution: monomer diffusion control and multiplicity of active sites. The first theory proposes that the difference in diffusional limitation at varying degrees of catalyst encapsulation by polymer is responsible for the broadness of MMD, whereas the second theory, the superimposition of MMDs generated by several types of dissimilar active sites.

Although the diffusional theory has enjoyed rigorous mathematical treatments, experimental evidence has lent greater credence to the alternative resolution. The most serious challenge to the diffusion theory was probably the fact that *chemical* modifications to the catalysts were able to vary the MMD (Zucchini and Cecchin, 1983; Karol, 1984). Chien et al. (1985) refuted the diffusion theory by showing that the alleged diffusion limitation made little difference in the slurry-phase polymerization behaviour of soluble poly(1-decene) and crystalline polypropylene. Modern high-activity catalysts do not necessarily

provide broad distributions under a gas-phase environment as predicted by the diffusion theory of Floyd et al. (1987).

While the diffusion theory has largely been discredited (Dusseault and Hsu, 1993), direct positive proofs for the multiplicity of active sites model are not available. The most often cited evidence for the multiplicity of active sites was provided by Wild et al. (1982). Using a technique of separating polyethylene molecules on the basis of crystallizability named temperature rising elution fractionation (TREF), Wild illustrated that the comonomer incorporation distribution of ethylene/ α -olefin copolymer was bimodal. Usami et al. (1986) supplemented the TREF studies with ^{13}C -NMR results to advance the theory that a discontinuity in the product of reactivity ratios ($r_1 \times r_2$) from one peak to the other observed in the TREF profile was the necessary and sufficient proof for the existence of multiple active centres.

Nevertheless, it should be emphasized that TREF only provides kinetic insights for copolymerization between ethylene and higher α -olefins and offers no supporting evidence for site heterogeneity during homopolymerization of ethylene. Addition of comonomer may arguably be the cause of the observed bimodal distribution in TREF in light of previously discussed "comonomer effect." While there is a myriad of investigations on the homopolymerization of propylene or other higher α -olefins in which the active centres were isolated on the basis of differences in Lewis acidity (Busico et al., 1985; 1986; Peña et al, 1991; Soga et al., 1988), stereoregularity (Suzuki et al., 1979; Keii et al., 1984), or oxidation state (Chien et al., 1989; Soga et al., 1981; 1982), only a limited amount of work has been done on ethylene homopolymerization (Chien and Bres, 1986; Zlotnikov et al., 1988).

Probably the most conclusive evidence for multiple sites for ethylene homopolymerization was furnished by Bu et al. (1995) who reported that the reaction rate order for an SMST catalyst was around 0.9 at 30°C and 1.5 at 70°C. As no single-site mechanism would allow the reaction order to traverse through the impervious Langmuir kinetic barrier of unity, there must be at least two types of sites on the surface of the catalyst.

2.2.2 Control of Molar Mass and Molar Mass Distribution

The control of molar mass distribution in Ziegler-Natta polymerization can be achieved by adjusting the operating parameters or by modifying the catalyst system. The amount and the type of chain-transfer agents (hydrogen, α -olefins, cocatalyst, etc.), Lewis bases, reactor temperature, and time have been explored to enhance or inhibit the manifestation of one particular type of active site in regulating the breadth of the overall molar mass distribution.

2.2.2.1 Hydrogen and α -Olefins

Molecular hydrogen has long been used to control the molar mass of the polymer. Without hydrogen, the catalytic process would produce polyolefin with too high a molar mass for most practical applications (Boor, 1979). It is generally agreed that the higher the concentration of hydrogen, the lower the molar mass, both M_n and M_w . Also well known is the similar effect of α -olefins on molar masses. Pasquet and Spitz (1991) studied the combined effect of hydrogen and 1-butene in gas-phase polymerization and found that 1-butene alone was a poor chain-transfer agent and hydrogen alone was somewhat better. Yet in the presence of 1-butene, hydrogen was much more effective in reducing the molar masses.

2.2.2.2 Cocatalyst

Lynch et al. (1991) noted that polyethylenes obtained from the TEAL system had lower molar masses (M_n as well as M_w) than did those from IPRAL under similar conditions. The more pronounced reduction in M_n , which led to greater Q , was attributed to the greater deactivation with TEAL. It was also found that both M_n and M_w can be simultaneously elevated if the size of the ligands attached to the aluminum in the cocatalysts was increased. Similar results were obtained with a second-generation ball-milled catalyst (Zucchini and Cecchin, 1983). However, in the presence of hydrogen, Marques et al. (1993b) reported that no correlation could be established.

2.2.2.3 Lewis Bases

Spitz et al. (1990) maintained that for ball-milled MgCl_2 catalysts, molar masses can be lowered and MMD narrowed by the inclusion of Lewis bases, either internal or external. As electron donors have generally been dispensed with in the current generation of polyethylene catalysts, control of MMD via external Lewis bases is not a preferred method since the inclusion of electron donors would compete with ethylene for active sites and thus compromise the activity.

2.2.2.4 Temperature

It is generally agreed that increasing the polymerization temperature lower the molar mass (Marques et al., 1993b). This has been widely attributed to a greater decrease in termination rate in comparison to propagation rate as temperature decreases. In slurry experiments, polydispersity was found to decrease with increasing temperature (Xiao and Lu, 1992); for gas-phase operations, however, an increase in MMD was observed (Jejelowo et al., 1991).

2.2.2.5 Polymerization Time

In ethylene polymerization, the molar mass was found to increase with the duration of polymerization up to a limiting value reached in about 10 minutes (Zlotnikov et al., 1988) or 90 minutes (Marques et al., 1993b), depending on the catalyst system. This is in sharp contrast to propylene polymerization, where Suzuki et al. (1979) found that the molar mass distributions for the atactic and isotactic fractions and for the entire sample did not vary appreciably with time (from 5 seconds to 3 hours). According to Kissin (1995), the change of average molar mass with time reflects the fact that the active centres that produce polymer molecules with lower MWs decay much faster.

Studies reviewed in the preceding sections represent only a small fraction of the publications in the area of catalytic Ziegler-Natta polymerization in slurry

reactors. The fraction of previous studies that is applicable to gas-phase polymerization is uncertain, for experimental results obtained from the slurry reaction cannot be used to reliably project the outcomes of the gas-phase, as demonstrated by Lynch et al. (1991). The catalyst used for the present study belongs to the family of the UNIPOL catalysts, and the unique characteristics enumerated by Karol et al. (1987) could not be examined fully if the reactions were to be carried out under a slurry environment. Descriptions of the gas-phase polymerization equipment previously designed by Lynch and Wanke (1991) are briefly presented in the following chapter; the exploration into the probable causes of irreproducibility are presented in Chapter 4.

3. EXPERIMENTAL

In this chapter, the equipment, materials, and procedures for gas-phase polymerization experiments are described briefly in Sections 3.1 through 3.3. Detailed information on the construction of the entire reactor system has been published elsewhere (Lynch and Wanke, 1991). Characterization techniques such as gas chromatography, gel permeation chromatography, temperature rising elution fractionation, melt index, and differential scanning calorimetry used in the present study are outlined in Sections 3.4 through 3.8.

3.1 Polymerization Equipment and Materials

Various components of the reactor system, represented schematically in Figure 3.1, are described in this section.

3.1.1 Reactor

The cylindrical reactor vessel with a capacity of approximately one litre was constructed from 316 stainless steel with a wall thickness of 1.5 cm. The inside diameter of the reactor was 11.4 cm and the depth, 10.2 cm. The top flange of the reactor was rigidly fixed to a support stand and the removable bottom section, bolted to the flange with a leak-proof seal provided by a Viton o-ring. All valves, fittings and tubing connected to the reactor were made of either 316 or 304 stainless steel.

Reactor pressure was maintained by means of a pressure regulator (Tescom Model 26-1600, 0 to 3.4 MPa range). A high precision pressure transducer (Omega Model PX621) connected between the pressure regulator and the feed entry port was used to monitor the pressure. A mechanical vacuum pump was used to remove impurities during reactor pretreatment.

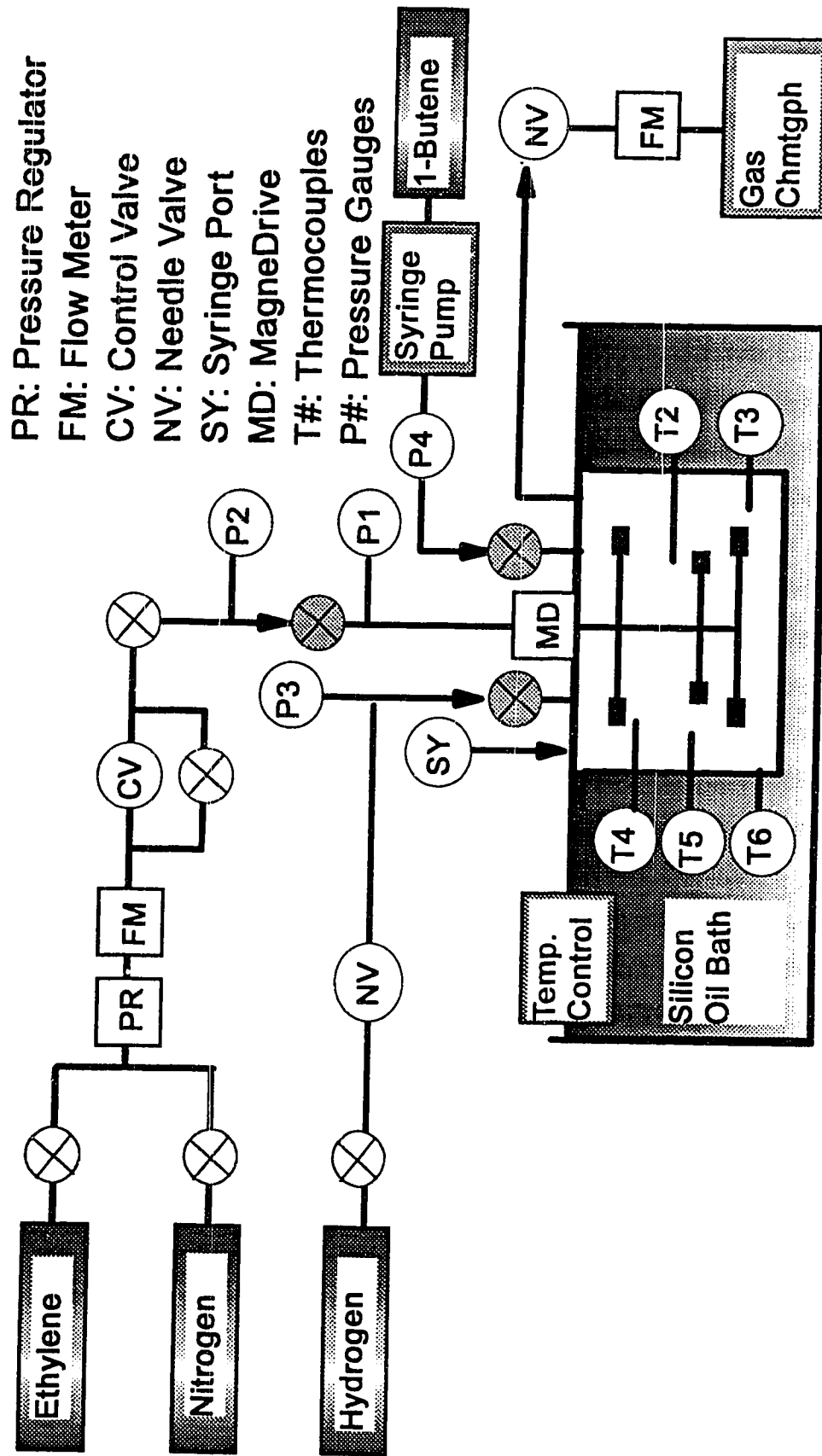


Figure 3.1 Schematic diagram of the reactor system

Reactor contents were stirred by an Autoclave Engineers Inc. Model 1.5-1-5 K-A236 Magnedrive II stirrer driven by a variable speed motor. Variable-angle paddle-type stirring vanes were attached to the stirrer shaft. They were fitted at various heights from the bottom of the shaft. In order to promote axial mixing, the vanes at the bottom were normally angled upwards and the vanes at the top, downwards.

Temperature control was achieved by immersing the reactor in a 26-litre bath filled with a medium viscosity oil, which was either Dow Corning 200 Fluid (100 CSt) or Esso Primoil 185. The latter was rather undesirable, for it degraded rapidly at the higher temperature (90°C) and emanated a repugnant odour. The temperature of the oil was maintained to within $\pm 0.1^\circ\text{C}$ by a Lauda Model MS constant temperature immersion circulator, which when used in combination with a cooling coil, enabled the bath to be operated over the range of 5 to 120°C. The oil bath could be raised or lowered and during the operation the surface of the oil was about 2 cm above the top surface of the flange. A stirrer driven by a constant speed DC motor was immersed in the oil bath to enhance agitation. Temperature in the reactor was monitored by six sheathed Type J thermocouples situated at various radial and axial locations.

3.1.2 Feed and Exit Streams

Polymer grade ethylene (from Matheson), ultra-high-purity hydrogen and pre-purified nitrogen (both from Linde) were passed through individual Alltech high pressure gas purifiers containing BASF R3-11 catalyst, Ascarite and molecular sieves (5A) for the removal of oxygen, carbon dioxide, and moisture, respectively. Without such treatment these feed gases may include as much as 10 ppm of oxygen containing compounds (H_2O , O_2 , CO_2 , and CO) which would readily deactivate the Ziegler-Natta catalyst system. Matheson mass flow meters (rated for 250 psi or lower) were used to monitor the flow rates of ethylene. Routine calibration of these mass flow meters against a bubble meter was performed to correct for baseline drift.

Liquefied 1-butene supplied by Novacor Chemicals Ltd. was introduced to the reactor without further purification via an ISCO 500D high pressure syringe pump which can be operated in one of four modes: constant volumetric flow, constant pressure, gradient volumetric flow, or gradient pressure. For most reactions the constant volumetric flow was used. External cooling water was used to prevent the vaporization of 1-butene in the syringe.

3.1.3 Data Acquisition

All thermocouples, pressure transducers, mass flow meters and mass flow controllers described above were interfaced with an OPTO 22 input/output system to a personal computer for data acquisition and control. Values of all monitored quantities were recorded every 20 seconds for all experiments.

3.2 Catalyst and Cocatalyst Handling

Handling and storage of catalyst and cocatalyst were done in a glove box (Model HE-493 from Vacuum Atmospheres Ltd). The inert-gas filled HE-493 provided a moisture- and oxygen-free environment, and whenever materials were transferred out of the glove box, the prechamber was evacuated to at least 0.050 torr before being refilled with nitrogen. Nitrogen gas was continuously cycled through the chemical purifier which contained two active ingredients capable of absorbing moisture and removing oxygen. Online moisture (MCM Dewmatic Model 600 Hygrometer) and oxygen analyzers (Custom Sensors & Technology Model 8203) constantly monitored the impurity levels in the glove box. Oxygen levels of less than 1 ppm and moisture levels of less than 4 ppm were normally maintained in the glove box.

A commercial catalyst (titanium tetrachloride bisupported on magnesium chloride and silica) provided by Novacor Chemical was used for the present study. For all experiments conducted in the current study, catalyst was introduced in the form of a suspension, which was prepared by placing a

prescribed amount of catalyst in a 100-cc volumetric flask filled with *n*-heptane, *n*-decane, or *n*-hexadecane. The most frequently used suspending liquid was *n*-heptane. The catalyst suspension, upon being thoroughly agitated by a magnetic stirrer, was drawn into the needle part (with a total volume of 1.0 ml) of a Hamilton Gastight syringe assembly. Likewise, samples of the liquid cocatalyst (either TEAL or TNHAL) or silicon tetrachloride obtained from Texas Alkyls were also transferred to the reactor by means of Hamilton Gastight syringes. All syringes were sealed with rubber septa prior to removal from the glove box in order to minimize the contact with atmospheric gases.

3.3 Polymerization Procedure

The following steps were developed for a typical gas-phase polymerization run if TNHAL was the cocatalyst. Aspects of the polymerization method that depart considerably from the operating procedure developed by Lynch and Wanke (1991) along with an alternative reactor pretreatment method using TEAL as the moisture scavenger are discussed in Chapter 4.

1. A seedbed (200 grams of sodium chloride obtained from Fisher Scientific) was placed inside a thoroughly cleaned reactor free of residual polymer or seedbed from the previous experiment.
2. The reactor was then sealed and leak-tested at 300 psi with nitrogen for a period of 30 minutes at room temperature. If the pressure drop after the temperature had attained a constant value (about 5 minutes) was 1 psi or less, the reactor was considered leakage-free and immersed into the oil bath and evacuated at 90°C overnight.
3. At the end of the evacuation period the reactor was cooled to the desired operating temperature. For copolymerization experiments, due to the comonomer activation effect, this initial temperature at which the catalyst was introduced was at least 5 to 10°C below the set point to avoid thermal runaway. This initial temperature offset

was smaller for homopolymerization. The magnitude of the initial offset depended on the amount of the catalyst and cocatalyst, and the concentrations of ethylene, 1-butene, and hydrogen.

4. For copolymerization experiments only: While the reactor was being cooled, liquid 1-butene was throttled from the supply tank into the cylinder of the syringe pump. The cylinder and the tube connected to the top of the flange was then compressed to 50 psi, a pressure slightly higher than the vapour pressure of 1-butene at the room temperature.
5. As the temperature of the reactor reached the desired initial value, the reactor was charged with 30 psi of ethylene, the upper threshold pressure at which injections of materials by Hamilton Gastight syringes can be performed safely. The prescribed amount of cocatalyst (typically 1.0 ml of neat TNHAL) was introduced to the reactor and stirred for 5 to 10 minutes in order to wet the seedbed evenly.
6. The catalyst suspension was injected into the reactor while stirring was temporarily suspended.
7. For copolymerization experiments only: following the catalyst injection, ethylene was added first to a total pressure of 50 psi. The ethylene feed stream was then isolated from the reactor and the desired amount of precharged 1-butene was pumped into the reactor.
8. The desired amount of hydrogen was added to the reactor.
9. With the pressure regulator set at the desired overall pressure, the ethylene flow was promptly started.
10. The reactor temperature was kept constant at the operating temperature by using the temperature controller on the oil bath.
11. After two hours of polymerization, the reactor was purged with carbon dioxide to deactivate the catalyst. The reactor was disassembled and the amount of polymer produced was weighed.

Removal of the sodium chloride seedbed from the polyethylene product was achieved by thorough rinsing of the reactor mixture with water, usually in a separatory funnel. Moist polyethylene sample was later washed with ethanol and vacuum filtered at room temperature. Baking the samples at elevated temperature was avoided as thermal degradation of the polymer would result prior to molecular characterizations.

3.4 Gas Chromatography

During the course of reaction the relative compositions of ethylene and 1-butene were monitored and analyzed by a Hewlett-Packard 5890A gas chromatograph equipped with two thermal conductivity detectors and a column packed with *n*-octane/Porasil. The flow rate of the sampling stream from the reactor through an 8-way valve to the GC analyzer was usually set at 20 sccm. Pre-purified helium (supplied by Matheson), flowing at the rate of 80 sccm, was used as the carrier gas. Retention times for ethylene and 1-butene at 100°C column temperature were approximately 1.15 and 2.05 minutes, respectively. The duration for each sampling cycle was 3 minutes, an interval too short for the registry of *n*-hexane (from TNHAL) or *n*-heptane (from the catalyst suspension). The molar response factor for ethylene was 48, and for 1-butene, 81. Due to the presence of hydrogen, a small portion of 1-butene was reduced to *n*-butane (retention time: approximately 1.85 minutes); the conversion of 1-butene to *n*-butane was found to be less than 5% at 100 psi P_{H₂}.

3.5 Gel Permeation Chromatography

Molar mass distribution was obtained with a Waters 150C GPC equipped with a differential refractometer analyzer. Four Shodex GPC/AT-80M/S columns, packed with styrene-divinylbenzene gels, were connected in series for the size exclusion chromatography. Temperature of the columns and the detector were maintained at 140°C. The carrier solvent, Fisher HPLC grade 1,2,4-trichlorobenzene containing 0.25 g/L of 2,6-di-*tert*-butyl-4-methyl-phenol antioxidant (from Aldrich Chemicals), was pumped at a rate of 1.0 ml/min through the columns. For each polyethylene sample analyzed, two solutions were prepared (0.02 wt% or less), and for each solution two repeat injections (100-300 μ L each) were performed. The reported number average and weight average molar masses are generally the averages of the four measurements. Prior to injections all samples were heated to 160°C for two hours in order to prevent the formation of supermolecular aggregates (Grinshpun et al., 1984). The universal calibration curve approach was used; a cubic function was adopted to fit the retention time with the molar masses of the standard references. Narrowly-distributed polystyrene samples with known molar masses (from TSK Standards), linear paraffins ($C_{20}H_{42}$, $C_{40}H_{82}$, and $C_{60}H_{122}$; supplied by Fluka), and NIST Standard Reference Material No. 1475, 1481, 1482, 1483, and 1484 were used as standards. It was assumed that values of the Mark-Houwink constants taken from the literature (Barlow et al., 1977) for polyethylene ($k=3.95 \times 10^{-4}$ dL/g; $\alpha=0.726$) and polystyrene ($k=1.90 \times 10^{-4}$ dL/g; $\alpha=0.655$) were valid for the entire range of molar mass studied. The Mark-Houwink constants used for HDPE were extended to LLDPE without correction, based on the assumption that a small number of side branches have little effect on the chain dimension in solution and introduce negligible uncertainty to the molar mass.

3.6 Temperature Rising Elution Fractionation

Temperature rising elution fractionation (TREF) profiles were obtained from the equipment built in the Department of Chemical Engineering at the University of Alberta (Chakravarty, 1993). The analytical fractionation (A-TREF) was preceded by a process of crystallization which involved the cooling of 0.1 wt.% polyethylene/*o*-xylene solution previously stirred for 2 hours at 120°C to -10°C at a rate of 1.5°C per hour. (To avoid stirring-induced entanglements which would hinder the process of molecular crystallization, the solution concentration should be reduced for samples with high molar masses where the average end-to-end distance may be shorter than the separation distance between molecules.) These samples, crystallized in vials, were packed into a column (45 mm in length and 6 mm in ID) along with inert diatomaceous earth and eluted by *o*-dichlorobenzene from -10 to 120°C at a rate of 2°C per minute. The concentration of polyethylene fraction in the solution was continuously monitored by an infrared detector whose wavelength was fixed at 3.41 μm (2930 cm^{-1}), the wavelength of methylene stretch. The absorption signal obeys the Beer's law over the range of concentration used (Lacombe, 1995).

3.7 Melt Index

Melt index (MI) was obtained from a melt flow indexer (Kayeness Model 7053). ASTM Method D 1238-94 Procedure A was followed to determine the rate of extrusion of 190°C molten polyethylene through an orifice (0.8000 cm in length; 0.2096 cm in ID) subject to a load of 2.16 kg over a ten-minute interval. A preliminary melting step, where polymer powders together with a small quantity of 2,6-di-*tert*-butyl-4-methyl-phenol antioxidant were loaded into the barrel and forced through the die, was used prior to the actual measurement to eliminate

pockets of air which would otherwise be trapped inside the extrudate should samples be measured directly from its nascent powdered form.

Samples with M_w greater than 2.0×10^5 were not measured directly as the materials were too solid-like under the testing condition with very little deformation under the stress applied. The formidable task of accurately cutting and weighing minute amount of polymer melt aside, the impact of shear stress variation at different cross section along the extrusion barrel on melt index has yet to receive its due recognition (Ghosh et al., 1995). Extending the time interval for measuring high- M_w polymer would lead to erroneous results, as the actual shear stress as alleged would decrease with the amount of polymer in the barrel.

3.8 Differential Scanning Calorimetry

Differential scanning calorimetry (DSC) measurements were made on a TA Instrument Model DSC2910 with a software package TA2200 to analyze the transition temperatures and the degree of crystallinity. Temperature calibration was accomplished by scanning through the melting point of an indium standard, which has a melting point of 156.6°C . Samples weighed in a Mettler balance (Model AC100 with ± 0.1 mg sensitivity) to be 5.0 ± 0.3 mg in size were sealed in non-hermetic aluminum pans with flat contact surface (supplied by Thermal Analysis) and subjected to the heating and cooling cycles. The programming steps were outlined in Table 3.1. Between each successive step shown, there was an isothermal interlude of five minutes (except between Steps 1 and 2) to ensure thermal equilibrium of the specimen and stability of the control signal. For HDPE samples, specimens were cooled to 40°C instead of 20°C .

Thermal characteristics as examined by DSC were strongly affected by the heating and cooling rates. At a slow heating rate, thin lamella would anneal into thicker lamella and melt at a higher temperature (Wunderlich, 1980; Hosoda et al., 1986); Hellmuth and Wunderlich (1965) observed that for polyethylene T_m is especially sensitive to heating rates lower than $10^\circ\text{C}/\text{min}$. The particular heating

Table 3.1 DSC Programme for polyethylene analysis

- Step 1. Equilibrating at 40°C.
Step 2. Heating at 10°C/min to 160°C.
- Step 3. Cooling at 5°C/min to 20°C.
Step 4. Heating at 10°C/min to 160°C.
- Step 5. Cooling at 10°C/min to 20°C.
Step 6. Heating at 10°C/min to 160°C.
- Step 7. Cooling at 20°C/min to 20°C.
Step 8. Heating at 10°C/min to 160°C.
-

rate was adopted based on the recent report by Ottani and Porter (1991) that at a heating rate 10°C/min or higher no reorganization was found. Heating rates higher than 10°C/min were avoided to prevent temperature gradients within the specimen. It was found that for the present equipment a cooling rate greater than 1°C/min would require the use of liquid nitrogen. The DSC facilities used for this study are located in Professor Michael C. Williams' laboratory.

4. REACTOR OPERATION

A significant amount of work in the present investigation of Ziegler-Natta copolymerization was devoted to the development of suitable laboratory procedures for obtaining reproducible results for gas-phase polymerizations. As mentioned in the previous chapters, in circumventing the problem of reproducibility, gas-phase operation was largely avoided in the academic and industrial research settings. Active ingredients of the catalyst system are less susceptible to poisons (e.g. oxygen, water, or carbon dioxide from any source) in the inert hydrocarbon solvent than in the gas-phase environment. Under the mild slurry conditions, other factors which may have significant impact on the performance of the catalyst in a gas-phase environment may not be noticed and much less investigated. In this chapter, aspects of polymerization method outlined in Section 3.3 that departed considerably from the operating procedure developed by Lynch and Wanke (1991) will be discussed in the following order: alternatives to the reactor pretreatment, timing of catalyst injection, and the selection of seedbed. Experimental results cited in this and subsequent chapters will be referenced by the run numbers; further information on any particular run can be found in the Appendix, The Annotated Summary of Experiments.

4.1 Reactor Pretreatment

Titanium tetrachloride, the active component of the Ziegler-Natta catalyst system, is extremely sensitive to any trace impurities such as moisture or oxygen. During the pretreatment period, which corresponds to the first two steps of the operating condition outlined in Section 3.3, it is desired to remove to the fullest extent possible traces of such catalyst poisons. Lynch and Wanke (1991) pretreated the reactor by a two-step procedure: first, baking the sealed vessel at 90°C *in vacuo*,

and second, injecting 2.0 ml of diethylaluminium chloride (DEAC) as the "moisture scavenger" to react with the water molecules which remained adsorbed on the reactor surface to produce ethane gas which was subsequently removed from the reactor along with unreacted DEAC by evacuation. The second evacuation step was implemented as overnight baking at 90°C did not sufficiently remove all the adsorbed molecules (Lynch and Wanke, 1991). The particular scavenging cocatalyst was chosen because DEAC is the cocatalyst for the Stauffer-type catalyst used in their study. The commercial catalyst used for the present study was activated by triethylaluminium (TEAL) in the production facilities, and replacing DEAC with TEAL as the moisture scavenger seemed appropriate.

During the earliest stage of the gas-phase polymerization studies, TNHAL was selected over TEAL as the cocatalyst of choice, as the TNHAL-activated catalyst exhibited a much higher activity than did the TEAL-activated catalyst (cf. Runs 6 and 10). Along with the change of cocatalyst was the substitution of TEAL by TNHAL as the moisture scavenger to avoid the unknown interactions between the TNHAL cocatalyst and the residual TEAL. The vapour pressure of TNHAL at 90°C was estimated to be less than 0.1 millitorr, a drastic reduction from that of TEAL (~5 torr). Although TNHAL can react with water to produce hexane, the cocatalyst in stoichiometric excess cannot be evacuated by the same mechanical pump. Recognizing the formidable task of evacuating any unreacted TNHAL with the device available, no attempt was made to remove TNHAL from the pretreatment after Run 18. Evacuation of the reactor after the 30-minute period was still applied to remove hexane, and the residual TNHAL was found capable of activating the catalyst injected into the reactor. However, removal of hexane was superfluous, for hexane was inert to the active components of the catalyst system. Beginning at Run 35, the following procedure was followed: after overnight baking at 90°C, the reactor was cooled to the reaction temperature, and cocatalyst was injected to the reactor just prior to the introduction of the catalyst. The second evacuation step was thus eliminated entirely.

This simplified pretreatment technique came at the expense of knowing the exact amount of TNHAL in the reactor when calculating the Al/Ti ratio. As the

overnight baking period was not controlled precisely, the moisture level on the reactor walls varied from one run to the next. The baking temperature can be increased to substantially reduce the prolonged baking period, but it was not feasible because the silicon oil would be lost through evaporation. Alternatives to the hot-oil baking technique were sought, as Al/Ti often plays a significant role in the phenomenological behaviour of the catalyst. Increasing the baking temperature was pursued first, as the residence time of the adsorbed species on the reactor surface decreases exponentially with respect to temperature. Experimental conditions for Runs 62 and 63 were identical except in the pretreatment techniques. In Run 63, the reactor was baked by blowing air (delivered by a heat gun, Master Appliance Corp. Model HG0391A) at 250°C to the reactor exterior for two hours. (During the baking period, the coldest part of the reactor as measured by Thermocouple 1 was 160°C.) The striking similarity between the two activity profiles (see Figure 4.1) suggests that the extended period of reactor baking can be greatly reduced when other heating devices such as a heat gun, heating mantle, or infrared radiator are used. Determining the relative cleanness of the reactor interior deliverable by these two approaches would likely require GC analysis of hexane content in the gas mixture.

The objective to establish a routine, TEAL-based pretreatment method capable of rendering reproducible reactor surfaces was also pursued. All polymerizations described hereafter in this section, unless otherwise noted, took place at 70°C, 200 psi ethylene and 100 psi hydrogen for two hours. In the first attempt, Run 113, the reactor moisture was reacted with 3.0 ml of dilute TEAL (1.0 M hexane solution) for 40 minutes and the mixture was then evacuated at 95°C. Just before the catalyst introduction, 1.0 ml of TEAL (neat) was injected. The activity of the catalyst was 240 g-PE/g-cat·h, which compared favourably with Run 107 (160 g-PE/g-cat·h) in which the reactor pretreatment was analogous to most of the TNHAL runs. In Run 115, the activity increased by about 40% (330 g-PE/g-cat·h) as the amount of neat TEAL was halved. In Run 116, no TEAL was added other than the diluted 3.0 ml used for pretreatment. The scant amount of TEAL remaining after evacuation was sufficient to nearly

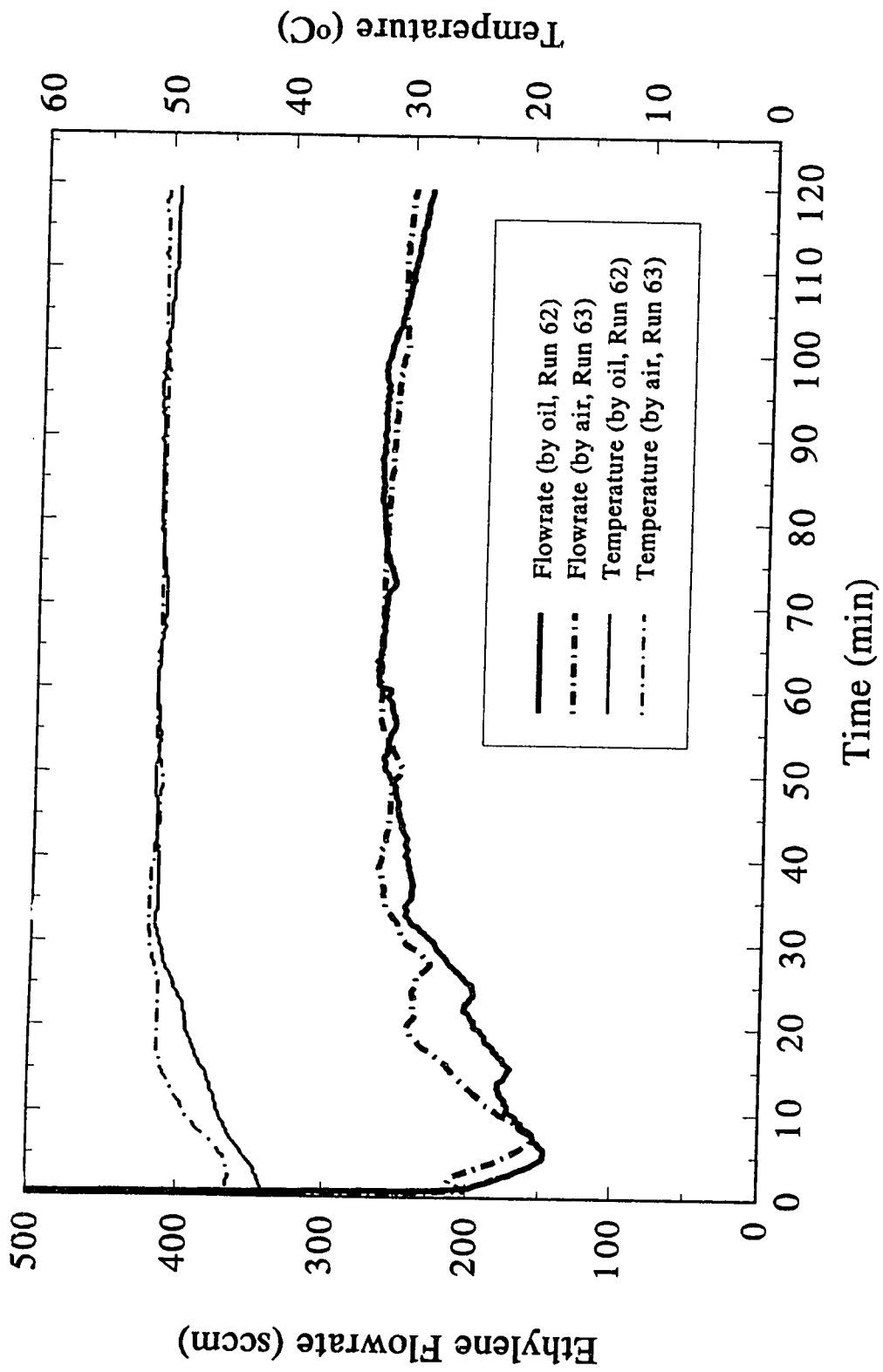


Figure 4.1 A comparison of two pretreatment methods

triple the activity to 900 g-PE/g-cat·h for the initial two hours. But when the experiment was repeated (Run 118), the activity was 800 g-PE/g-cat·h.

The sizable difference in activity between Runs 116 and 118 again presented the challenge of reproducibility. The presence of TEAL in these two runs was certain, for the type of catalyst ($\text{SiO}_2/\text{MgCl}_2$ -supported TiCl_4) would be inactive without any cocatalyst, but the amount of its presence was not. The uncertainty in the amount of TNHAL as a direct consequence of the pretreatment method was tolerated with the understanding that the catalyst complexed with the cocatalyst of long ligands was less sensitive to the Al/Ti. However, it has been demonstrated here that with TEAL as the cocatalyst, such uncertainty would raise questions on the integrity of the kinetic studies. To fully ascertain the Al/Ti in the reactor, which is to be accomplished by adding a precise amount of cocatalyst into the reactor, demands the complete removal of the initial moisture-scavenging TEAL from the reactor.

Several improvised pretreatment methods were tested in Runs 125, 128, and 129, and except for Run 128, the activities were comparable to those of Runs 116 and 118. The method used in Run 128 (Table 4.1) was repeated three times (Runs 131-133) and in all cases the catalyst displayed no activity unless TEAL was supplemented. Thus, the objective of developing a reproducible pretreatment method rendering a moisture-free and cocatalyst-free environment was accomplished. The prolonged baking period was not needed in this method, and the amount of cocatalyst was under control, enabling the investigations on the effect of Al/Ti ratio on activity.

Table 4.1: Pretreatment procedure used in Run 128

- 1 Place 200 grams salt bed into the reactor; Test leakage with 300 psi nitrogen for 20 minutes; Start heating the oil bath
 - 2 Immerse the reactor into 95°C hot oil; Evacuate the reactor for 40 minutes
 - 3 Inject 3.0 ml of 1.0M TEAL into the reactor with 30 psi nitrogen background pressure; Stir the seedbed for 20 minutes; Raise the heating oil temperature to 105°C
 - 4 Evacuate for 20 minutes at 105°C
 - 5 Add 300 psi ethylene; Stir 5 minutes
 - 6 Evacuate while cooling the vessel to 65°C
 - 7 Inject cocatalyst
 - 8 Inject catalyst
-

4.2 Catalyst Injection

After the cocatalyst has been introduced into the reactor, the catalyst suspended in solvent (generally heptane) were then injected into the reactor through a syringe. The catalyst suspension was introduced into the reactor under different ethylene and nitrogen pressures as shown in Table 4.2, and after a prescribed amount of mixing time (0 or 15 minutes), the reaction was allowed to proceed under the set conditions as indicated.

It is well known that for polymerization to occur, Ti^{+4} must be reduced to Ti^{+3} and Ti^{+2} by a reducing agent such as TEAL, and overreduction of Ti^{+4} to Ti^{+1} would render the catalyst inactive. Typically catalyst was injected into pure ethylene (as in Run 107) and with very little delay polymerization took place at 200 psi of ethylene on the sites which had just been reduced from Ti^{+4} to Ti^{+3} .

Table 4.2: Composition of the gas mixtures into which catalyst was injected (Polymerization condition: C₂H₄=200 psi; H₂=100 psi; Temp.=70°C; Time=2 hr)

Run	Ethylene (psi)	Nitrogen (psi)	Delay Time (min)	Yield (g)
107	50	0	0	19.0
110	50	0	15	14.1
111	25	25	15	11.6
108	0	50	0	9.5
109	0	50	15	1.7

Further reduction of Ti⁺³ was hindered, as layers of polyethylene grown around the catalyst particles limited the TEAL diffusion to the active sites. It appeared that the layers of polyethylene formed around the catalyst particles had a protective function against such overreduction. This protective layer against overreduction by TEAL was considerably less during the initial 15-minute prepolymerization period of Run 110, where only 50 psi ethylene engaged in the protection of active sites. After the 15-minute delay, a significant amount of active sites had been reduced to inactive oxidation states, hence the 25% reduction in overall activity. As the protective layer was further reduced by nitrogen dilution (Run 111), the drop in activity was an additional 15 percent.

Under the pure nitrogen environment, active centres were not protected by the polyethylene forming around the catalyst particles. TEAL reduction of bare catalyst continued until ethylene was introduced into the reactor to compete with TEAL for active titanium species. Comparing with Run 107, the 50% reduction in overall activity in Run 108 suggested that the presence of monomer molecules during the initial contact between the catalyst and the cocatalyst appeared to be most crucial. Such loss of activity was further exacerbated by a fifteen-minute delay of reaction (Run 109).

It can be surmised that the first layers of polyethylene around the catalyst particle form an effective diffusional barrier against the cocatalyst from overreducing the active sites, and among the variables which determine the level of protection are the monomer concentration (or pressure) and the delay time. Attempts were made to investigate whether higher alkanes can shield the active sites from the strong cocatalyst TEAL. Three catalyst suspensions were made: one heptane (Run 118), one decane (Run 127), and one hexadecane (Run 125), and the order of the activity was decane > heptane > hexadecane. It can be inferred from the order of activity that decane did shelter the active centres better than did heptane. However, dispersion appeared to have a stronger effect than did diffusion, or hexadecane would have the highest averaged activity. Hexadecane was the most viscous among the three solvents (Table 4.3), and the stirring of the seedbed with 1 ml of hexadecane as observed from the transparent Lexan vessel was correspondingly the poorest.

Table 4.3: Viscosities of catalyst suspending media

Run	Solvent	Viscosity (cp) at 70°C	$M_n \times 10^{-3}$	$M_w \times 10^{-3}$
118	heptane	0.17	27	104
125	hexadecane	0.67	29	111
127	decane	0.29	28	104

The significance of stirring was further illustrated by the difference in the activity profiles of these three runs (see Figure 4.2). In all these runs the temperature was well controlled to be around the temperature set point of 70°C. While the activity profiles were very dissimilar, the reaction kinetics on the molecular level was comparable: samples of these three runs were found to have nearly identical molar mass distributions.

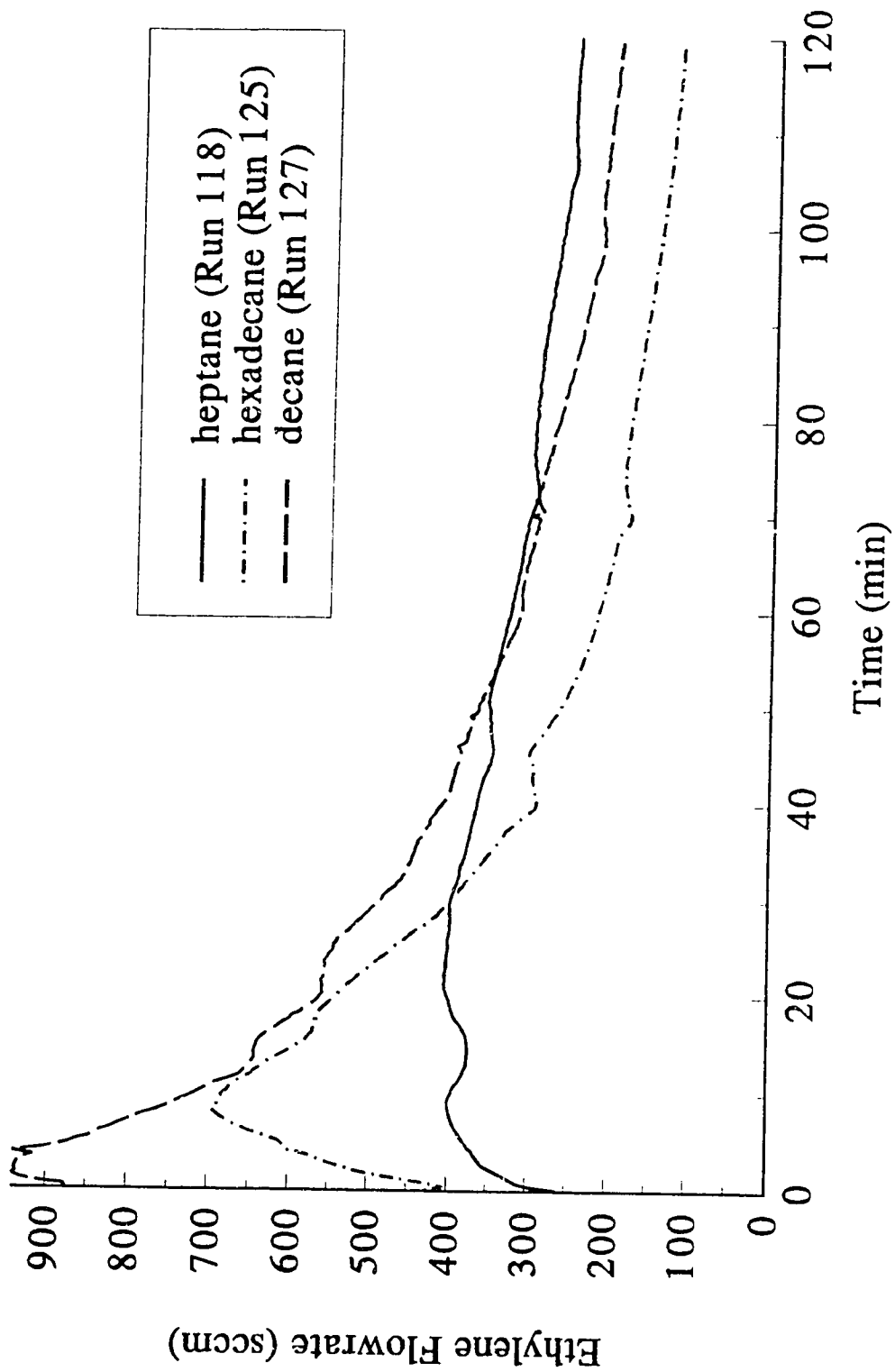


Figure 4.2 Effect of catalyst suspending medium on the activity profile (flowrate normalized to 30 mg catalyst)

Numerous studies on Ziegler-Natta polymerization have been undertaken to model the reaction mechanism, kinetic behaviours, and molecular compositions; Figure 4.2 underscores the difficulty of inferring molecular information based on the apparent, macroscopic rate behaviour. In this particular instance, it would be highly unlikely for a model to predict that nearly identical molar mass distributions can be arrived at from vastly different kinetic profiles.

4.3 Choice of Seedbed

For most Ziegler-Natta catalysts, a seedbed is generally required for gas-phase polymerization. As the present investigation includes kinetic studies and product characterization, one overriding concern in choosing the proper seedbed was the ease of separating polymer from the solid mixture. Several types of seedbed (glass beads, sodium chloride crystals, and polyethylene powders) were tested between Runs 2 and 12. When no solid support was used (Run 2), a layer of polyethylene built up on the bottom of the vessel. The use of commercial polyethylene as a support was not an option. Separation of polyethylene from the Teflon seedbed used by Lynch and Wanke (1991) would be tedious for extracting large quantities needed for materials testing. Sodium chloride (approximately 500 μm in size) was ultimately chosen over other alternatives as polymer can be isolated from the product-support mixture by repeated rinsing in water. The thoroughness of NaCl removal can be checked by the dielectric strength of the solution.

As mentioned in Chapter 1, temperature control is a major concern for any gas-phase polymerization reactor. In the present semibatch reactor, heat released by the growing polymer particles is transferred to the constant temperature oil bath in part through the collisions between polymer particles and the reactor walls. The advantages of sodium chloride particles over glass beads, in the context of heat transfer, included the smaller particle sizes and the higher thermal conductivity (see Table 4.4). The smaller density difference between the growing polyethylene particles and NaCl crystals, crucial to the mixing of particles, was

Table 4.4: Thermophysical properties of selected seedbeds (Perry, 1984)

Seedbed	Density (g/cm ³)	Thermal Conductivity (W/m-K)
polyethylene	0.91-0.97	0.38
Teflon	2.2	0.26
salt	2.2	7.1
glass	2.8	0.81

yet another factor in favour of the sodium chloride crystals over glass beads as the support.

5. PROPAGATION KINETICS

The kinetic profile of the copolymerization reaction on a supported Ziegler-Natta catalyst is characterized by a period of rapid increase in activity followed by a period of rapid decay. This initial surge in activity is commonly referred to as the "comonomer effect." The cause of the comonomer effect is not entirely understood, as stated in Section 2.1.1. In this chapter, results of the study of the effects of operating conditions on this kinetic behaviour will be presented and discussed. A brief description of all the experimental runs is provided in the Appendix.

5.1 Effects of Hydrogen and Temperature on Copolymerization Rates

Figure 5.1 shows the ethylene consumption rate (Q_E) versus time (under constant amount of 1-butene precharge) at several different hydrogen pressures (0-200 psi). It was observed that Q_E always reached a maximum within the first ten minutes and decayed rapidly afterwards. Accompanying this rate maximum was the observed 5–10°C temperature excursion above the temperature set point (70°C) for a period of about 30 minutes (Figure 5.2). This rate enhancement was most pronounced in the absence of hydrogen and became less significant at higher hydrogen pressures.

Published studies on copolymerization studies have seldom addressed the thermal characteristic just described, for the results discussed in the open literature were mostly produced in slurry systems. In the gas-phase reactor, the collision between the polymer particles and the reactor interior provides a significant contribution to the overall heat transfer to the constant temperature oil bath. While both the conduction through the wall and the convection with the temperature bath remain unchanged, the efficacy of heat removal in the gas-phase

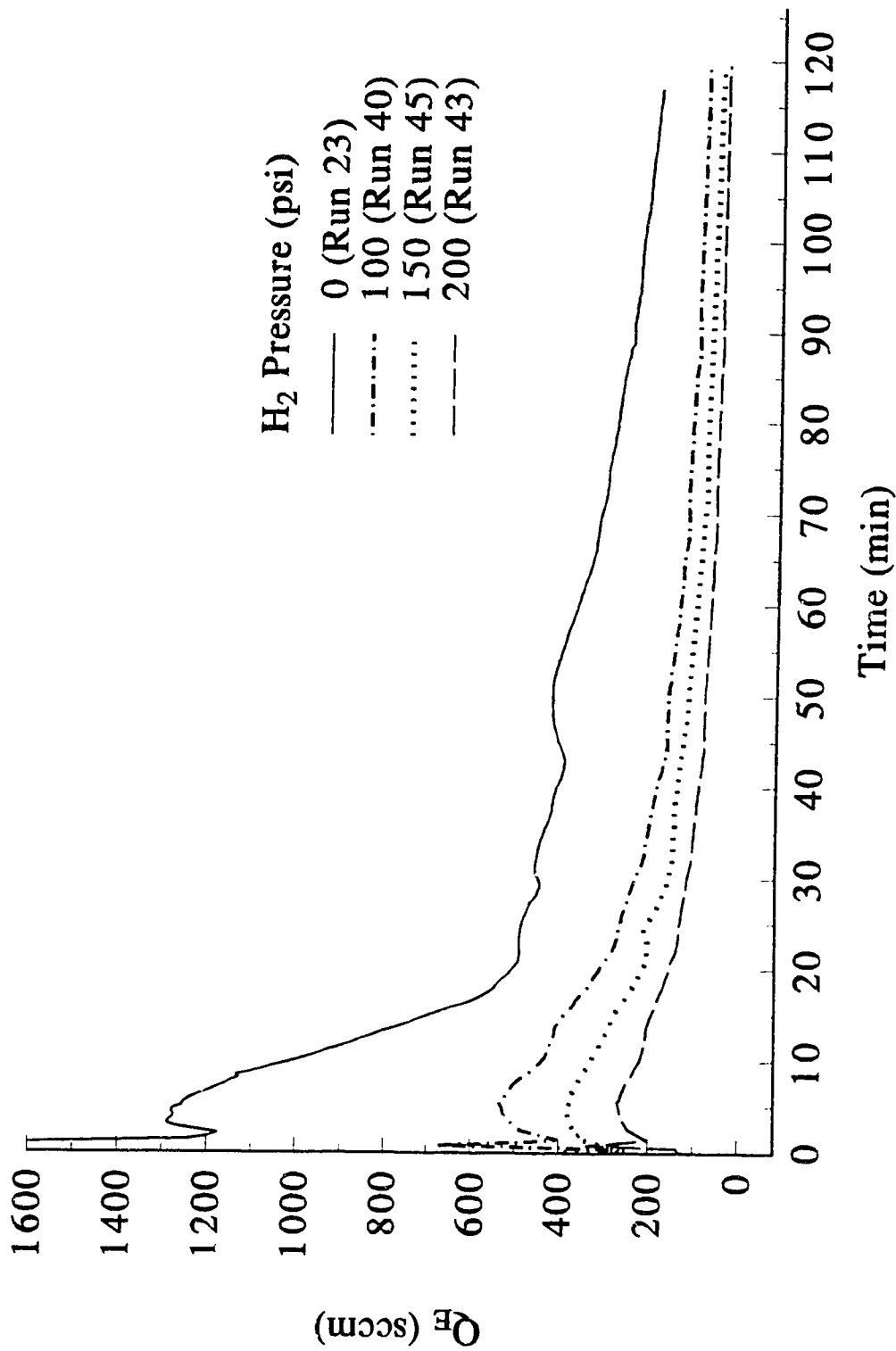


Figure 5.1 Effect of hydrogen pressure on the instantaneous ethylene consumption rate in ethylene/1-butene copolymerization: reaction at 70°C with 30 mg catalyst, 10 ml of liquid 1-butene precharge, 160 psi of ethylene, and 1.0 ml TNHIAL.

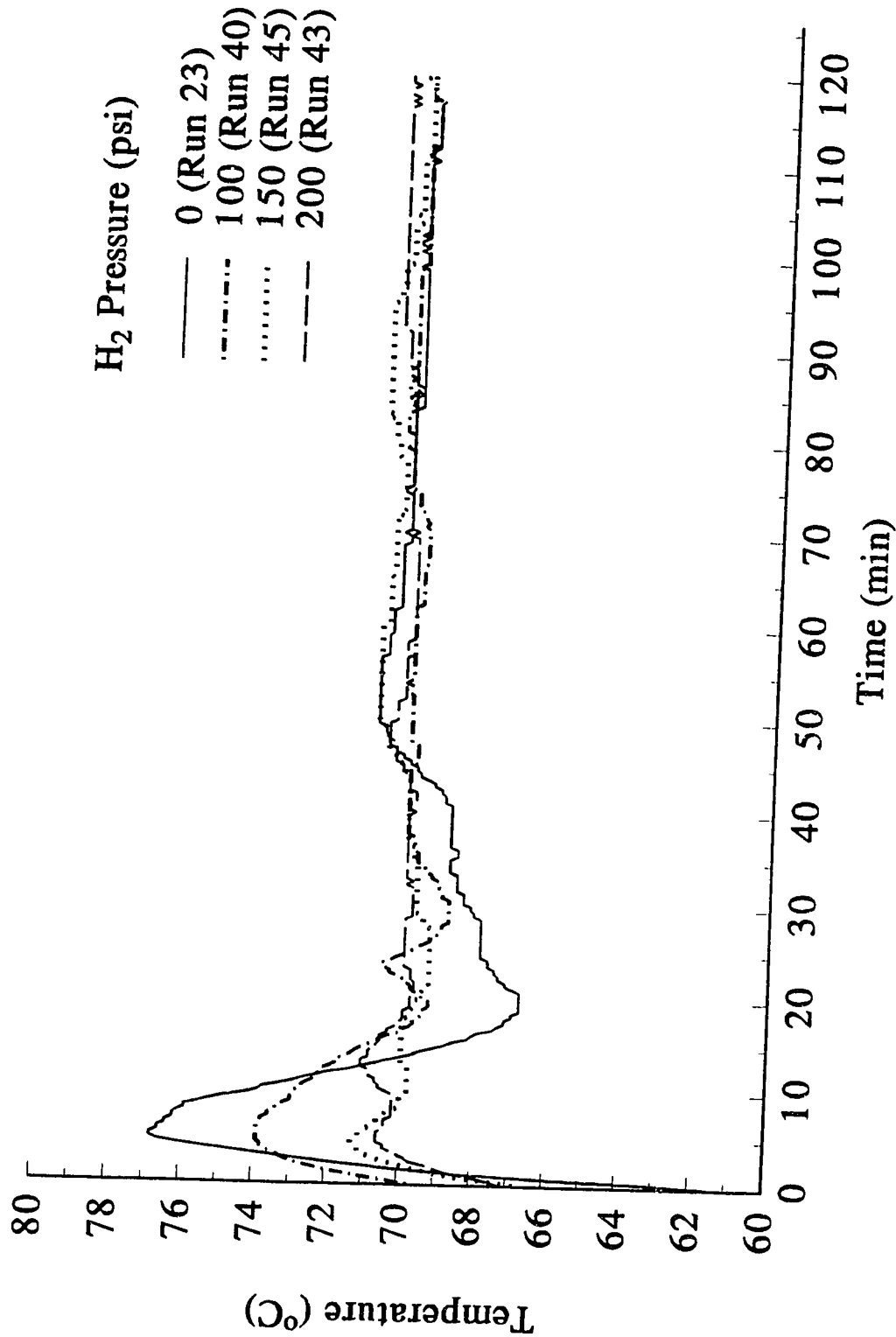


Figure 5.2 Effect of hydrogen pressure on the reaction temperature

reaction is substantially inferior to that in the slurry reaction. This thermal instability problem, compounded with the complications described in Chapter 4, makes rigorous discussion of catalyst activity inappropriate.

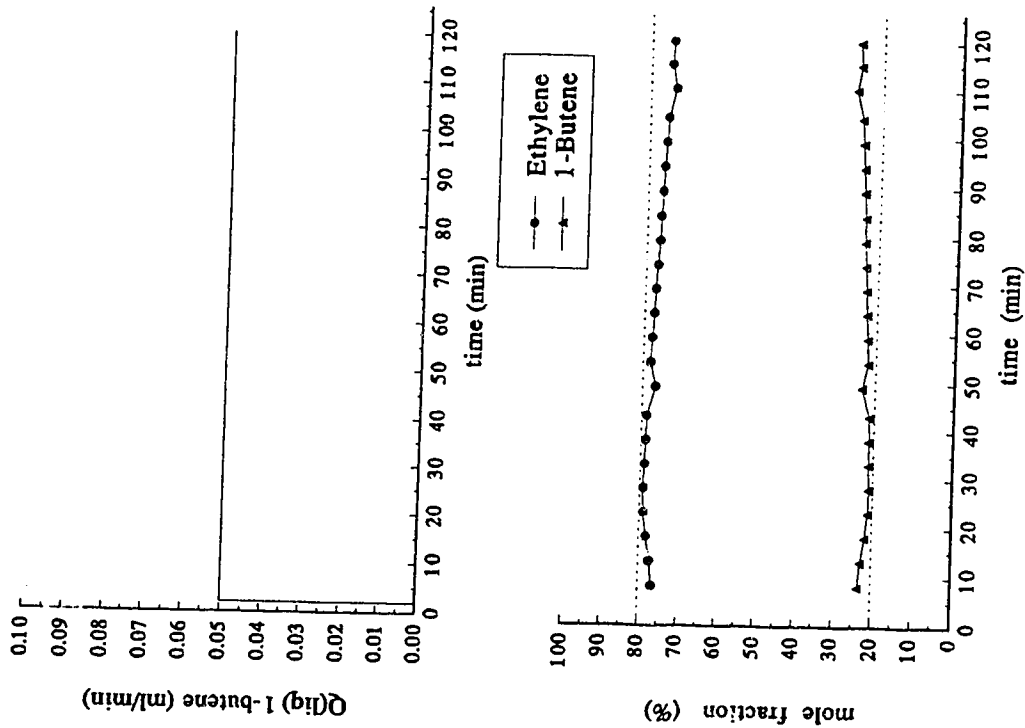
Nevertheless, some general observations can still be made about the kinetic behaviour as the temperature returned to the steady state value. According to the GC analysis, the gas-phase composition varied very little with time after the initial transient period. If the amount of gas-phase 1-butene sampled to the gas chromatograph was replenished accordingly by a constant feed of liquid 1-butene (usually at a rate of 0.05 ml/min), the composition of the mixture, regardless of the hydrogen pressure, was remarkably stable, as shown in Figure 5.3. The steadiness of gas-phase composition was also observed in experiments carried out at 50°C. As illustrated in Figure 5.4, the 1-butene fraction after the first 30-minute period was constant and independent of the initial 1-butene feed patterns which were used to maintain a flat profile. Such observation of limited 1-butene consumption following the initial 30-minute period indicates that 1-butene incorporation was essentially zero after the first few minutes of the reaction.

5.2 Effect of Ti Oxidation States on Copolymerization

With 1-butene consumption following the initial period of polymerization (~30 minutes) being limited at best, a copolymerization mechanism which would adequately describe the phenomenon should have a sensitive time dependence. A number of studies have been conducted to better understand the comonomer effect in slurry-phase operation (Tait et al., 1988; Chien et al., 1993). These studies focused only on the initial rise to $R_{p,max}$; little has been reported regarding the ensuing decay of activity.

Karol et al. (1993) suggested that the rapid decay of catalytic activity was possibly caused by variations in the oxidation state of titanium. Similar contemplations on the oxidation state in the context of ethylene/ α -olefin copolymerization were reported by Soga et al. (1981; 1982) who proposed that

20 psi H₂



100 psi H₂

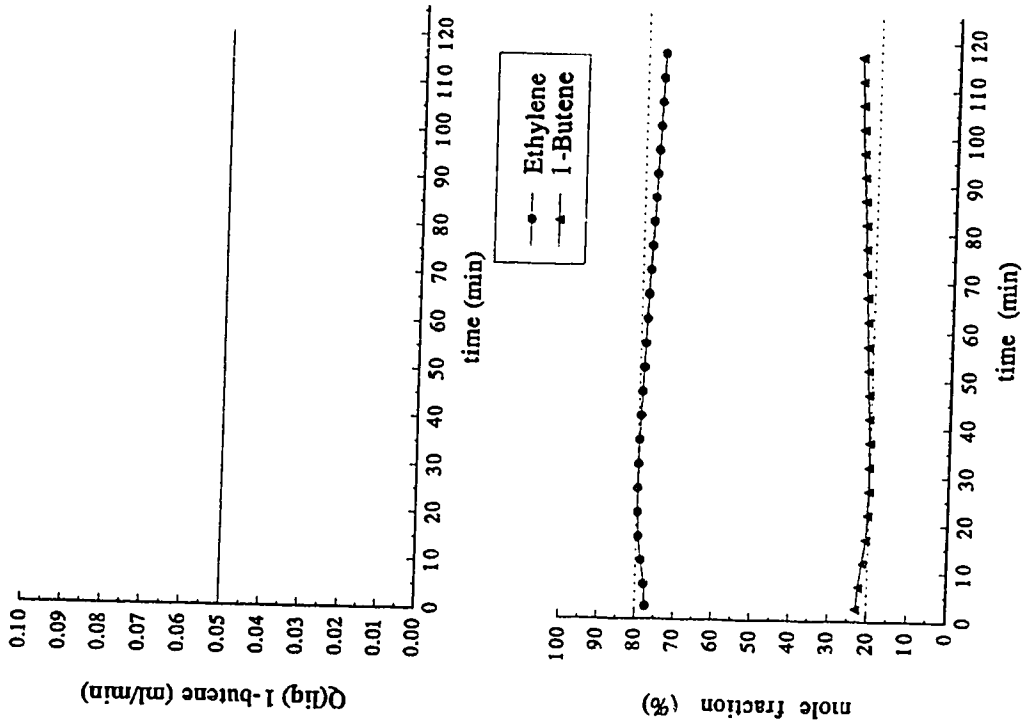


Figure 5.3 Mole fraction of ethylene and 1-butene versus time at different hydrogen pressures

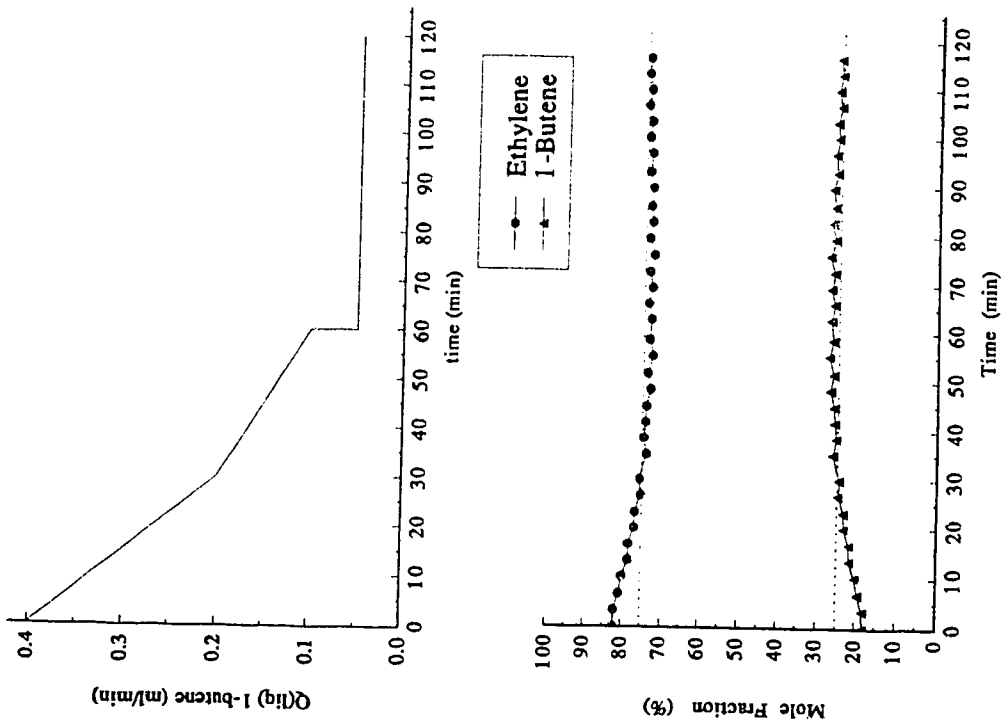
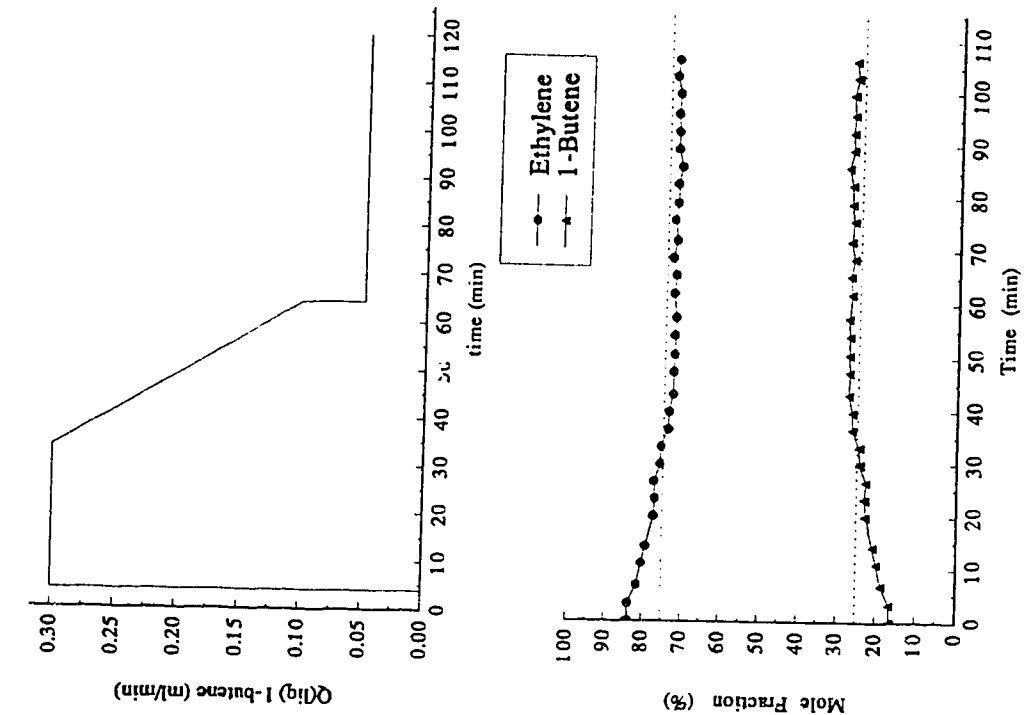


Figure 5.4 Mole fraction of ethylene and 1-butene versus time under different 1-butene feed patterns

copolymerization of ethylene with α -olefins occurred on the Ti^{+3} sites whereas homopolymerization of ethylene occurred on Ti^{+2} .

A combination of these two postulates leads to the hypothesis that surface Ti^{+4} initially reduced by cocatalyst to Ti^{+3} copolymerized ethylene and 1-butene, and the Ti^{+3} further reduced by TNHAL to Ti^{+2} was active only for ethylene homopolymerization. This hypothesis would allow a strong dependence on time, as the process of oxidation state reduction by cocatalyst was continuous, especially when TNHAL was used in great excess. As the population of Ti^{+3} gradually evolved into Ti^{+2} , the frequency of 1-butene insertion into growing chains declined. In fact, Soga and Yanagihara (1988) have demonstrated that when a very weak cocatalyst was used to reduce the catalyst in a copolymerization reaction, no ethylene homopolymer would form.

5.3 Fractional Conversion of 1-Butene to *n*-Butane

Traces of *n*-butane were detected in the GC spectra for reactions involving 1-butene and hydrogen. The intensity of the *n*-butane peak increased with increasing hydrogen pressure but was almost negligible for $P_{H_2} \leq 20$ psi. The ratio of *n*-butane/1-butene as a function of reaction time is shown in Figure 5.5. It is evident that the conversion of 1-butene reached a steady value after about 20-30 minutes for P_{H_2} under 100 psi and somewhat longer for higher P_{H_2} .

A prominent feature in the plot of *n*-butane/1-butene ratio versus time was the sizable gap in the steady-state values between 100 psi and 150 psi of hydrogen. If hydrogenation that took place on the surface of the stainless steel reactor walls was the major route to *n*-butane production, the increase in the steady-state value would be expected to be more gradual than abrupt. It seemed more likely that the conversion of 1-butene occurred mainly on the surface of the catalyst, noting that the amount of catalyst for Runs 43 and 45 was twice as much as for Runs 27 and 40.

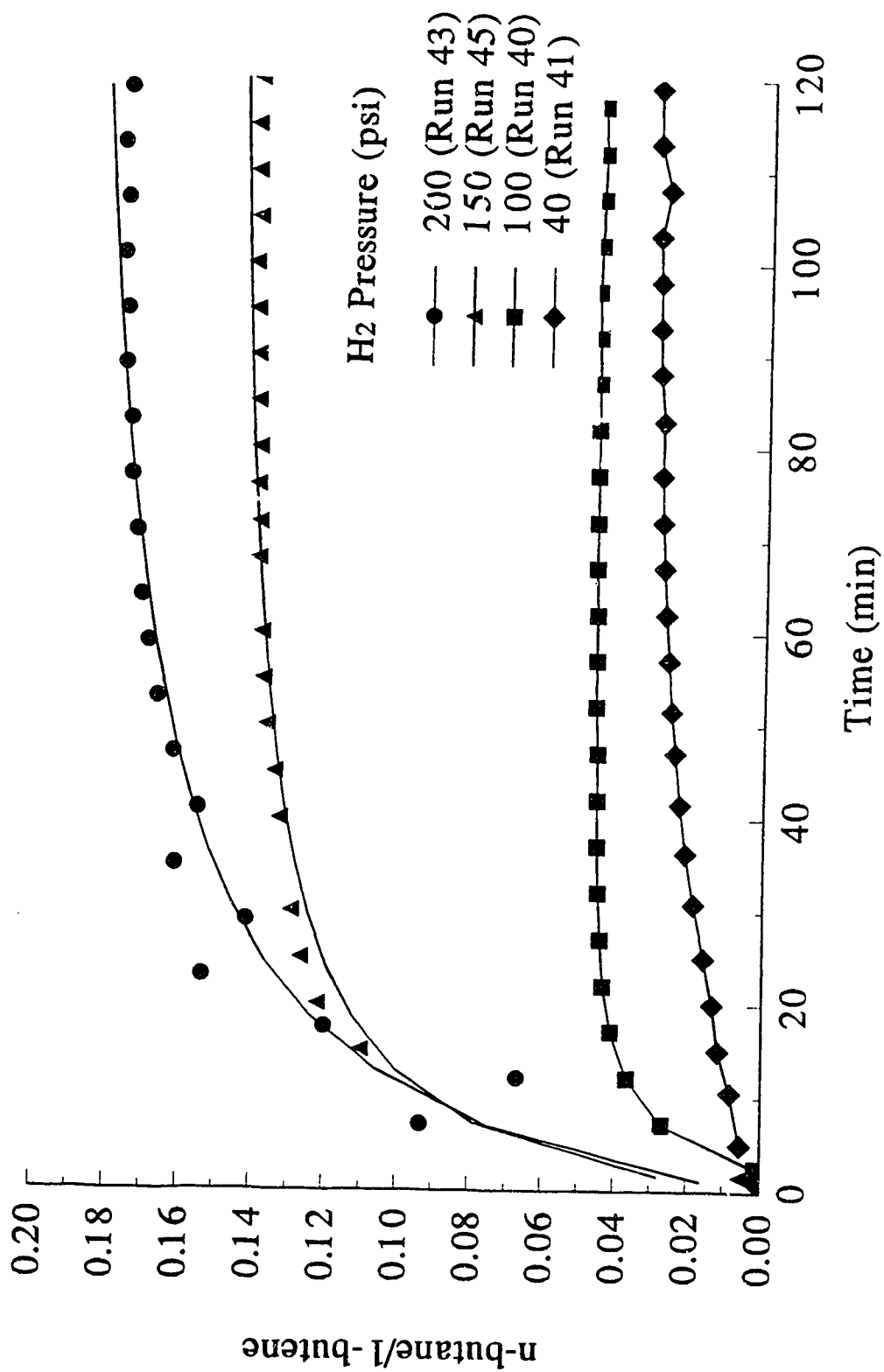


Figure 5.5 Fractional conversion of 1-butene to *n*-butane as a function of reaction time

The time required for the partial conversion of 1-butene to *n*-butane to stabilize coincided remarkably well with the apparent period of 1-butene incorporation discussed in Sections 5.1 and 5.2. It appeared that while 1-butene was being copolymerized with ethylene on Ti^{+3} , *n*-butane was formed, quite possibly on the same type of active titanium site. The build-up of *n*-butane within the reactor was rapid at first and then became gradual. The ensuing period of steady *n*-butane/1-butene ratio indicated that no further conversion of 1-butene into *n*-butane took place on Ti^{+2} . (On the other hand, it was also possible that Ti^{+2} was responsible for α hydrogenation and Ti^{+1} was unreactive to 1-butene.)

5.4 Effects of Comonomer Precharge on Copolymerization

Variation of comonomer incorporation with precharged amount of 1-butene was found to be dramatic. As shown in Figure 5.6, the amount of 1-butene precharge strongly influences the shape of the TREF profile. (The lower the temperature, the greater the branching frequency.) For a homopolymer without any side branches (Run 48), the profile was a single symmetric peak centred around 102°C. A 6°C downward shift was observed for the sample produced with 5 and 10 ml of 1-butene precharge (Runs 49 and 40), or approximately 20 and 40 psi of 1-butene partial pressure in the gas-phase reactor. For these samples a broad secondary peak between 50 and 90°C emerged, indicating the presence of highly branched molecules. Increasing the amount of 1-butene further led to a greater presence of the branched molecules that eluted over a lower temperature range relative to the linear molecules that eluted in the high temperature range.

Since branching frequency decreases with elution temperature, a semi-quantitative comparison between different profiles can be made by integrating each curve with respect to temperature (Figure 5.7). With only 5 ml 1-butene precharge (Run 49), the fraction of branched polyethylene (defined here as the fraction of polymer soluble in *o*-dichlorobenzene below 90°C) was about 34%. As

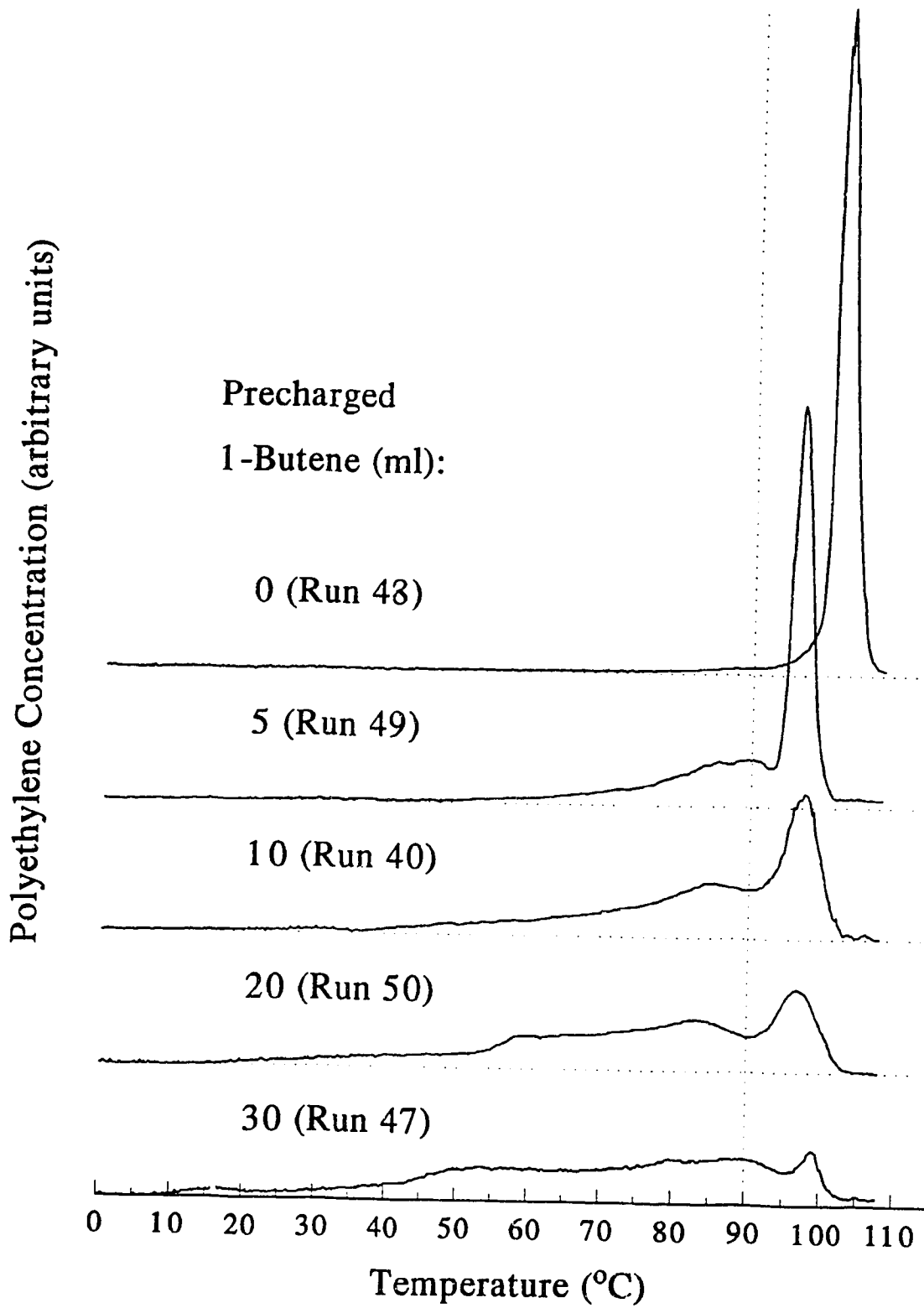


Figure 5.6 TREF profiles of LLDPEs produced at various 1-butene precharges

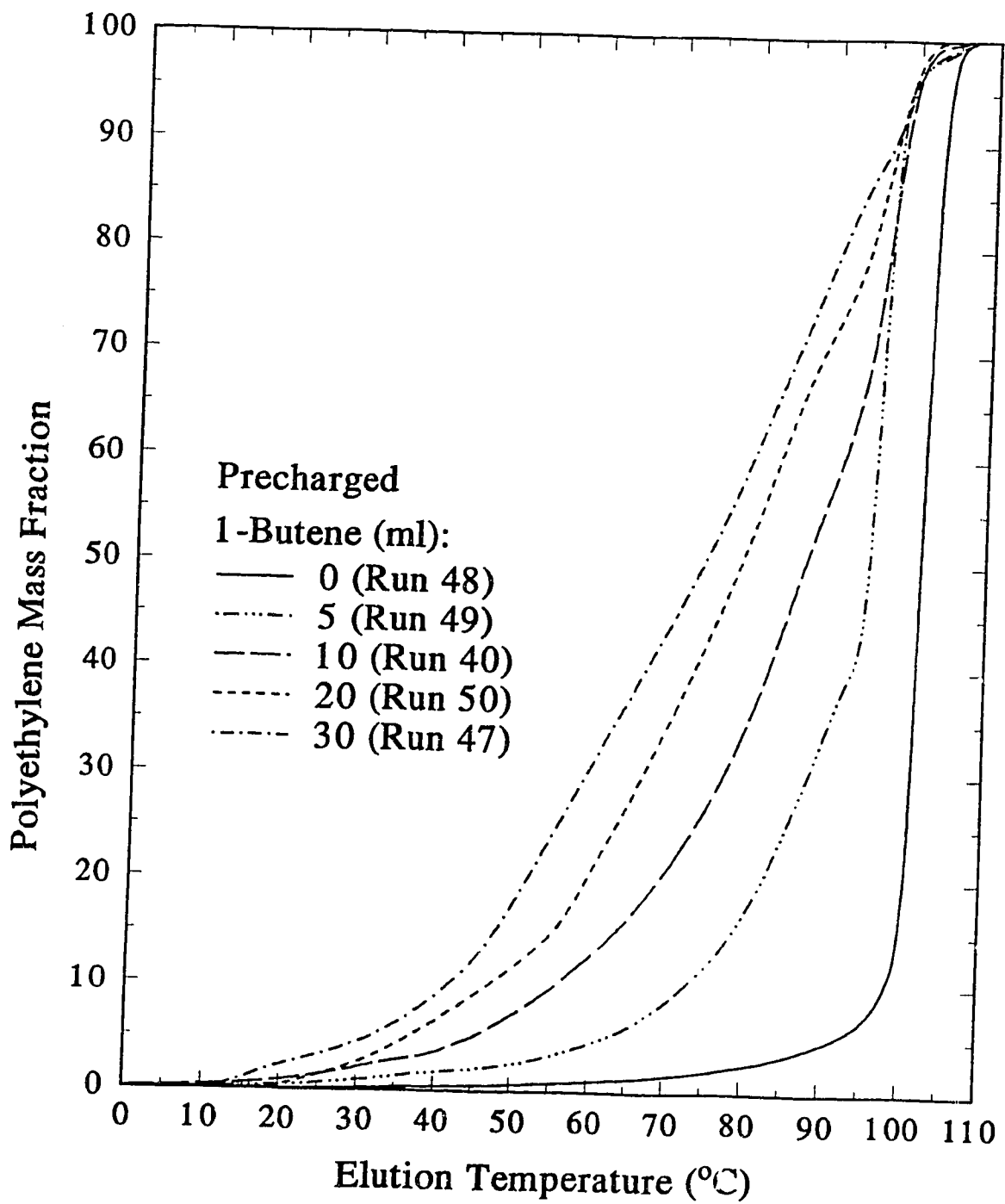


Figure 5.7 Integrated TREF profiles of LLDPEs

the amount of precharge was doubled to 10 ml (Run 40), 57% of the sample was eluted below the same cut-off temperature. The fractions of polymer dissolved below 90°C for 20- and 30- ml precharge were 72% (Run 50) and 80% (Run 47), respectively.

The aforementioned results were based on experiments with varying amounts of liquid 1-butene precharged to the reactor. In Run 59 (200 psi ethylene, 100 psi hydrogen, 1.0 ml TNHAL), however, 1-butene was only fed at a rate of 0.1 ml of liquid per minute. The presence of 1-butene enhanced the activity, since over twice as much polymer was produced in Run 59 as in Run 71, an ethylene homopolymerization run which had the same operating condition as Run 59. Therefore, the amount of comonomer needed to enhance the activity was small. It was however observed that without a substantial amount of initial 1-butene, only a limited amount of 1-butene was incorporated. This is shown in Figure 5.8, where the TREF profiles for Runs 59 and 71 were plotted. For the homopolymer (Run 71), the elution profile was a symmetric peak centred around 100°C. The shape became slightly skewed for the copolymer (Run 59). Although the lower overall elution temperature for Run 59 identified the sample to be a copolymer, the conspicuous absence of a sizable secondary peak suggested that highly branched molecules which would otherwise elute from the column at around 50-90°C were not produced.

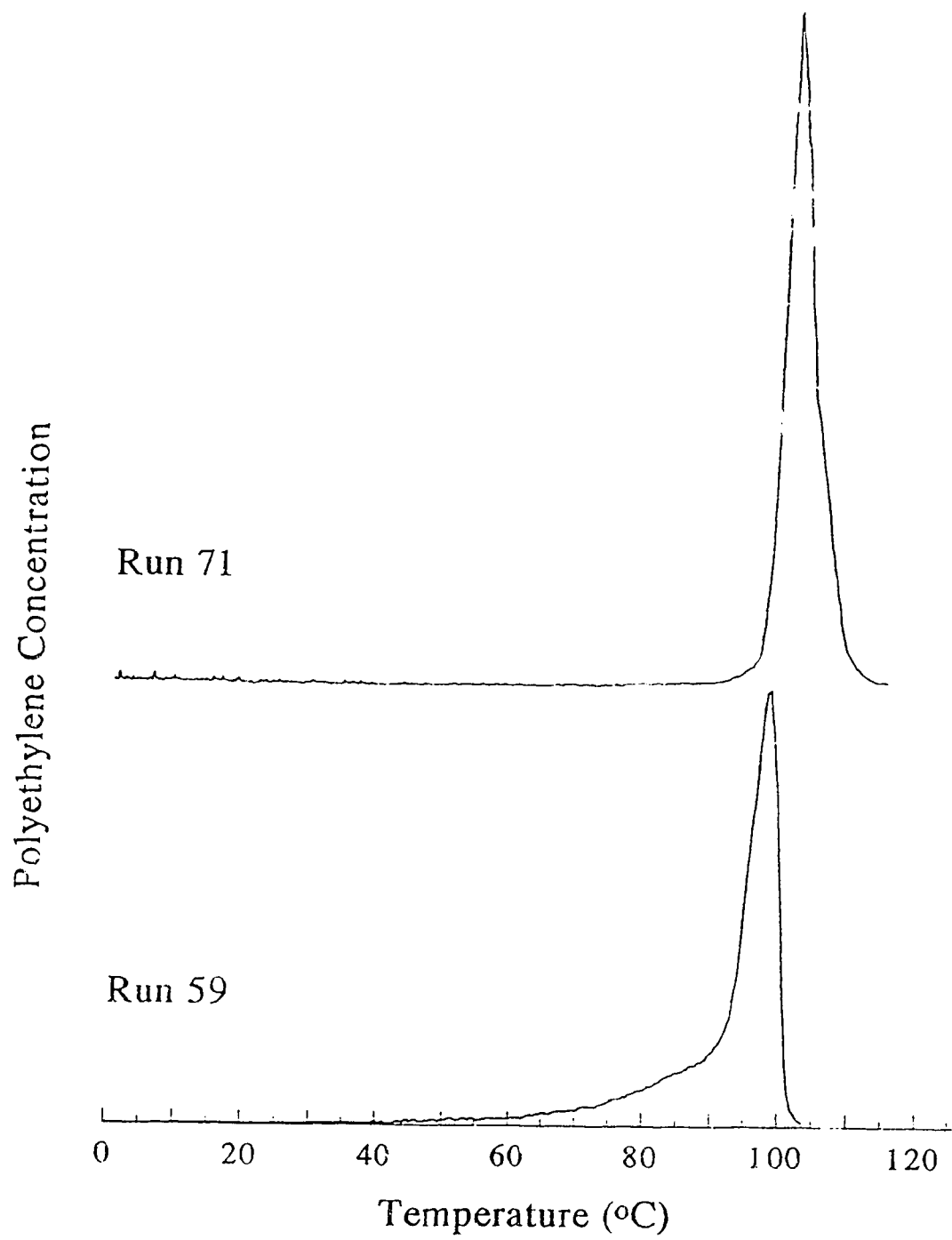


Figure 5.8 TREF profiles of HDPE and LLDPE without 1-butene precharge

6. CHARACTERIZATION OF POLYETHYLENE

Part 1: Molar Mass Distribution, Molar Mass, and Melt Index

Several analytical techniques were employed to characterize the samples produced in this study. In addition to temperature rising elution fractionation, which was used in the previous chapter to illustrate the pattern of comonomer incorporation as affected by the amount of 1-butene precharge, gel permeation chromatography and differential scanning calorimetry were used to study the effects of reactor operating parameters on the molar mass distribution and the crystal structure, respectively, of the polyethylene samples. In this chapter, discussions on the manifestations of molar size distribution, including number-average molar mass (M_n), weight-average molar mass (M_w), polydispersity (Q), and melt index (MI) are presented. The discussion of thermal characterization of the polymer samples via DSC is deferred until the subsequent chapters.

6.1 MOLAR MASS DISTRIBUTION

The effects of hydrogen and 1-butene on the molar mass distribution are shown in Figures 6.1 and 6.2. It was clear from these figures that both hydrogen and 1-butene can serve as chain transfer agents, as increasing the amount of hydrogen or 1-butene shifted the MMDs downwards. In Figure 6.1, the shape of the distribution does not vary significantly except in the transition from zero hydrogen to 40 psi hydrogen. The peculiar shape of the MMD for zero hydrogen was due to complete exclusion of largest molecules from the pores of the packing materials in the GPC columns and should not be considered as a credible representation of the actual distribution of the molar mass especially at $M > 10^6$. In the presence of hydrogen the MMD appeared to be closer to the shape of a single log-normal distribution; however closer examination indicated that the

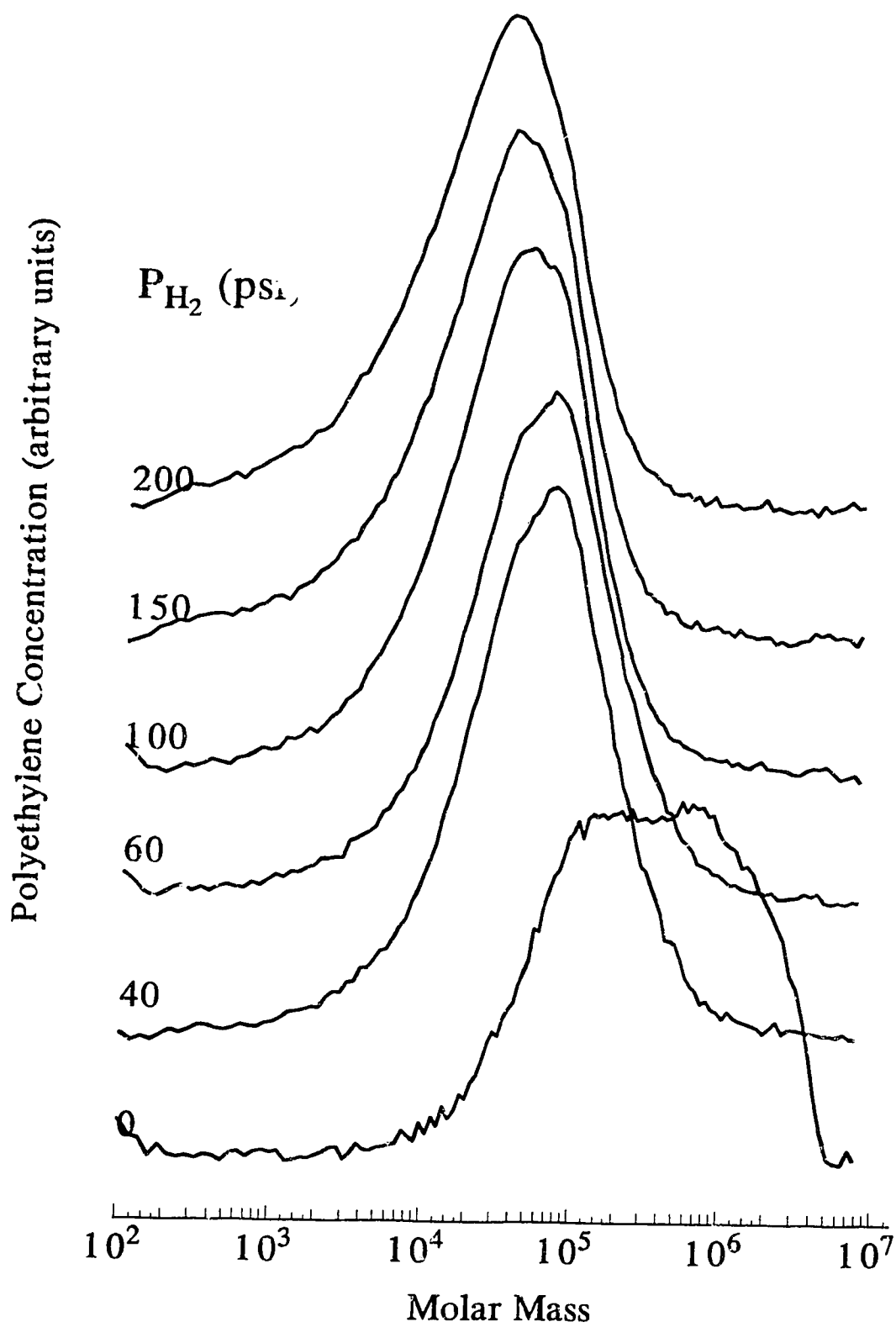


Figure 6.1 Effect of hydrogen on molar mass distribution

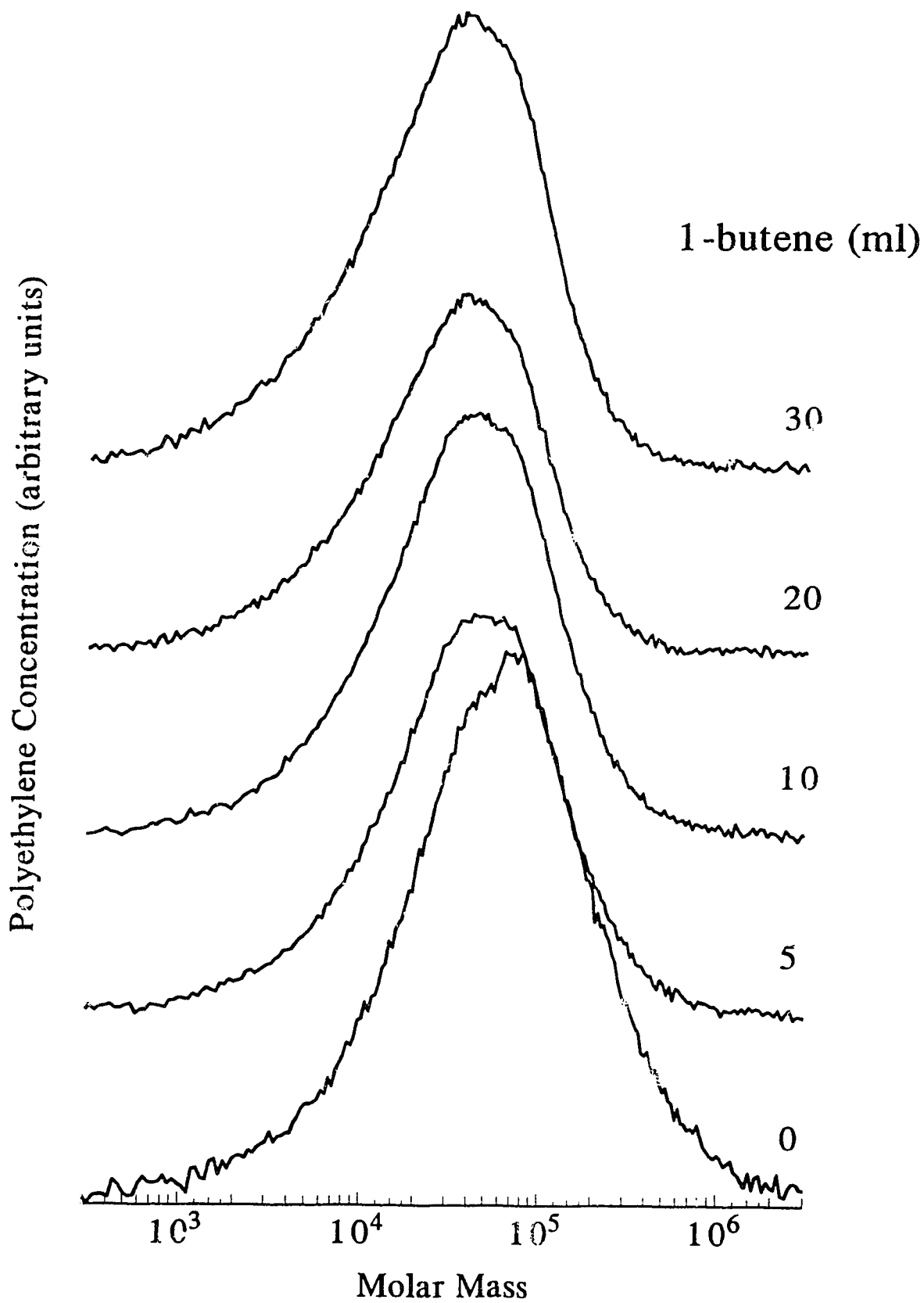


Figure 6.2 Effect of 1-butene on molar mass distribution

MMDs were made up of at least two MMDs, as "shoulders" near the apexes were readily recognizable on the individual distributions. One of these distributions appeared to be relatively insensitive to hydrogen pressure with a maximum at 5×10^4 , while the maximum for the other distribution decreased from about 8 to 2×10^4 when the hydrogen pressure was increased from 40 to 200 psi. These observations suggested that hydrogen was a more effective chain transfer agent for one type of site than for the other. A similar phenomenon was also observed in Figure 6.2 for the 1-butene series, as increasing the amount of 1-butene shifted the shoulder of the MMD from the left to the right side of the distribution.

Molar mass distributions shown in Figures 6.1 and 6.2 were rather broad, with Q being 4 or higher. The unusual broadness of MMD characteristic of polyolefins produced over Ziegler-Natta catalyst has been of considerable academic interest and among the major theories reviewed by Keii (1990), the multiplicity of active sites theory appeared to be most credible. The shape of MMD, according to the theory, is the result of various active sites producing separate molar mass distribution. However, the possibility that different types of active site would respond differently to hydrogen as the chain-transfer agent has never been addressed directly before.

As a result of the molar mass distribution shifting downwards with respect to increased hydrogen or 1-butene, both the number-average and weight-average molar masses dropped accordingly (see Figures 6.3 and 6.4)¹. In terms of number-average molar mass, the value decreased by about a factor of ten from 10 to 200 psi hydrogen. (M_n for zero hydrogen should be deemed unreliable as previously described in this section.) Changing the amount of comonomer precharged into the reactor dropped the M_n from 2.6×10^4 to 1.1×10^4 between 0 and 30 ml of 1-butene. The variation in M_w as a result of hydrogen or of 1-butene was also monotonic.

It was noted that, between 10 and 100 psi of hydrogen, polydispersity Q was relatively constant (see Figure 6.5). The deviation of Q at pressure above 100

¹Data are provided in Tables 6.1 and 6.2.

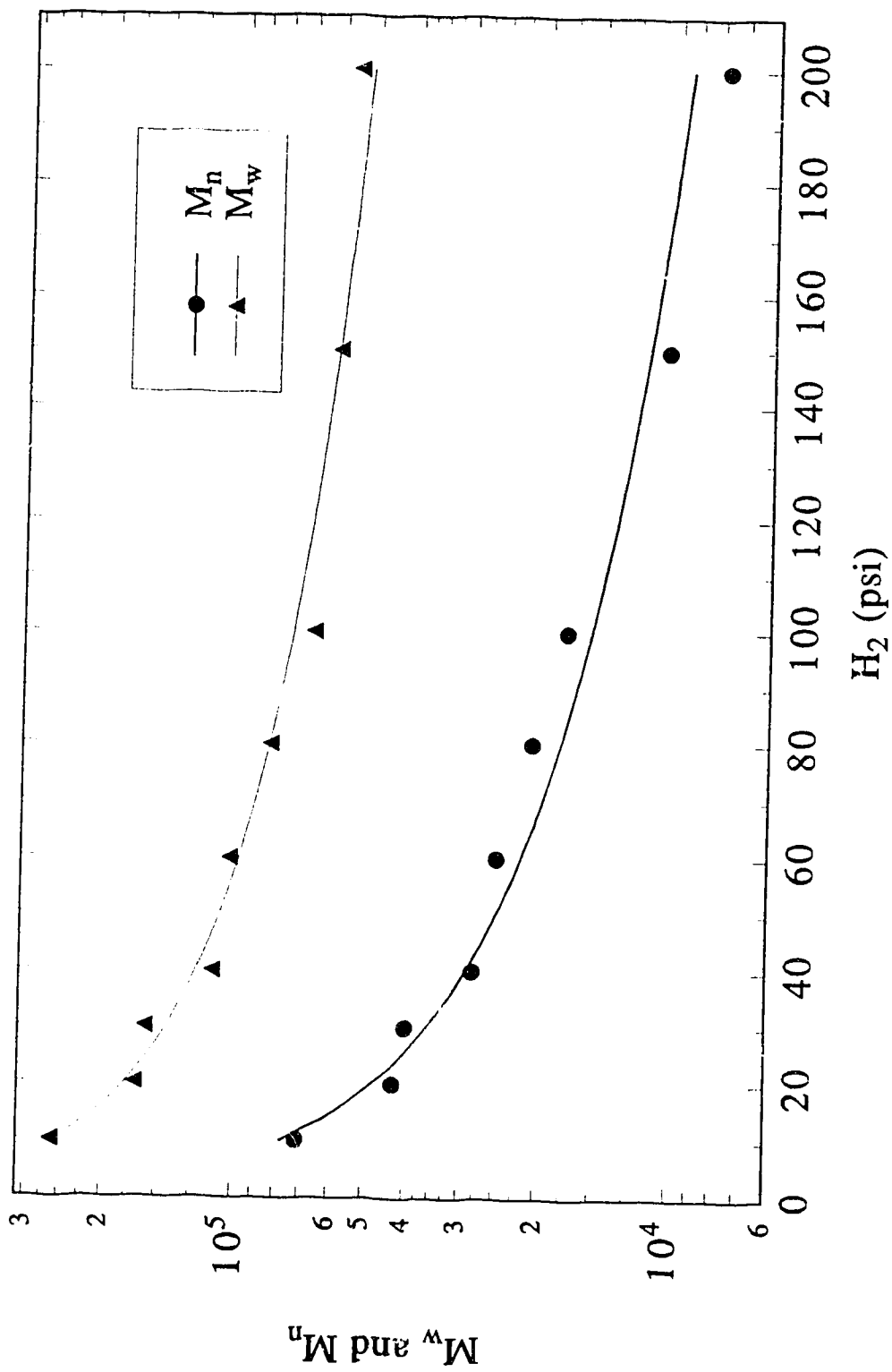


Figure 6.3 Effect of hydrogen on M_n and M_w

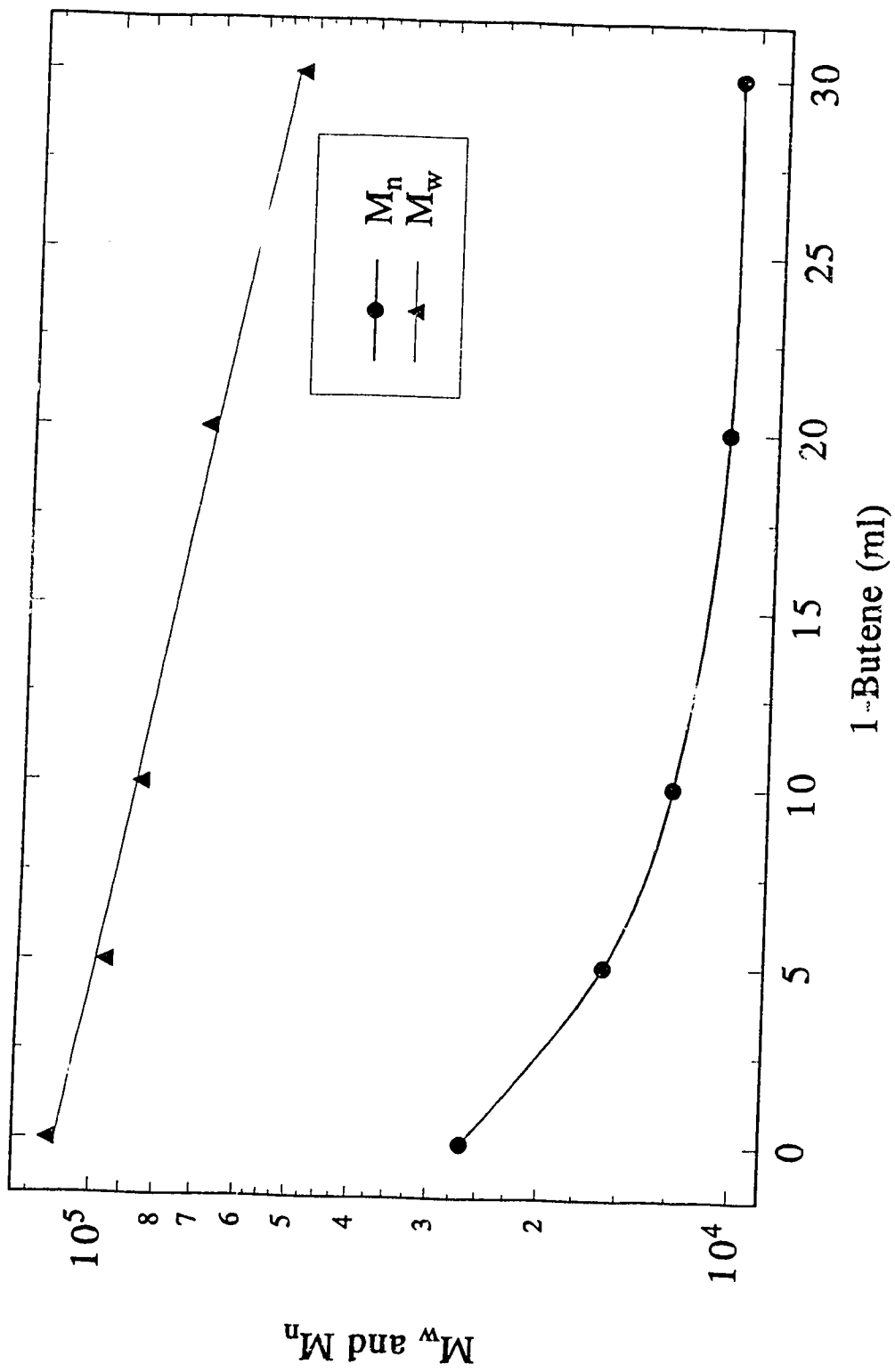


Figure 6.4 Effect of 1-butene on M_n and M_w

Table 6.1 Effect of hydrogen on M_n , M_w , and melt index of linear low density polyethylene. Reaction conditions: ethylene=160 psi; 1-butene=10 ml (40 psi); cocatalyst=1.0 ml TNHAL; temperature=70°C.

Run	Hydrogen Pressure, psi	$M_n \times 10^{-3}$	$M_w \times 10^{-3}$	Melt Index (190/2.16)
23	0	106.0	612.0	0.005 (est.)
34	10	70.8	259.8	0.08 (est.)
30	20	42.5	167.7	0.345
31	30	39.9	159.4	0.406
27	40	28.1	112.1	1.30
38	60	24.9	103.1	1.80
39	80	20.8	83.8	2.52
40	100	17.4	67.1	6.02
45	150	10.4	60.0	9.26
43	200	7.8	55.7	16.2

Table 6.2 Effect of precharged 1-butene on M_n , M_w , and melt index of linear low density polyethylene. Reaction conditions: hydrogen=100 psi; cocatalyst=1.0ml TNHAL; temperature=70°C; ethylene+1-butene=200 psi.

Run	1-Butene Precharged, ml	$M_n \times 10^{-3}$	$M_w \times 10^{-3}$	Melt Index (190/2.16)
48	0	26.5	116.6	0.74
49	5	16.0	96.8	3.02
40	10	13.1	86.9	4.87
50	20	10.7	71.0	10.3
47	30	10.6	52.6	18.1

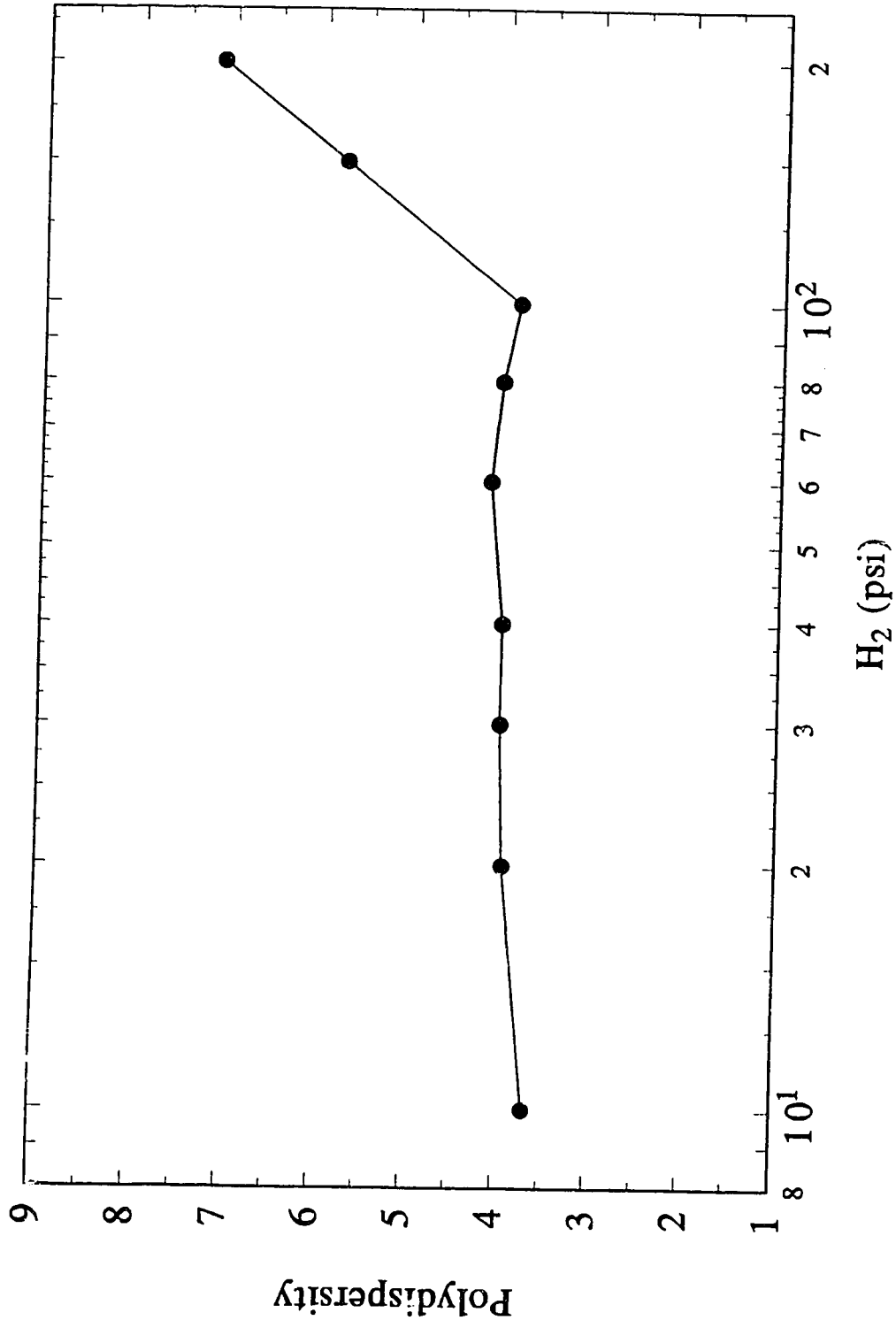


Figure 6.5 Effect of hydrogen on polydispersity

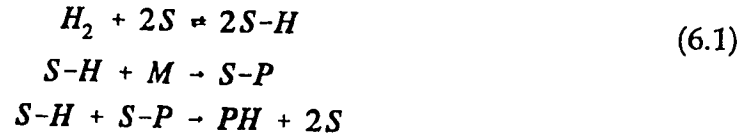
psi probably can be regarded as an experimental anomaly, for the respective MMDs (see Figure 6.1) both encompassed a significant portion of small molecules, and according to ASTM D5296, GPC measurements are invalid for $M < 2000$.) On the other hand, based on the argument presented earlier in this section, one may support the increase in polydispersity at higher P_{H_2} as one of the two recognizable distributions was more susceptible to hydrogen than the other. According to the latter argument, the invariance of polydispersity between 10 and 100 psi was due to the overlay of the two separate distributions. This argument is difficult to refute due to the scarcity of available data above 100 psi and the absence of credible data below 10 psi. Theories on the effect of hydrogen on polydispersity reviewed by Keii (1991) do not settle the dispute, for the possibility that one type of active site responds differently to hydrogen than the other, as stated earlier, has never been considered.

While both hydrogen and 1-butene can limit the molar mass, hydrogen remains the preferred chain transfer agent as it does not introduce an additional structural variable (i.e. branching frequency) into the polymer molecules. Since hydrogen does not propagate a growing chain, the termination rate order can be determined (Section 6.2) and the knowledge of the rate order can be used for mechanistic investigation of the surface reaction.

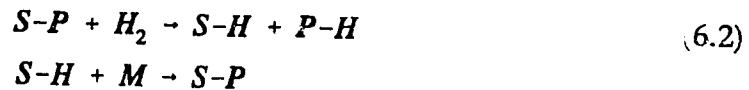
6.2 HYDROGEN TERMINATION RATE ORDER

Whether hydrogen terminates a growing chain via a first- or half-order mechanism has not been determined conclusively from slurry-phase experiments (Keii, 1987), let alone from gas-phase experiments. It has been suggested that, depending on the catalyst system, the termination rate order n can be either 0.5 or 1.0. Based on the argument presented in the previous section, it is even plausible that the termination rate order may be specific to the type of active site

on the surface. A plausible half-order dependence proposed by Keii (1987) can be summarized as



where hydrogen is dissociatively adsorbed (S-H) and the propagating polymer molecules are terminated by the surface interaction between an active polymerization centre (S-P) and an adjacent adsorbed hydrogen (S-H). On the other hand, a possible first-order mechanism would be (Keii, 1987)



where direct insertion of molecular hydrogen terminates the growing polymer chain.

In studying the effect of hydrogen on the molar mass of polyethylene, Marques et al. (1993b) plotted $1/M_v$ against P_{H_2} and $(P_{H_2})^{1/2}$ and decided the value of n based on the linearity of each fit. That is,

$$\begin{aligned}
 \frac{1}{M_v} &= a + b P_{H_2}^{1/2} \\
 \frac{1}{M_v} &= a + b P_{H_2}
 \end{aligned}
 \tag{6.3}$$

Since the average degree of polymerization \bar{x} is related to M_n (Stevens, 1990), not M_v , the use of purely empirical M_v was likely due to the availability of dilute solution viscometry measurements. As M_n was evaluated in the current study, the empiricism of M_v can be avoided.

The rationale for Eq. 6.3 is as follows. Since polymer chains are not terminated by coupling, the average degree of polymerization π and the number-average molar mass are related according to

$$\frac{M_n}{M_0} \approx \pi = \frac{R_p}{R_t} \quad (6.4)$$

where M_0 is the molar mass of the monomer, and R_p and R_t are the rate of propagation and of termination, respectively.

In the slurry reaction, growing polymer chains are terminated through transfer to hydrogen $R_{t,H}$, cocatalyst $R_{t,A}$, and through β -hydride elimination $R_{t,\beta}$ (Chien and Kuo, 1986). With all these individual contributions included, Eq. 6.4 becomes

$$\pi = \frac{R_p}{R_{t,\beta} + R_{t,A} + R_{t,H}} \quad (6.5)$$

Rearranging Eq. 6.5 and substituting $R_{t,H} = k_{t,H} (P_{H_2})^n$, the effect of hydrogen on M_n can be evaluated according to

$$\frac{M_0}{M_n} \approx \frac{1}{\pi} = \frac{R_{t,\beta} + R_{t,A}}{R_p} + \frac{R_{t,H}}{R_p} = a + bP_{H_2}^n \quad (6.6)$$

assuming that $R_p/k_{t,H}$ is not affected by P_{H_2} . Rather than ascribing a value to n , as in the case of Eq. 6.3, the use of Eq. 6.6 permits the evaluation of n . The result of non-linear regression of M_n versus P_{H_2} based on the data tabulated in Table 6.1 shows that n has a value of 0.62 (see Figure 6.6). (Only the data between 10 and 100 psi were plotted, as Al/Ti was halved for 150 and 200 psi.)

If $R_{t,H}$ is the predominant mode of chain termination in the gas-phase reaction, the constant term in Eq. 6.6 should be negligible. Dropping a from Eq. 6.6, a power-law equation emerges:

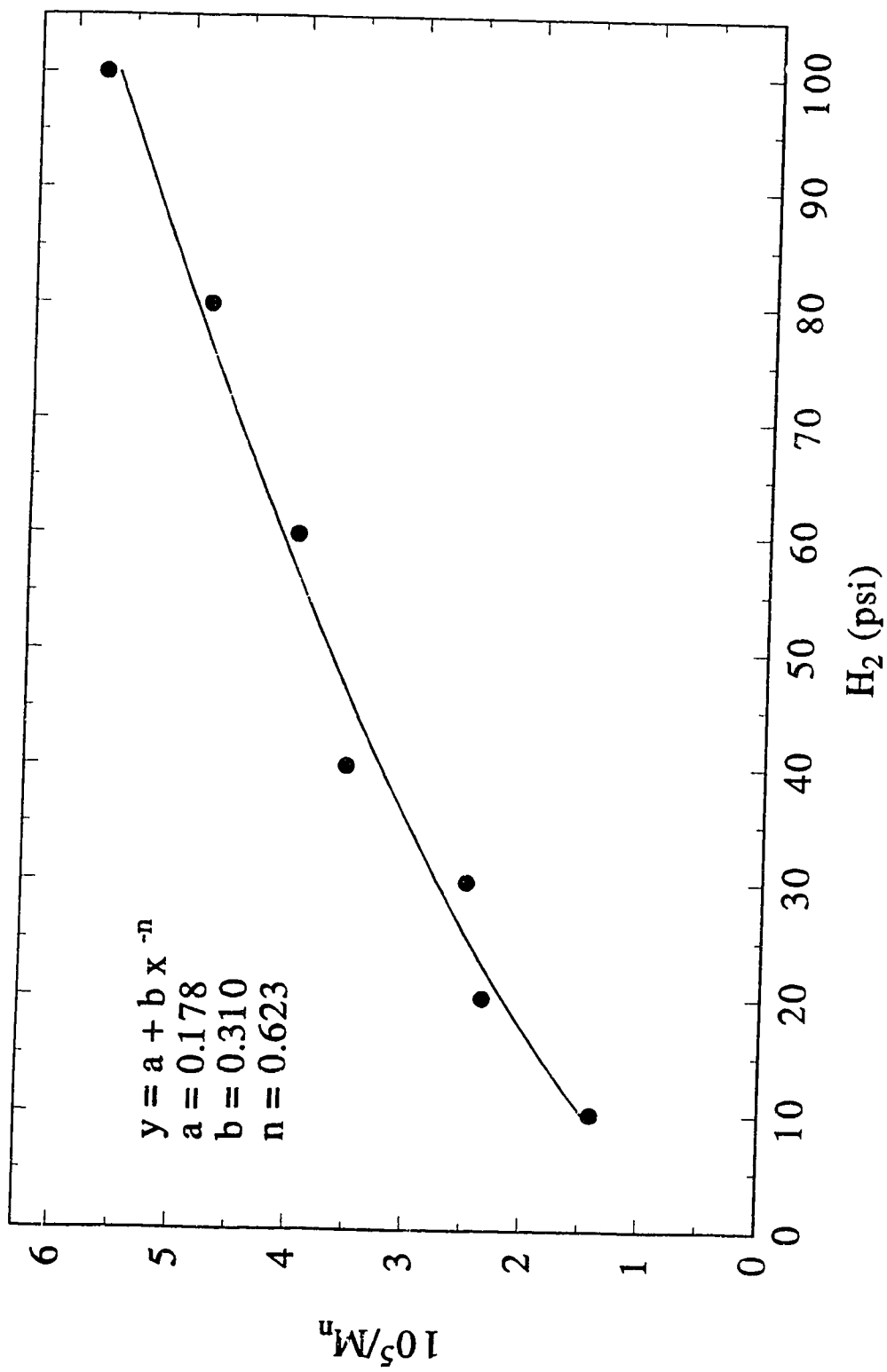


Figure 6.6 Effect of hydrogen on M_n

$$\frac{M_0}{M_n} \approx \frac{R_{t,H}}{R_p} = \frac{k_{t,H} P_{H_2}^{-n}}{R_p} = c P_{H_2}^n \quad (6.7)$$

The rate order as determined by directly curve-fitting M_n versus P_{H_2} in a log-log plot was 0.59, which was only slightly lower than 0.62 (see Figure 6.7). Such remarkable agreement between the two methods of determination indicated that $R_{t,H}$ was the overwhelming route to chain termination in gas-phase reaction. Incidentally, it was noted that for solution phase polymerization, the rate order was 0.58 (Jaber and Ray, 1993).

With n being neither half nor unity but 0.6, the possibility that hydrogen termination can occur via different mechanisms was considered. The simplest equation expressing the proposed termination mechanism would be

$$R_{t,H} = k'_{t,H} P_{H_2}^{0.5} + k''_{t,H} P_{H_2}^{1.0} \quad (6.8)$$

and the result of the curve-fitting is shown in Figure 6.8. Eq. 6.8 succinctly restates the hypothesis offered in the previous section: hydrogen is a more effective chain-transfer agent for one type of site (via first-order kinetics) and less effective for the other (via half-order kinetics). Using this hypothesis with the observation by Lacombe (1995) that the sites responsible for copolymerization were more hydrogen sensitive could lead to a possible pairing between atomic hydrogen termination (Eq. 6.1) with homopolymerization and molecular hydrogen termination (Eq. 6.2) with copolymerization. In the absence of further studies, this linkage between propagation and termination mechanisms is possible but not conclusive.

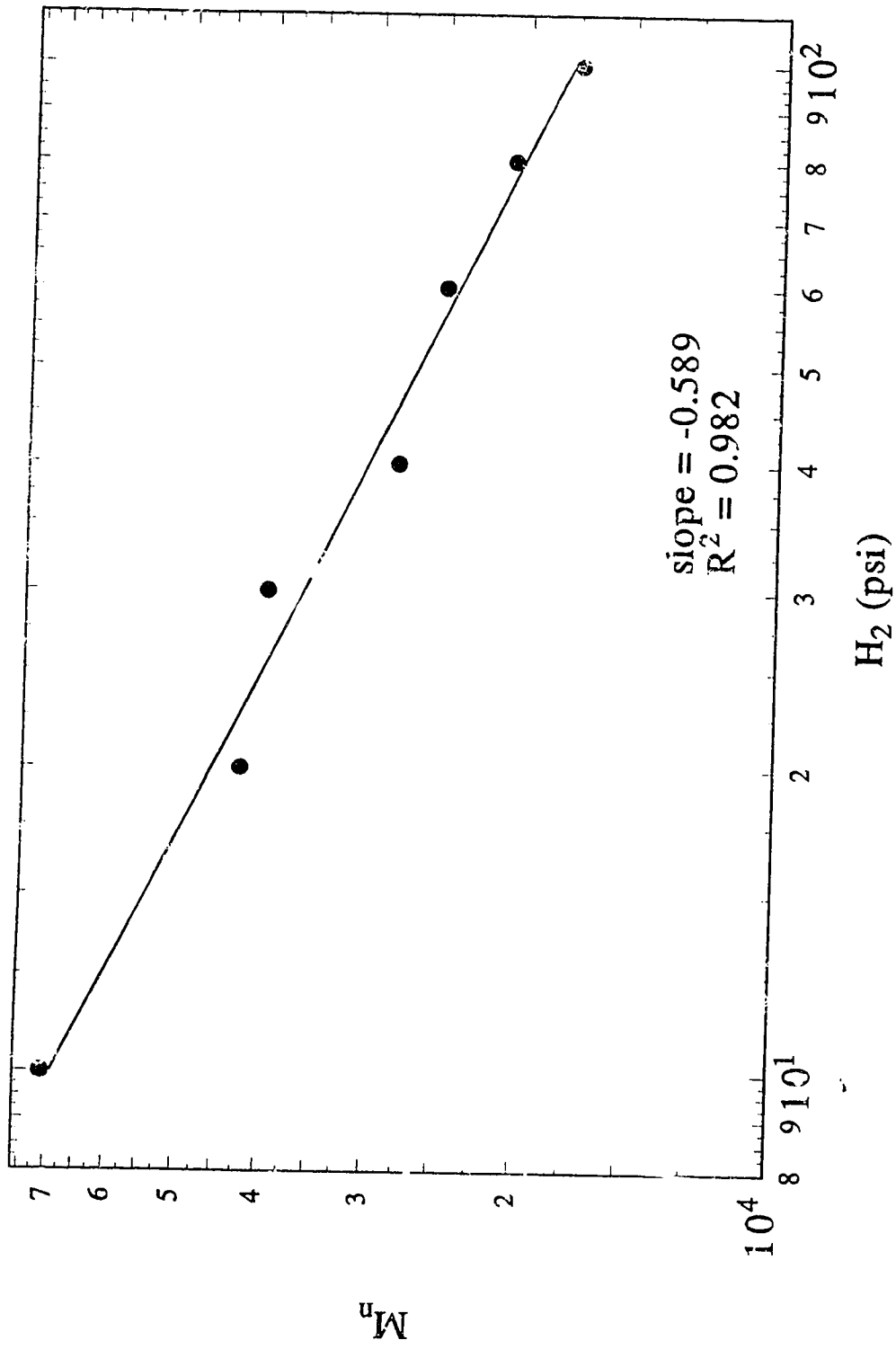


Figure 6.7 Fractional order dependence of M_n on hydrogen pressure

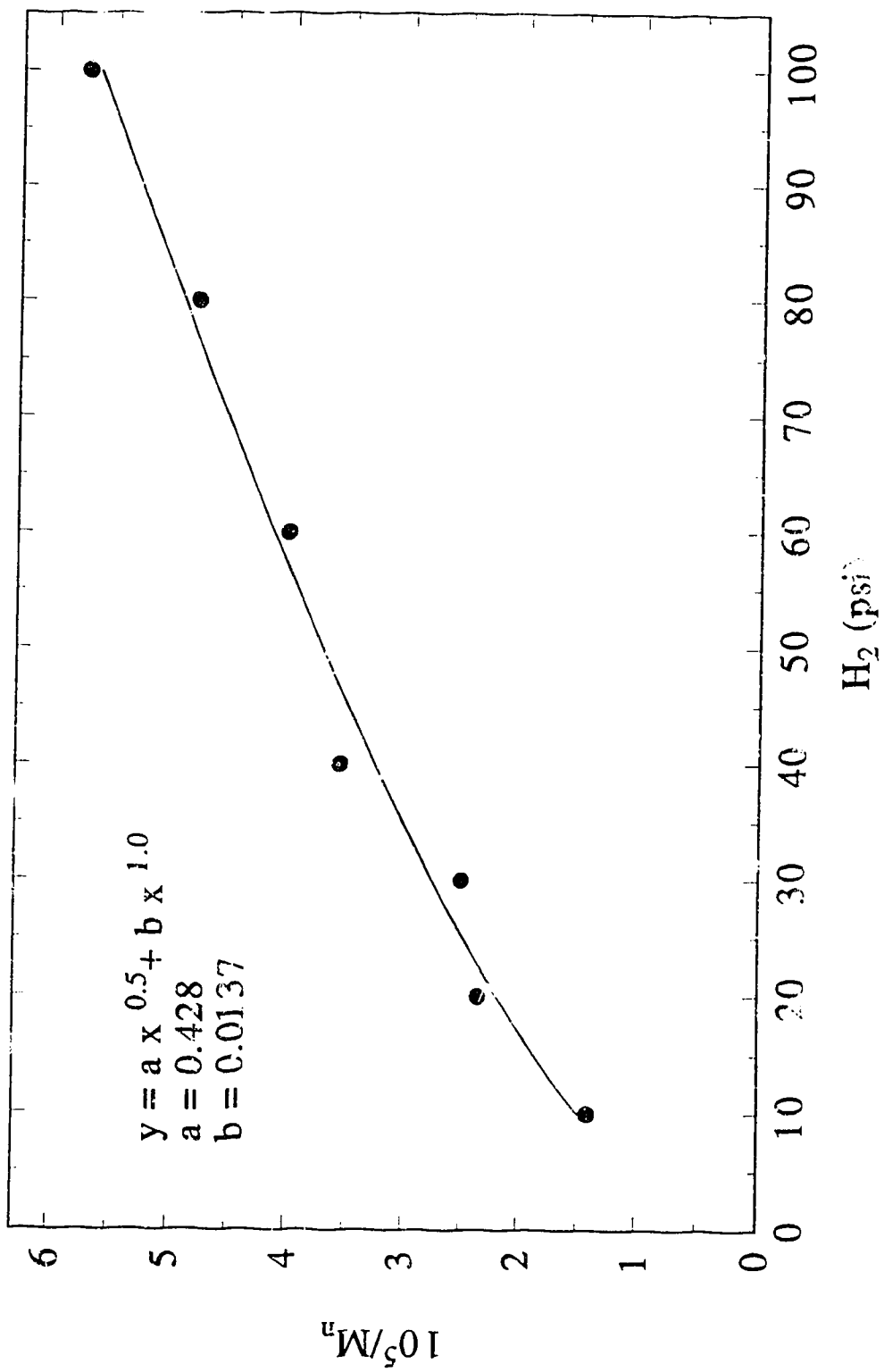


Figure 6.8 M_n versus hydrogen, mixed order curve-fitting

6.3 MELT INDEX

Melt index (see ASTM D1238 for equipment and operational details) and density are the most widely used product specifications in the polyolefins industry. The former is related to the liquid-state deformability under a set of measuring conditions, whereas the latter is related to the solid-state crystallinity at room temperature. Presentation of melt index in the broader context of molar mass distribution is warranted because of the close relationship between melt index and molar mass, as will be shown later in this section; discussions of density measurement will be deferred until Section 7.4.

The effect of hydrogen on MI is shown in Figure 6.9. Increasing the amount of hydrogen increased the melt index almost quadratically for the polymers produced in the present study. As film-blowing grade LLDPE resins typically have a melt index of 1.0, the two samples produced at 40 and 60 psi of hydrogen would be most suitable for such application. According to Figure 6.9, the amount of extrudate to be collected from the capillary die within a 10-minute interval would be below 0.1 gram for samples produced with 10 H₂ psi or less.

According to the derivation by Bremner et al. (1990), melt index is inversely proportional to viscosity. As the effect of weight-average molar mass on the zero-shear viscosity of polymer melt is well recognized,

$$\eta(\dot{\gamma} \rightarrow 0) = \tau_{i0} \propto M_w^{3.4} \quad (6.9)$$

a simple power-law relationship between melt index and M_w would result in the shear-independent Newtonian regime:

$$MI \propto M_w^{-3.4} \quad (6.10)$$

An overall slope of 3.3 between melt index and M_w shown in Figure 6.10 suggested that the apparent shear stress exerted by the load (ca. 298 kPa) was not

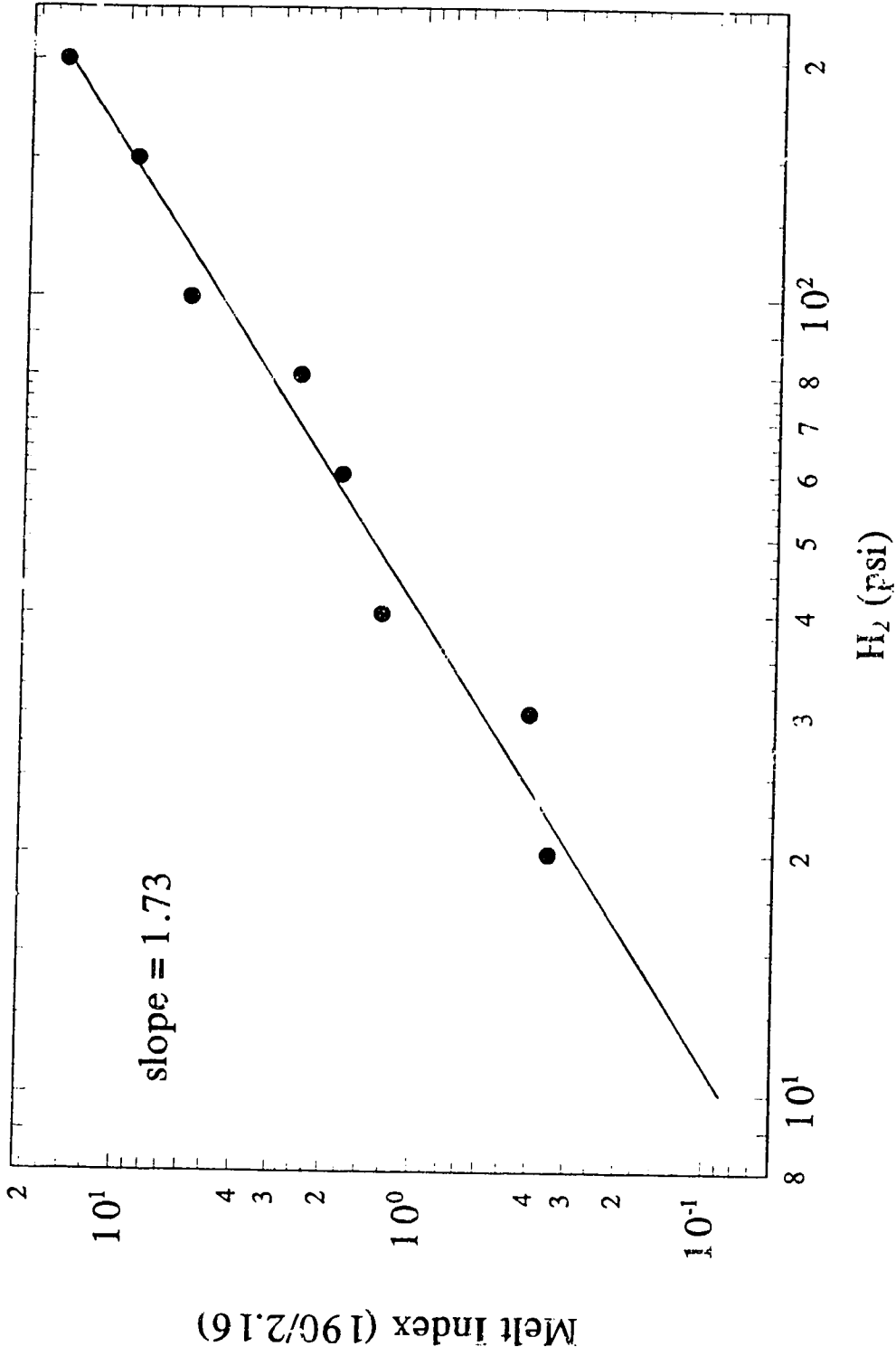


Figure 6.9 Melt index dependence on hydrogen pressure

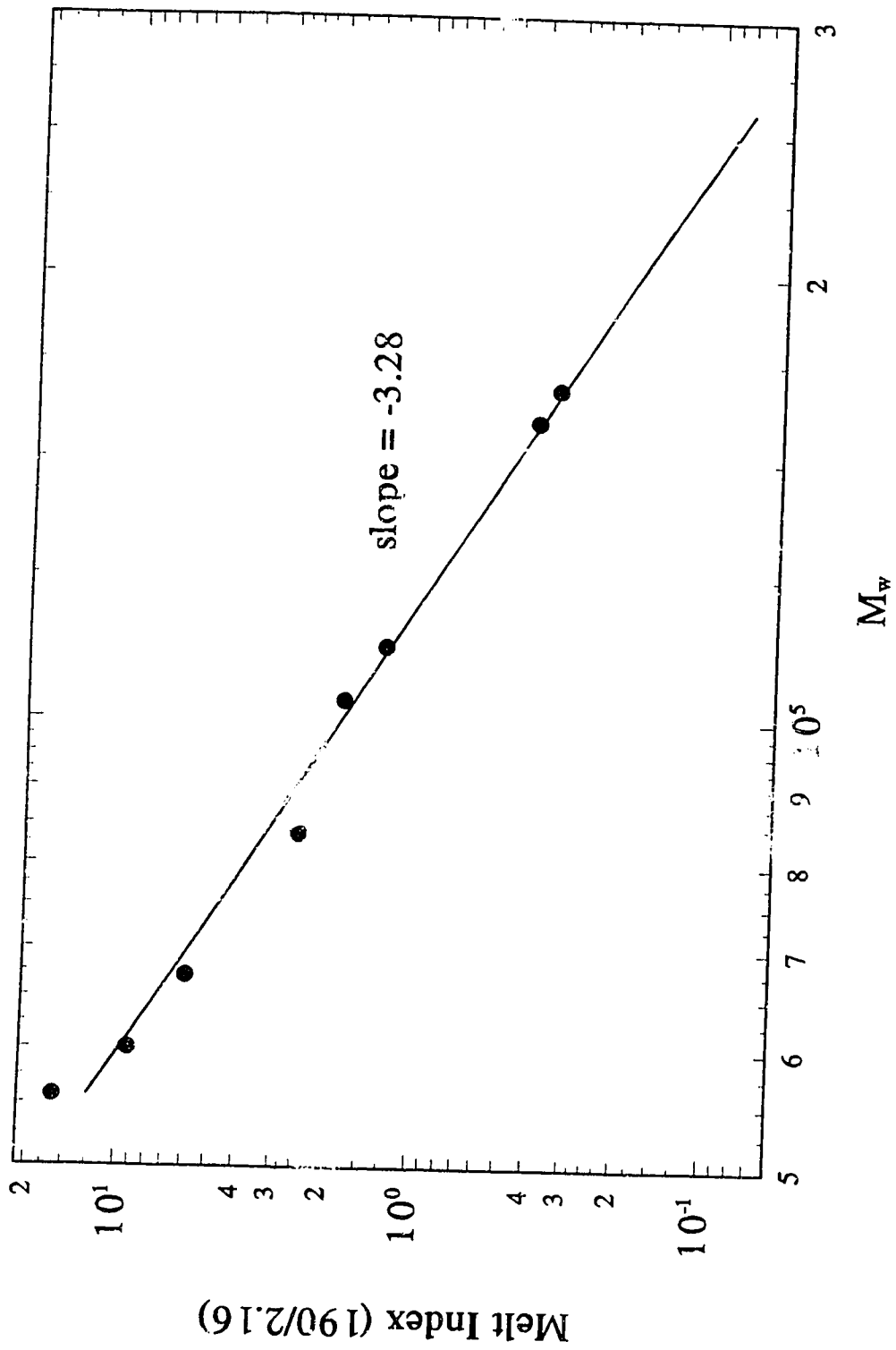


Figure 6.10 Relationship between melt index and M_w

sufficient to induce non-Newtonian behaviour. Based on the correlation in Figure 6.10, the melt indices for the two samples which were not measured directly are estimated to be 0.08 (Run 34) and 0.005 (Run 23).

Upon closer scrutiny, the slope at the lower M_w region in Figure 6.10 was considerably steeper (ca. 4.4). One simple explanation is illustrated in Figure 6.11, a plot of steady shear viscosity for a polymer such as polyethylene or polystyrene with different M_w . At the shear-independent Newtonian plateau, viscosities (or MI') are indifferent to whether the measurements are made under constant shear rate (Line A) or constant shear stress (Line B). However, at a higher shear stress (Line C), it is entirely possible for the viscosity of the higher- M_w polymer to intersect with the constant stress curve inside the shear-independent Newtonian regime, and for the lower- M_w polymers, outside. It is clear that the lower the M_w , the greater the difference between $\eta(C)$ and $\eta(B)$. While the slope for $\eta(A)$ or $\eta(B)$ versus M_w is a constant around 3.4, the slope between $\eta(C)$ versus M_w is a function of M_w .

In deriving the relationship between melt index and M_w , Bremner et al. (1990) assumed that K' , the ratio between η and η_0 , was a constant for all polymers. This is equivalent to stating that $\eta(C)/\eta(B)$ was a constant. Although this assumption was later qualified to all polymers "of a given family," i.e. samples with similar branch type, polydispersity, or comonomer content (Bremner et al., 1991), the possibility that $K'=f(M_w)$, however, was never mentioned.

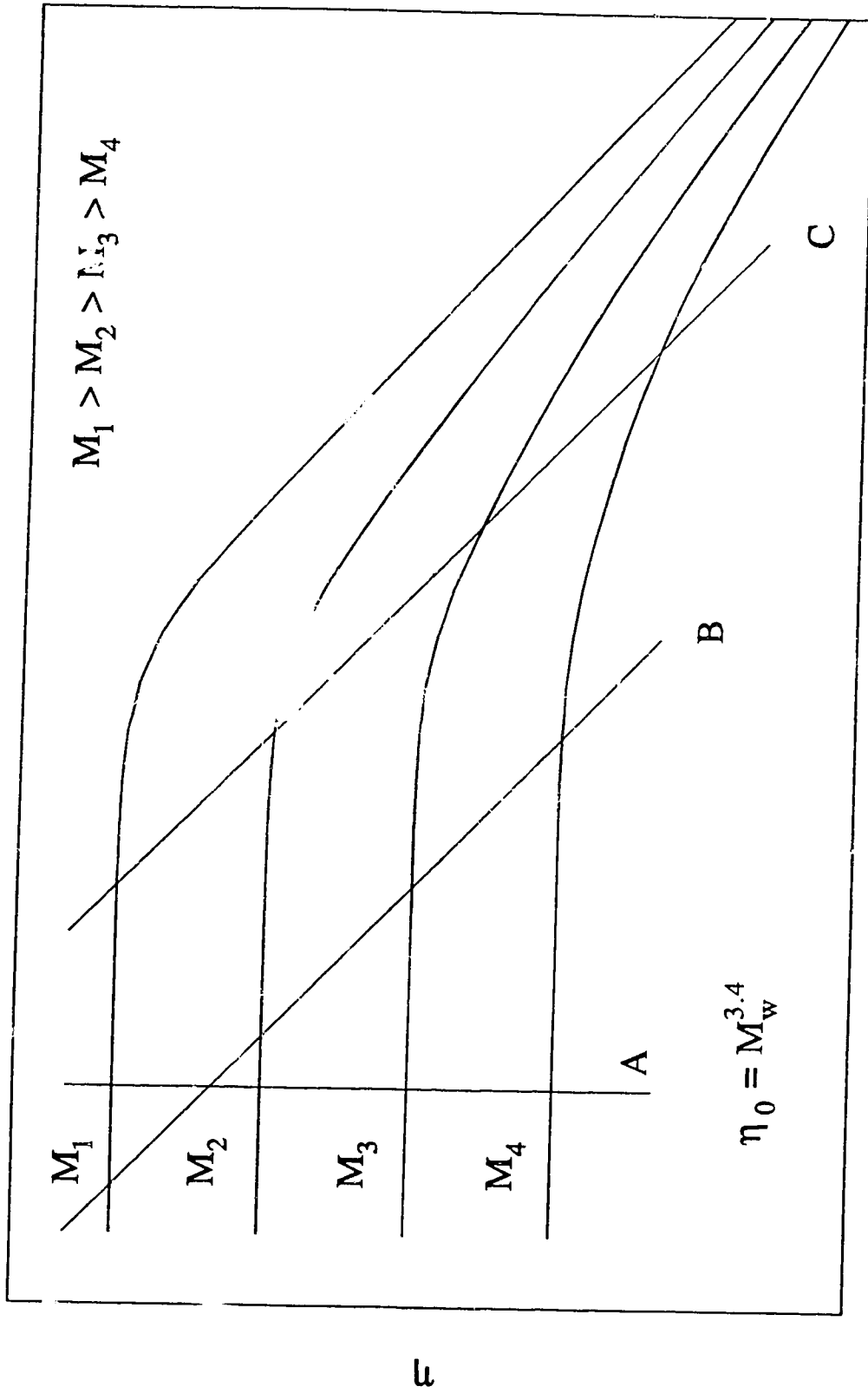


Figure 6.11 Shear viscosity versus shear rate for a typical polymer

7. CHARACTERIZATION OF POLYETHYLENE

Part 2: Crystallinity, Melting Temperature, Density, and Miscibility

Crystallinity of LLDPE is generally considered to be influenced by the amount of comonomer incorporated into the otherwise linear HDPE, for side branches disrupt the chain-folding process. Polymer crystallinity can be determined through differential scanning calorimetry (DSC), as the amorphous domains do not undergo phase transition at the melting temperature. The percent crystallinity (X_c) of a polymer can be calculated from the enthalpy of fusion as

$$X_c = \frac{H}{H_c} \quad (7.1)$$

where H_c is the enthalpy of fusion for 100% crystalline polymer (293 J/g), and H the enthalpy of fusion for the sample calculated by integrating the area between the endotherm and the baseline.

Closely associated with crystallinity is the melting temperature (T_m), which is related to the average thickness of the crystalline lamella (l_{avg}). For ethylene homopolymers, l_{avg} can be estimated according to the Thomson-Gibbs equation:

$$l_{avg} = \frac{2 \sigma_e T_{eq}}{\Delta H_c \rho_c (T_{eq} - T_m)} \quad (7.2)$$

where T_{eq} is the equilibrium melting temperature of crystalline polyethylene (145°C), σ_e is the lamellae surface energy (9.3×10^{-4} J/m²), and ρ_c (1.0100 g/cm³) is the density of pure crystalline polyethylene (Ottani and Porter, 1991). Depending on the rate of heating used in DSC, an ethylene homopolymer can melt over a 10-20°C range, and from Eq. 6.2 it is possible to relate the melting range to the distribution of lamellae thickness. Reflecting the structural heterogeneity of ethylene/ α -olefin copolymers produced by Ziegler-Natta catalysts, the melting

interval of LLDPE samples is significantly greater than 20°C, and the quantitative relationship between l_{avg} and T_m expressed in Eq. 7.2 becomes dubious (Wunderlich, 1980).

It should be stated at the outset that the credibility of X_c calculated from integrating the area between the endotherm and the baseline has been questioned recently (Foreman and Blaine, 1995). DSC endotherms superimpose the heat capacity contribution from the amorphous domain with the enthalpy contribution from the crystalline domain; separation of these two sources would require the technique of temperature modulation. For the present study, a high heating rate (10°C/min) was used to suppress the superposition of these sources. It should be noted also that a unified method of reporting T_m has yet to emerge. Several published studies on the melting behaviours of HDPE prefer to report the onset of melting rather than the peak of the endotherm as the equilibrium melting temperature to minimize the superheating effect (Wunderlich, 1980) as well as the heat transfer resistance across the specimen (Wang and Harrison, 1993). However, polymer melting is rarely conducted at equilibrium, and it is also inadequate to use an onset temperature to represent LLDPE's multimodal endotherm. Furthermore, it has been argued that, on the grounds of compositional heterogeneity, T_m for LLDPE does not exist (Harrison, 1995). As this chapter concerns HDPE as well as LLDPE, it is necessary to define a T_m which can be consistently located for any given DSC trace irrespective of its shape. The following discussions adopt the convention which assigns final peak temperature of the endotherm before its return to the baseline as T_m .

In the following sections, the effects of M_w and branching on X_c and T_m will be examined for samples prepared under very different reactor operating conditions. In Section 7.1, samples of ethylene homopolymer are used to establish the role of M_w ; in Section 7.2, the role of increasing branching frequency in ethylene/1-butene is examined; and in Section 7.3, the effect of M_w on branched polyethylene is considered. Comments on density and crystallinity are made in Section 7.4. The endotherms of these samples are subjected to further scrutiny in Section 7.5 from the perspective of polymer blends.

7.1 Effect of Molar Mass on Crystallinity and Melting Temperature in Ethylene Homopolymer¹

In Figure 7.1, the crystallinity is shown as a function of M_w for a series of ethylene homopolymers produced at 50°C under different hydrogen pressures (10-200 psi). As seen from Figure 7.1, X_c for linear polyethylene powder ranged from 64 to 69%. The dependence on molar mass was rather weak, indicating that the size of the molecule was a rather minor factor in determining the perfection of chain-fold. Such phenomenon can be understood as follow: during polymerization, polyethylene molecules crystallize as they are formed, segment by segment, and the perfection of the crystallization process is only slightly affected by the overall sizes of the individual molecules.

Also shown in Figure 7.1 is the crystallinity of resins prepared under different cooling rates (5, 10, and 20°C/min). Except for the sample with the highest M_w (7.1×10^5), crystallinity increased upon melting-recrystallization. The magnitude of ΔX_c shown in Figure 7.1 clearly established the relationship between M_w and ΔX_c : the higher the M_w , the lower the mobility of molecules in the molten state due to entanglement, the lower the increase in crystallinity. The monotonic relationship between the rate of crystallization and polymer morphology is also apparent from Figure 7.1: the slower the cooling process, the greater the improvement in crystallinity upon recrystallization.

The relationship between T_m and M_w for the same homopolymers of ethylene was plotted in Figure 7.2. T_m for polyethylene powder increased monotonically with respect to M_w from 135.3°C to 140.6°C for M_w of 1.1×10^5 to 7.1×10^5 . While crystallinity of the nascent powder was relatively independent of M_w , the average lamellae thickness (l_{avg}) was not l_{avg} as estimated according to Eq. 7.2 almost doubled from about 15 to 29 nm.

¹Data are provided in Table 7.1.

Table 7.1 Percent crystallinities and melting temperatures of HDPE produced at 50°C under constant ethylene pressure. Data are plotted in Figures 7.1 and 7.2.

Run	HDPE		Powder		Crystallized 5°C/min		Crystallized 10°C/min		Crystallized 20°C/min	
	H ₂ (psi)	M _w × 10 ⁻⁵	X _c	T _m	X _c	T _m	X _c	T _m	X _c	T _m
72	10	7.10	64.0	140.6	59.6	136.1	57.9	135.6	56.8	135.1
71	50	2.94	65.2	138.7	70.2	135.8	67.6	135.3	65.9	135.1
70	100	1.58	65.4	137.1	73.3	135.7	70.8	135.6	70.4	134.8
70	200	1.09	69.2	135.3	81.9	134.5	79.7	134.4	78.2	134.0

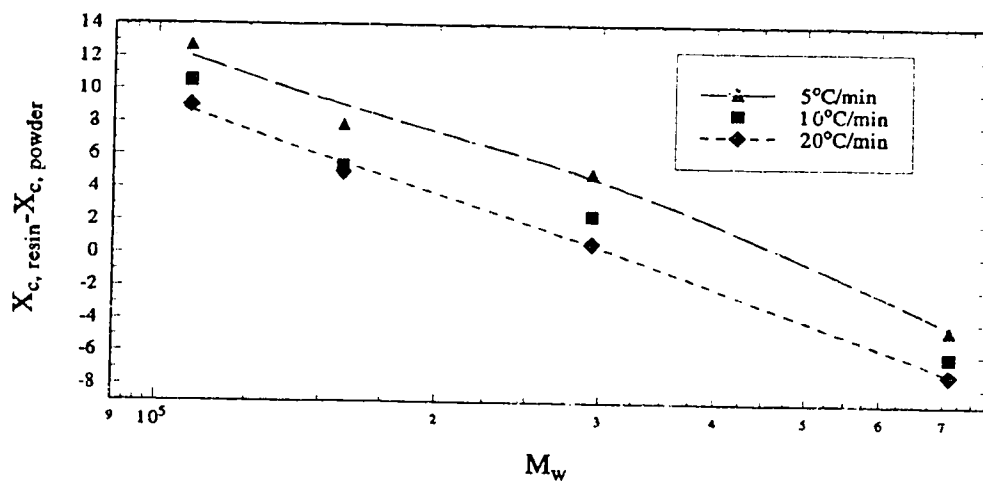
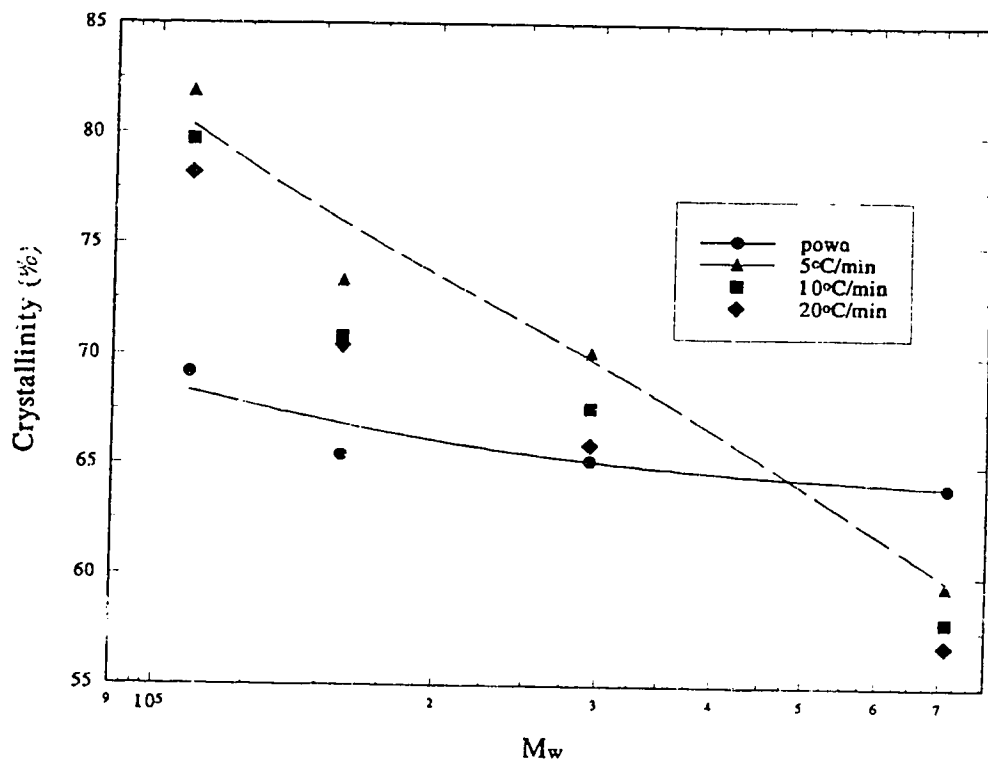


Figure 7.1 Percent crystallinity versus M_w for ethylene homopolymers

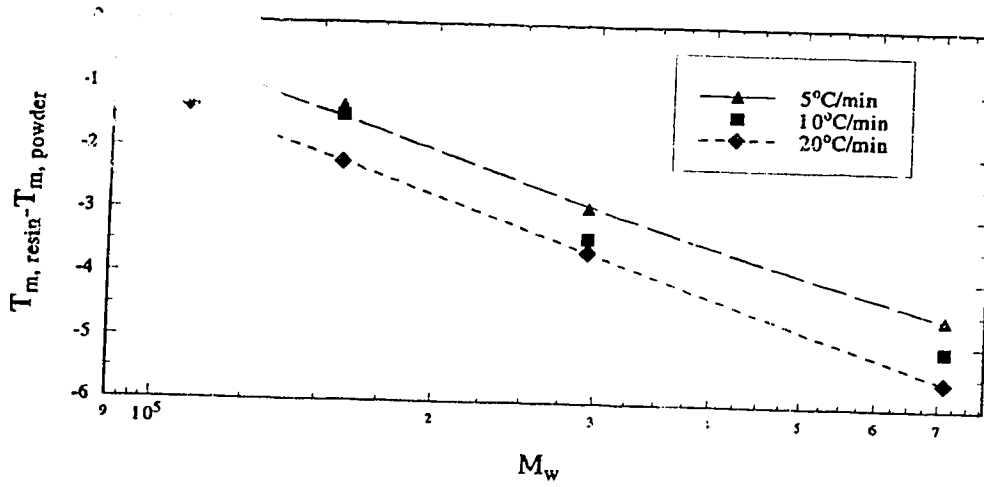
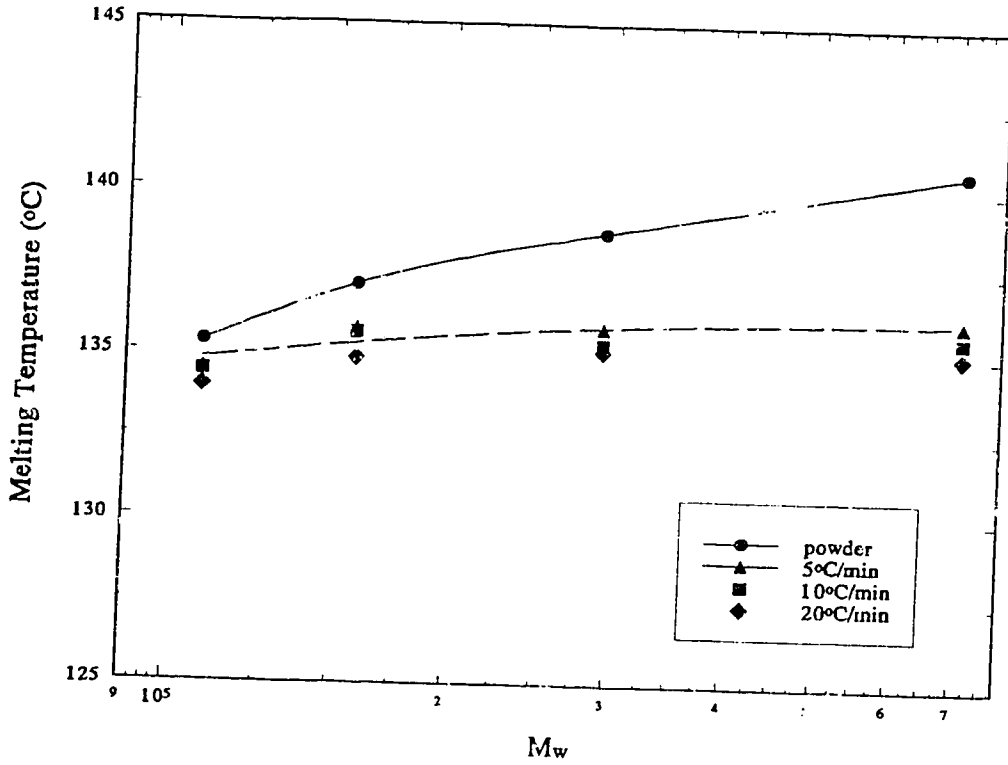


Figure 7.2 Melting temperature versus M_w for ethylene homopolymers

The dependence of T_m on M_w was also observed for recrystallized melts, but the increase of T_m with respect to increasing M_w was only 1.5°C. In all cases the T_m decreased upon recrystallization, and the extent of T_m depression was also monotonic with respect to the rate of crystallization: the faster the cooling, the greater the ΔT_m .

The coupling of X_c elevation and T_m depression upon melt recrystallization suggests that the increase in the size of crystalline domain was accompanied by a decrease in the average thickness of lamella. It appeared that a balancing mechanism was in force between these two physical properties often considered to be analogous.

7.2 Effect of Branching on Crystallinity and Melting Temperature in Ethylene/1-Butene Copolymer²

Crystallinity as affected by branching frequency is shown in Figure 7.3. LLDPEs in this series were produced at different ethylene/1-butene ratios under constant hydrogen pressure (100 psi) and temperature (70°C). As indicated in Chapter 5, the amount of 1-butene incorporation in LLDPE increased with increasing amount of precharged 1-butene in the reactor. As 1-butene can also facilitate chain transfer, the higher the comonomer concentration, the lower the M_w . According to Figure 7.3, crystallinity decreased with increasing branching frequency both in powder and in resin, indicating that the side branches disrupted the chain-folding process regardless whether polyethylene was in the form of powder or melt.

Branching frequency has a greater manifestation in terms of ΔX_c . The extent of morphological improvement upon melt recrystallization was more pronounced for samples with little or no side branches. For all samples the increase in crystallinity was most significant at the lowest cooling rate, but the difference due to cooling rate diminished with increasing branching frequency.

Figure 7.4 shows the increase of T_m with respect to decreasing branching frequency, a relationship analogous to the one observed between percent crystallinity and M_w shown in Figure 7.3. It was noted however that at high branching frequency, fast cooling may actually produce a higher melting resin.

It was noted that the $X_{c, \text{ powder}}$ of Run 48, an ethylene homopolymer, was higher than all the samples of the same genre examined in Section 7.1. Although $X_{c, \text{ powder}}$ was not a sensitive function of M_w during segment-wise chain-folding during polymerization, as discussed in the previous section, the kinetics of crystallization was temperature dependent. It appeared that the higher the polymerization temperature, the greater the crystallinity of as-polymerized powders.

²Data are provided in Table 7.2.

Table 7.2 Percent crystallinities and melting temperatures of LLDPE produced at 70°C under constant hydrogen pressure. Data are plotted in Figures 7.3 and 7.4.

Run	LLDPE		Powder		Crystallized 5°C/min		Crystallized 10°C/min		Crystallized 20°C/min	
	C ₄ (ml)	M _w × 10 ⁻⁴	X _c	T _m	X _c	T _m	X _c	T _m	X _c	T _m
48	0 (HDPE)	11.66	72.1	135.8	77.9	135.2	75.2	135.0	72.8	134.6
49	5	9.68	60.5	127.1	65.3	129.0	63.5	128.4	62.2	127.9
50	20	7.10	34.9	122.5	38.8	123.9	40.0	123.6	41.0	123.2
47	30	5.26	24.3	122.1	25.7	122.7	25.4	122.9	25.3	123.1

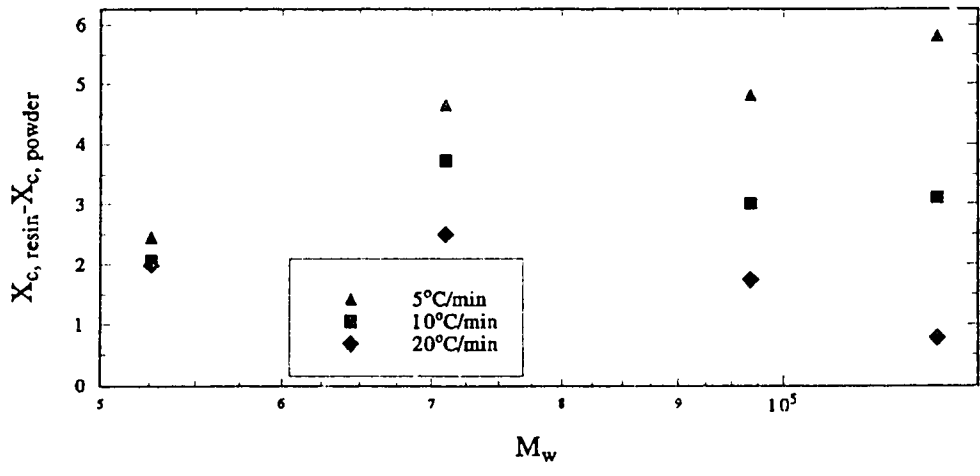
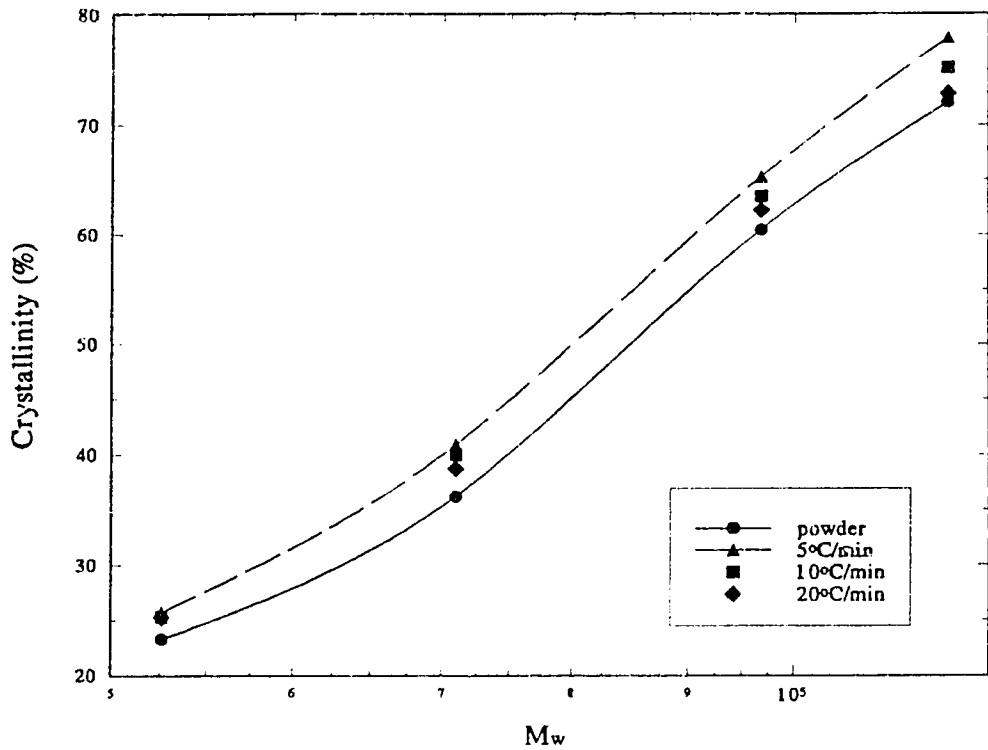


Figure 7.3 Percent crystallinity versus M_w for LLDPE: effect of branching

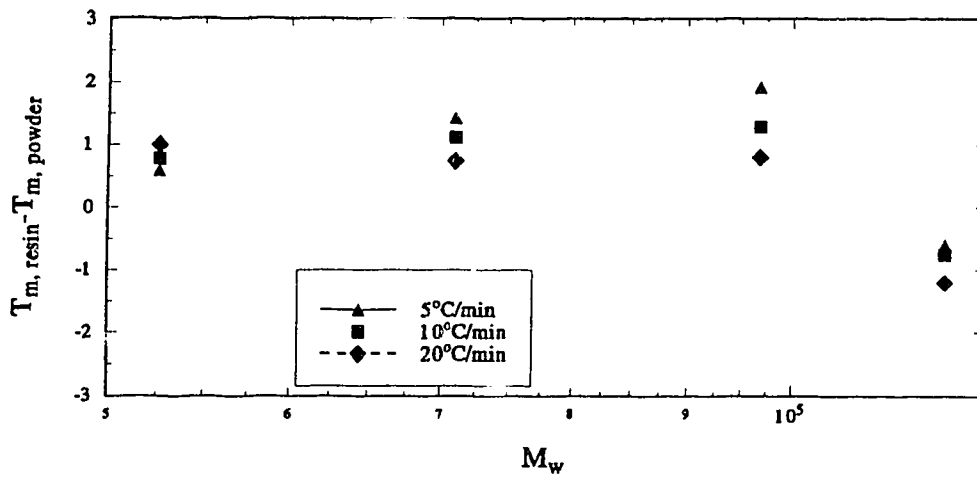
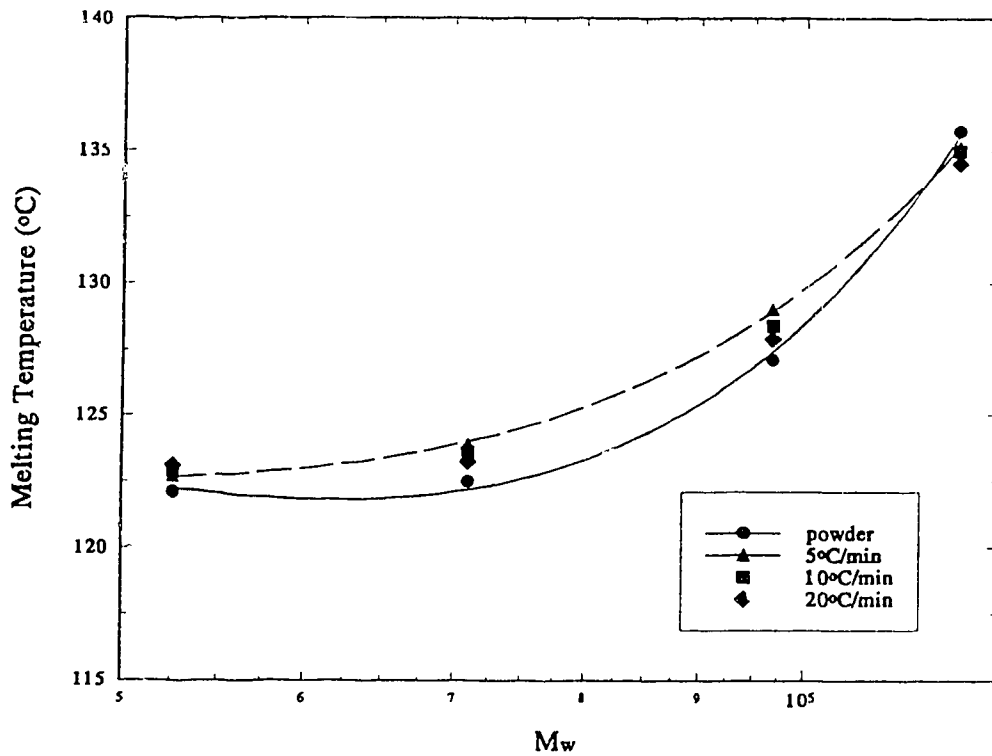


Figure 7.4 Melting temperature versus M_w for LLDPE: effect of branching

7.3 Effect of Molar Mass on Crystallinity and Melting Temperature in Ethylene/1-Butene Copolymer³

The crystallinities of LLDPE produced under the constant 1-butene precharge (10 ml) at 70°C under various hydrogen pressures (0-200 psi) are shown in Figure 7.5. The factor governing the crystallization behaviour of these LLDPEs is the size of the molecule, since the extent of 1-butene incorporation in these samples was nearly identical (Lacombe, 1995). The crystallinities of LLDPE samples were approximately constant at 45% in the powder form, unaffected by M_w . This phenomenon is very similar to that shown in Figure 7.1, where M_w for ethylene homopolymer powders also affected the crystallinity little. Therefore, the rationale that the segment-wise chain-folding is not affected by the overall size of the molecule during polymerization can be applied to both HDPE and LLDPE.

After the samples were recrystallized from the molten state, the crystallinity strongly depended on M_w ; the lower the molar mass, the higher the crystallinity. Such influence of M_w on crystallinity was also very similar to that shown in Figure 7.1.

The difference between nascent powder and recrystallized resin for LLDPE is further illustrated in Figure 7.6. For powders, T_m increased slightly with increasing M_w , whereas for resins, T_m decreased slightly with increasing M_w . (Such dependence of T_m (resin) on M_w was not observed for homopolymers shown in Figure 7.2). As a result, melting temperature may either increase or decrease with melt recrystallization, depending on M_w .

In summary, M_w remains the dominant factor in determining both the crystallinity and the melting temperature for LLDPE resins with similar branching frequency, and the types of dependence are nearly identical to those observed in ethylene homopolymers.

³Data are provided in Table 7.3.

Table 7.3 Percent crystallinities and melting temperatures of LLDPE produced at 70°C under constant 1-butene precharge. Data are plotted in Figures 7.5 and 7.6.

Run	LLDPE		Powder		Crystallized 5°C/min		Crystallized 10°C/min		Crystallized 20°C/min	
	H ₂ (psi)	M _w × 10 ⁻⁴	X _c	T _m	X _c	T _m	X _c	T _m	X _c	T _m
23	0	61.2	44.6	127.9	36.4	121.7	35.4	121.1	35.1	120.7
34	10	26.0	45.0	125.2	41.3	124.2	40.2	123.6	39.6	123.4
27	40	11.2	44.2	123.0	46.1	124.6	44.0	124.6	44.4	124.2
40	100	6.71	45.6	123.5	48.6	125.3	46.9	125.2	46.6	124.8

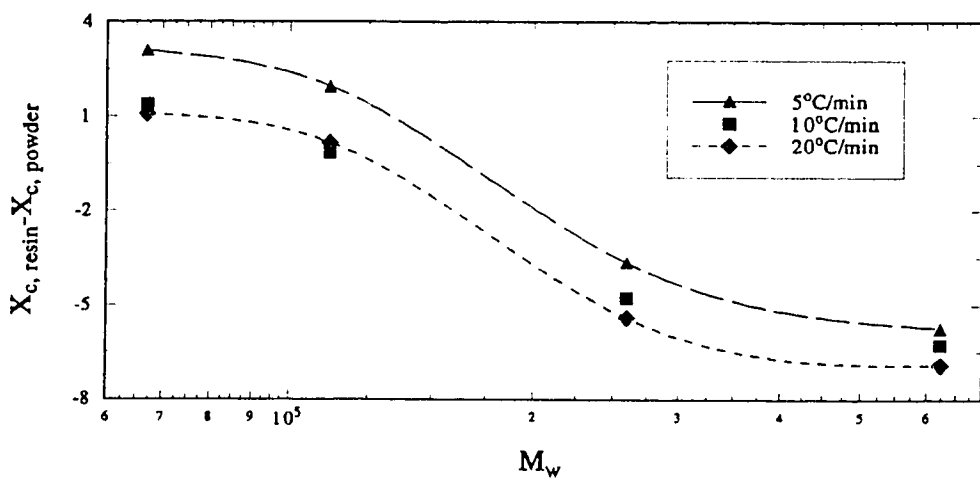
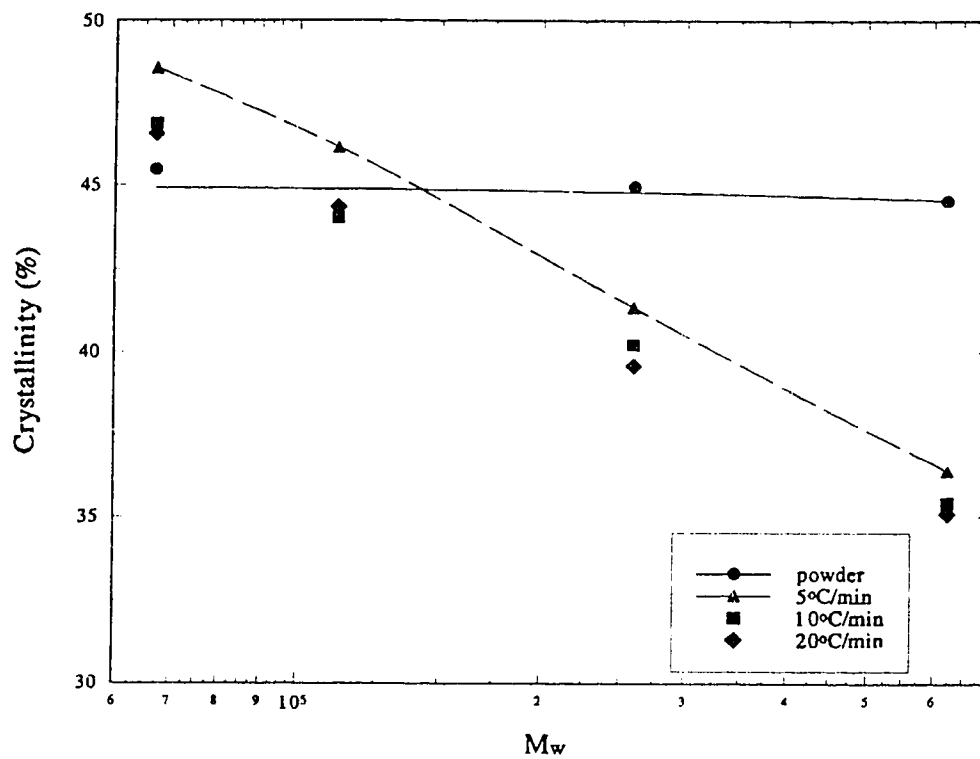


Figure 7.5 Percent crystallinity versus M_w for LLDPE: effect of M_w

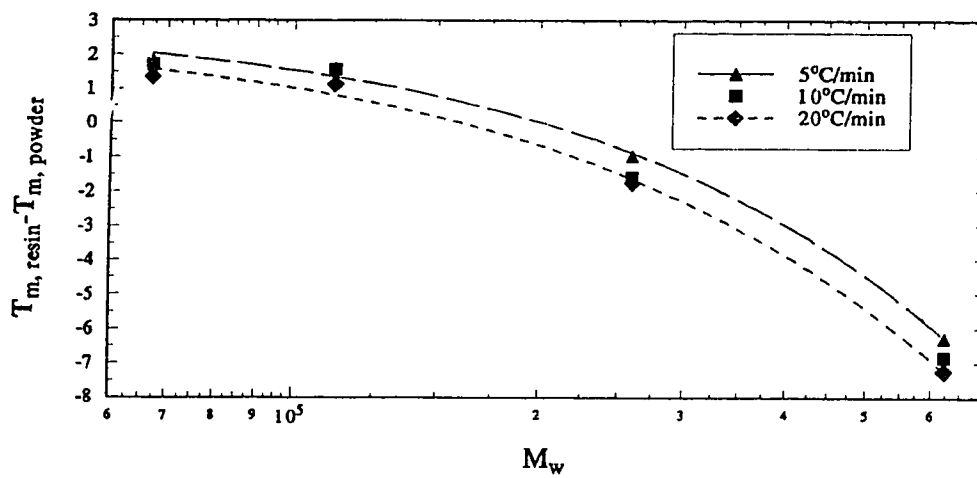
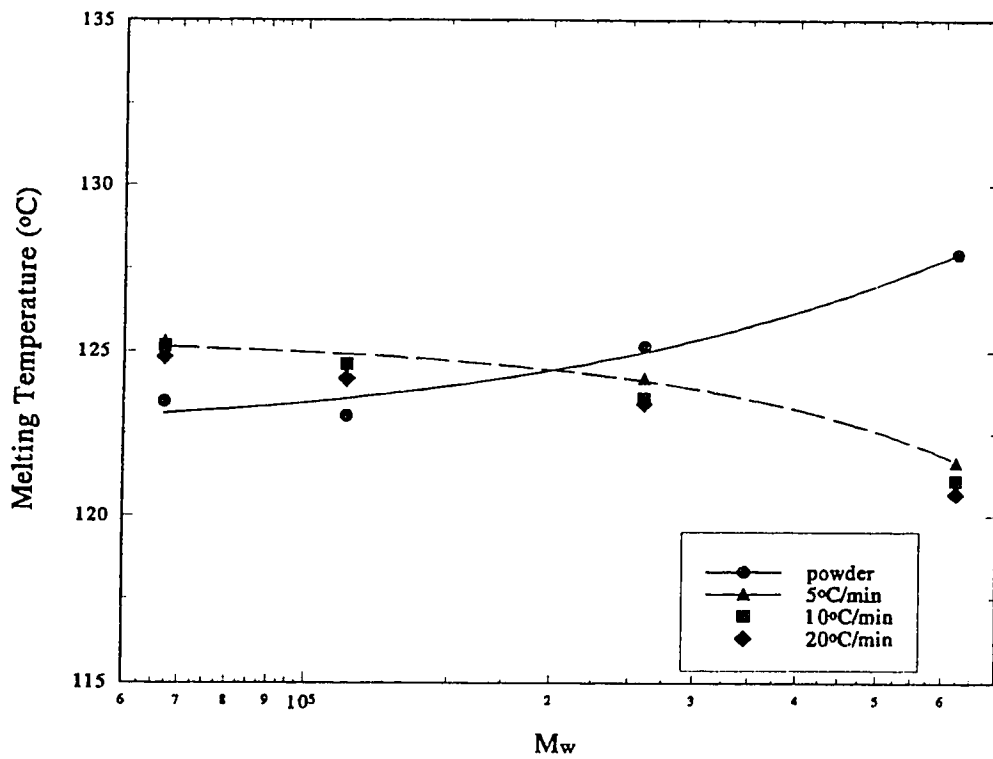


Figure 7.6 Melting temperature versus M_w for LLDPE: effect of M_w

7.4 Density

As density of LLDPE is closely related to crystallinity, no measurements were made for the samples produced in this study, for meticulous conditioning of the samples would be required to ascertain the exact thermal history whose impact on crystallinity has been documented in the previous sections. On the other hand, it is known that crystallinity and density are related according to the dilatometric equations (Karbashewski et al, 1992; Sehanobish et al., 1994):

$$\rho = X_c \rho_c + (1-X_c) \rho_a \quad (7.3a)$$

$$1/\rho = X_c/\rho_c + (1-X_c)/\rho_a \quad (7.3b)$$

where ρ_c and ρ_a are the densities for 100% crystalline and 100% amorphous polyethylene. Evaluation of density based on X_c shown in Tables 7.1 through 7.3 is straightforward. According to Table 7.4, ethylene homopolymers studied in Section 7.1 with X_c between 60 and 80% have their densities ranging from 0.94 to 0.98 g/cc, whereas the density varies from 0.90-0.93 g/cc for the LLDPEs studies in Section 7.3 with X_c around 35-50%.

Table 7.4 Density of polyethylene according to dilatometry equation

Crystallinity (%)	Density (g/cc) Eq. 7.3a	Density (g/cc) Eq. 7.3b
0	0.8520	0.8520
5	0.8599	0.8587
10	0.8678	0.8655
15	0.8757	0.8725
20	0.8836	0.8795
25	0.8915	0.8867
30	0.8994	0.8940
35	0.9073	0.9014
40	0.9152	0.9089
45	0.9231	0.9165
50	0.9310	0.9243
55	0.9389	0.9322
60	0.9468	0.9403
65	0.9547	0.9484
70	0.9626	0.9568
75	0.9705	0.9652
80	0.9784	0.9739
85	0.9863	0.9827
90	0.9942	0.9916
95	1.0021	1.0007
100	1.0100	1.0100

Note: Values for 100% crystalline and 100% amorphous polyethylene are adopted from Janzen (1992): $\rho_a=0.8520$ g/cc, $\rho_c=1.0100$ g/cc.

7.5 Linear-Low Density Polyethylene: A Blending Perspective

The ramifications of structural heterogeneity of polyethylene on the processing characteristics of melts and the physical properties of solids are of significant research interest both in academia and in industry. Numerous studies on TREF, TREF-GPC, or TREF-DSC have shown convincingly that linear-low density polyethylene is comprised of at least two fractions, with one fraction consisting of linear molecules and the other branched (Wild et al., 1982a; Usami et al., 1986; Kelusky et al., 1987; Mirabella and Ford, 1987; Hosoda, 1988; Kakugo et al., 1991; Defoor et al., 1992; Karbasheski et al., 1992; Zhou and Hay, 1993; Balbontin et al., 1994; Joskowicz et al., 1995; Takoka et al., 1995). LLDPE samples produced in the laboratory had a multimodal branching distribution, as shown in Figure 5.6. It has been reported that the linear portion of LLDPE contributes to its inferior processability, lower onset of sharkskin and melt fracture, and higher zero-shear viscosity (Karbasheski et al., 1991).

DSC endotherms for ethylene homopolymers and ethylene/1-butene copolymers were readily distinguishable by shape. According to Figure 7.7, endotherms for the HDPE samples studied in Section 7.1 were (almost) symmetrical for both nascent powders and recrystallized resins (cooled at 5°C/min) even though they differed in size and in position. On the other hand, the LLDPE samples studied in Section 7.2 were considerably more complex. Increasing the amount of precharged 1-butene from 0 to 30 ml dramatically altered the shape of the endotherms as shown in Figure 7.8. For the powders, the heat trace changed from a single melting peak centred around 133°C for the HDPE (Run 48) to a multiple-melting peak (Run 47). (Despite its odd shape, the endotherm for Run 47 was remarkably reproducible.) For resins, these LLDPE endotherms assumed a bimodal shape commonly associated with TREF: one sharp peak (around 122°C) and one broad peak at the lower temperature range. Also as in the case of TREF, the greater the comonomer content, the better defined the low-temperature peak. In essence, due to molecular reorganization,

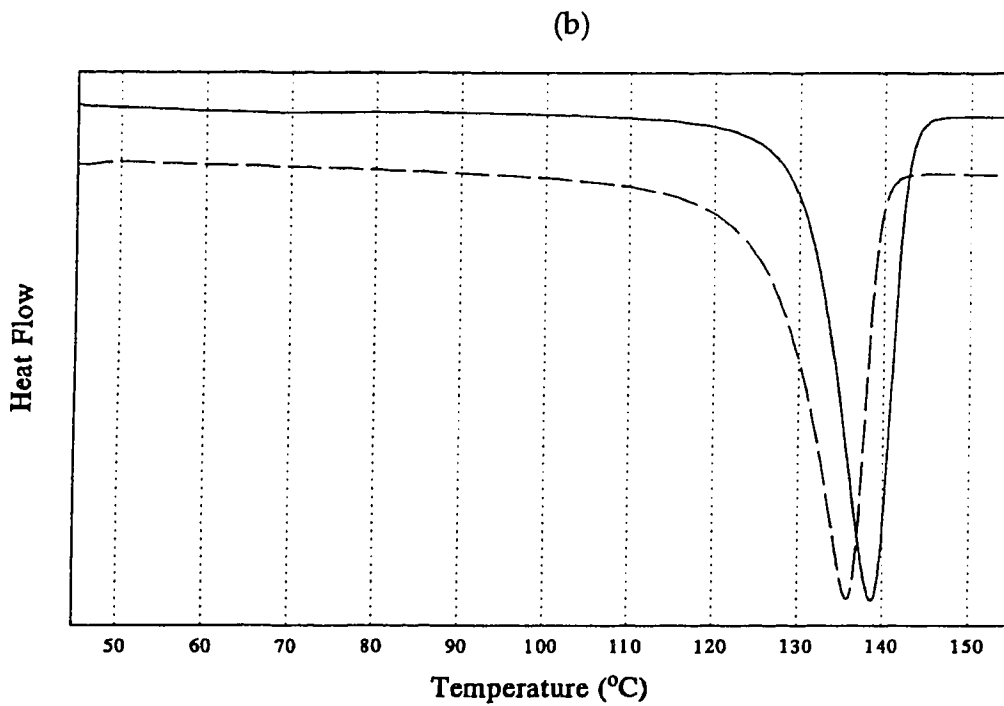
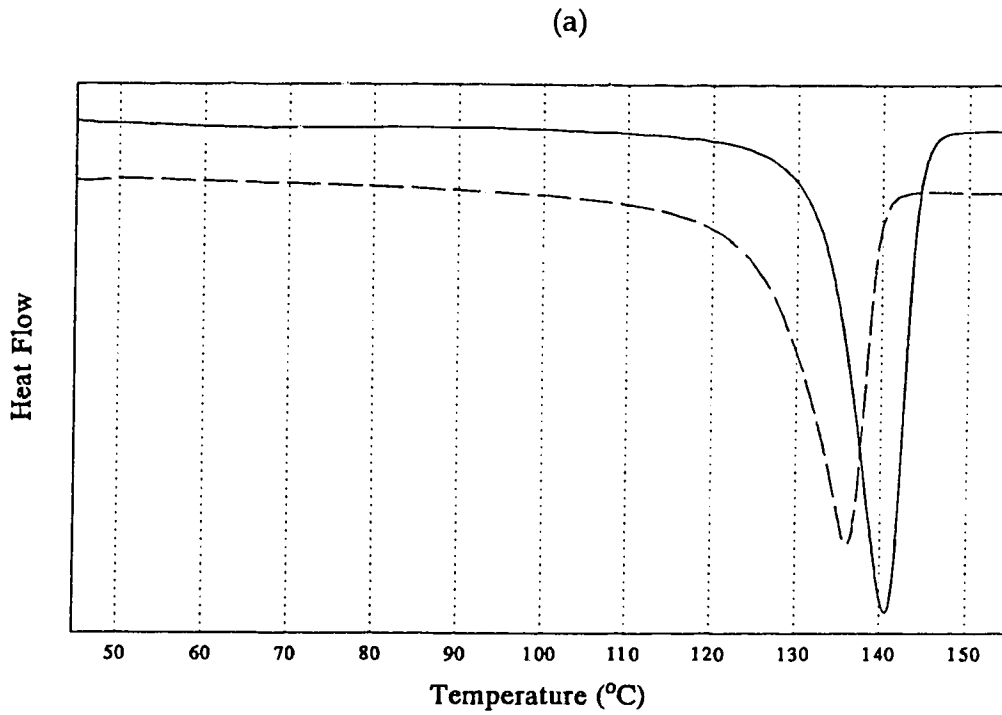
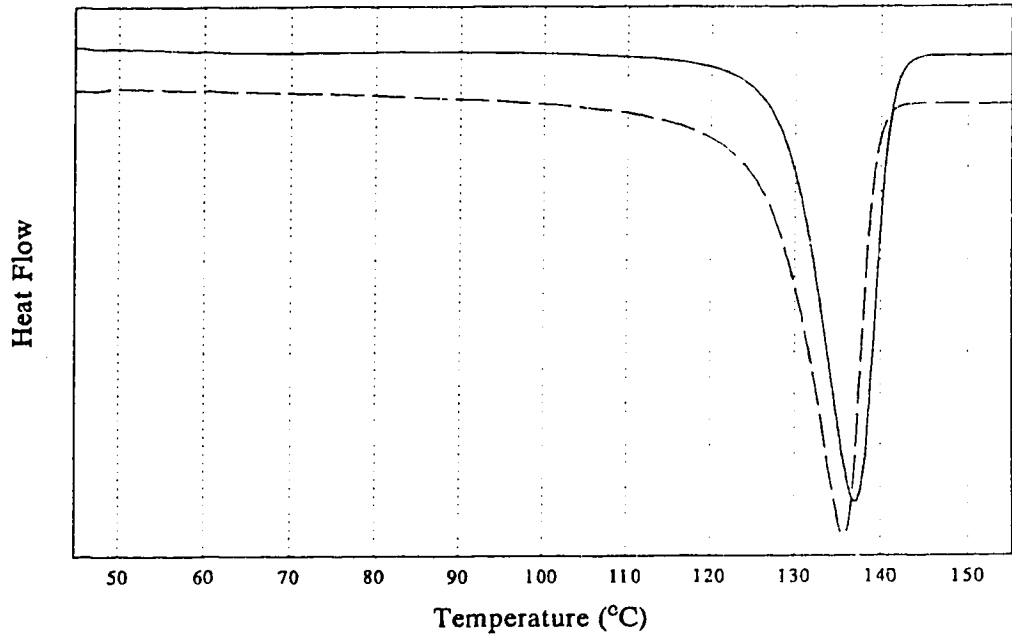
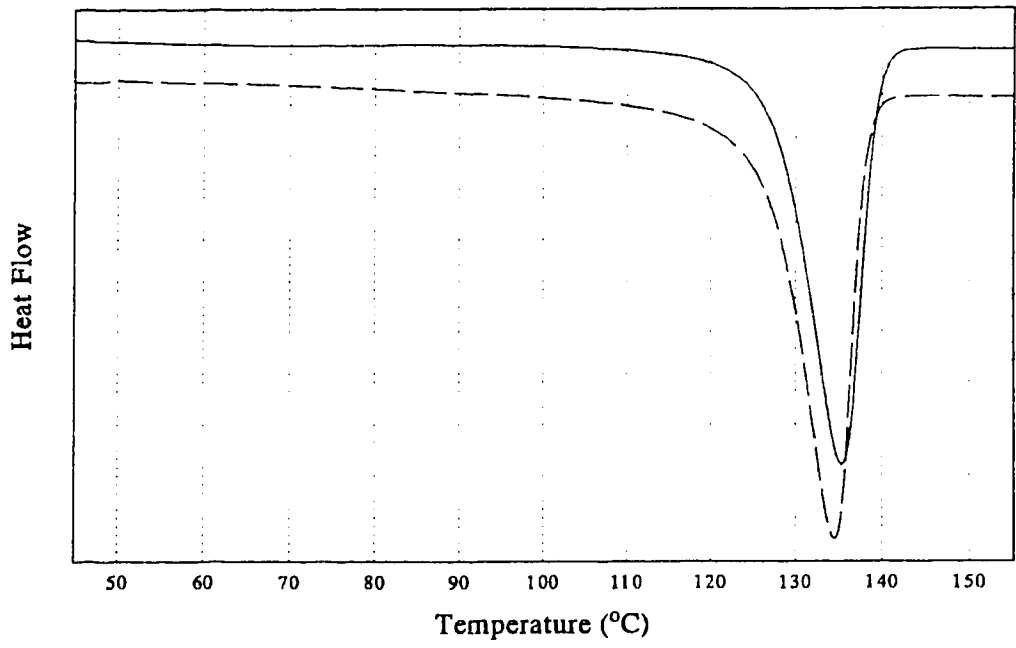


Figure 7.7 Endotherms (offset for clarity) of samples examined in Section 7.1: (a) 10 psi H₂ (Run 76); (b) 50 psi H₂ (Run 72); (c) 100 psi H₂ (Run 71); (d) 200 psi H₂ (Run 70). Solid line: powder; dashed line: resin.

(c)



(d)



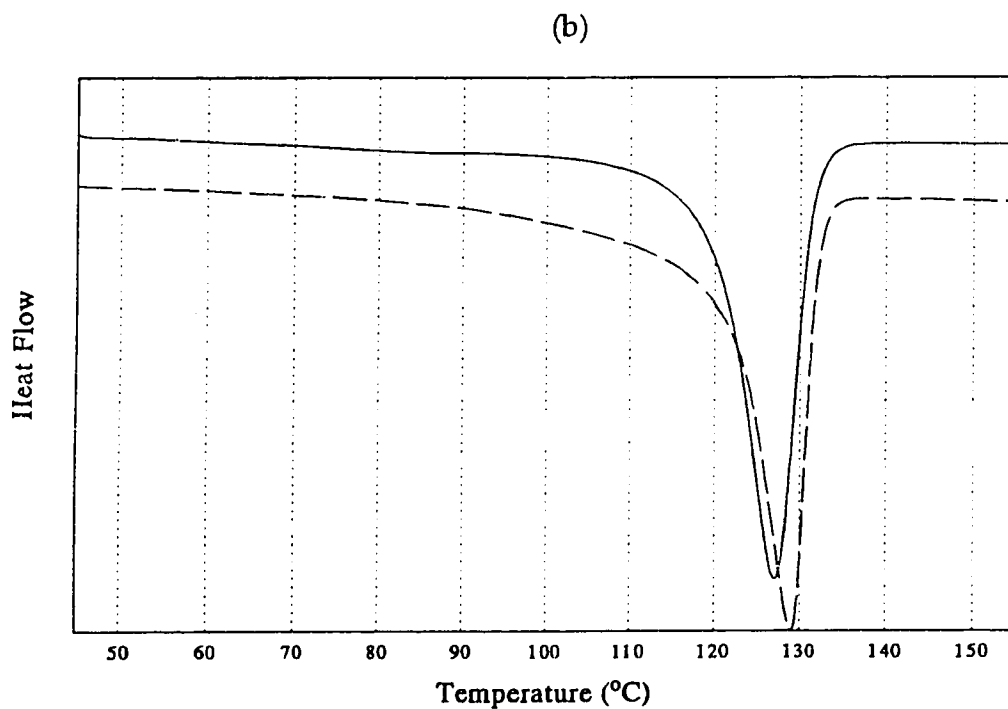
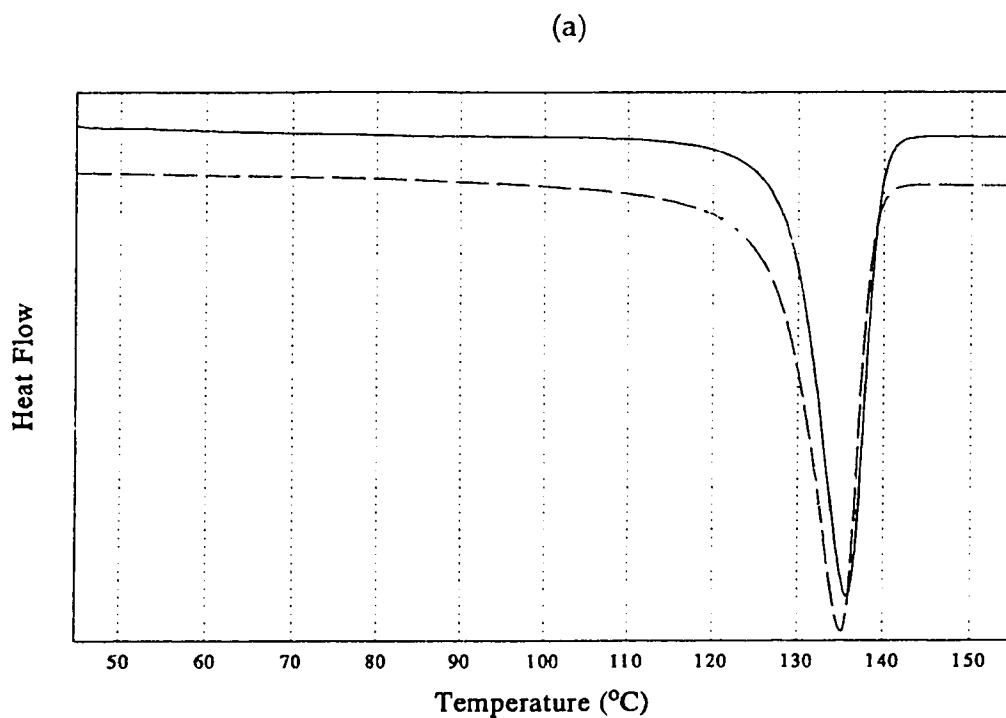
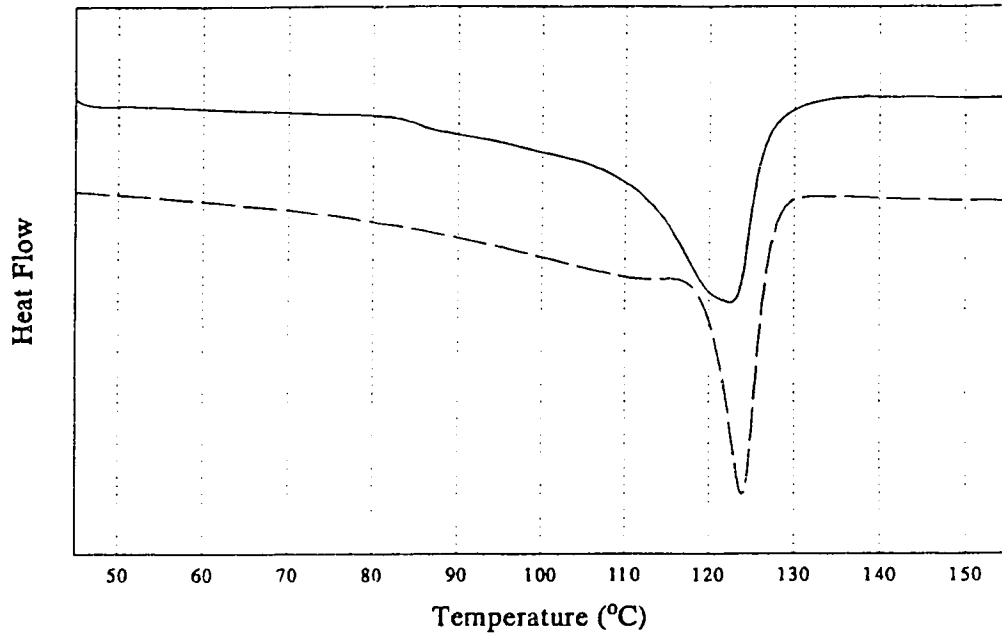
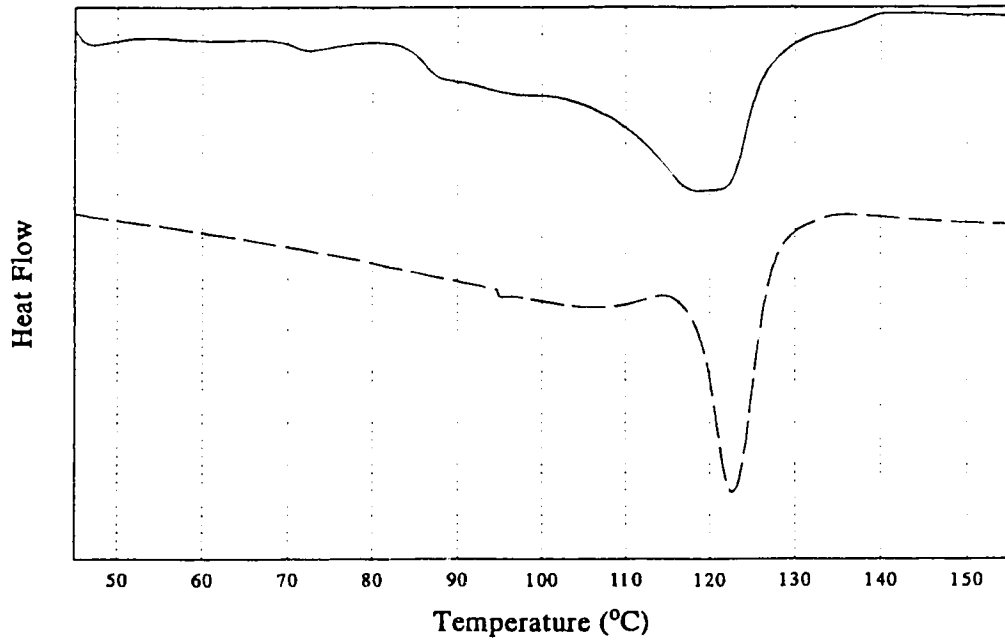


Figure 7.8 Endotherms (offset for clarity) of samples examined in Section 7.2: (a) 0 ml 1-butene (Run 48); (b) 5 ml 1-butene (Run 49); (c) 20 ml 1-butene (Run 50); and (d) 30 ml 1-butene (Run 47). Solid line: powder; dashed line: resin.

(c)



(d)

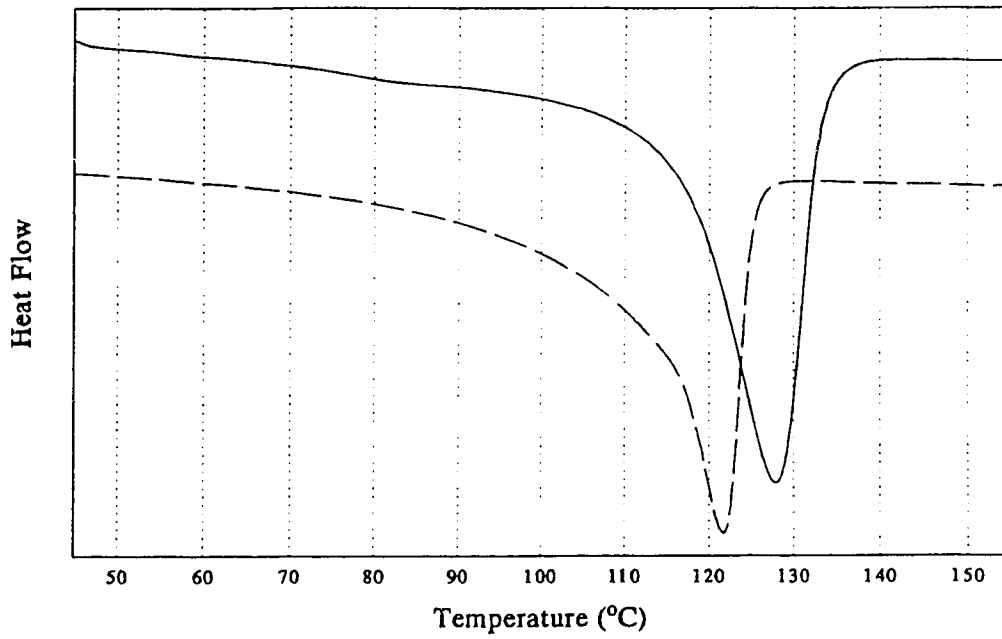


recrystallized melts and nascent reactor powders have lamellae size distributions which are significantly different.

Based on the evidence shown in Figure 7.8, LLDPE with multimodal lamellae sizes can be considered as blends of ethylene/1-butene copolymers with varying degrees of comonomer incorporation. Characterization techniques such as small-angle x-ray scattering (SAXS), wide-angle x-ray diffraction (WAXS), small-angle light scattering (SALS), synchrotron-sourced x-ray scattering (SSXS), small-angle neutron scattering (SANS), transmission electron microscopy (TEM), scanning electron microscopy (SEM), and Raman spectroscopy have been applied in addition to DSC to investigate the miscibility of polyethylene blends (Ree et al., 1987; Kyu et al., 1987; Hu et al., 1987; Wang et al., 1990; Tashiro et al., 1992a-b; 1994a-d; Tashiro 1995; Hill et al., 1992; 1993; Hill and Barham, 1992a-b; 1994; Puig et al., 1993). At issue of these studies is whether blends of polyethylenes with varying degrees of branching are miscible ($\Delta G_{\text{mix}} < 0$) under various thermodynamic and processing conditions. If the answer is negative, no amount of mixing or blending can prevent phase separation, and phase-separated rheology in the melt will lead into phase-separated morphology in the solid (Domoulin et al., 1987). Theoretical calculations by Wardhaugh and Williams (1995) have predicted that an LLDPE melt is immiscible and may even form intramolecular phase-separated domains.

Figure 7.9 shows the melting curves (powders and melts) of the LLDPE samples studied in Section 7.3. It was noted that all powders had relatively symmetric, unimodal endotherms characteristic of single-phase melt. Upon melt recrystallization, however, all these endotherms became bimodal, indicating multiphase blends. Such transformation of (near) single-phase blend in powder to multiphase blend in resin cannot be detected by a procedure like TREF which involves the process of dissolution and recrystallization prior to elution fractionation. The extent of phase separation among resins was controlled by the molar mass, as the lower the molar mass, the sharper the linear, high-melting peak.

(a)



(b)

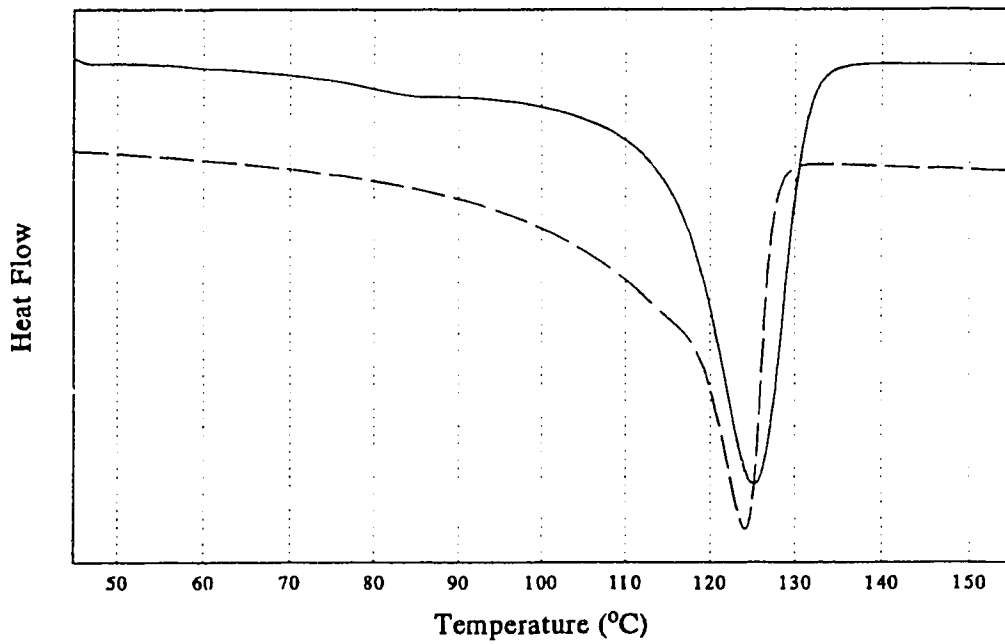
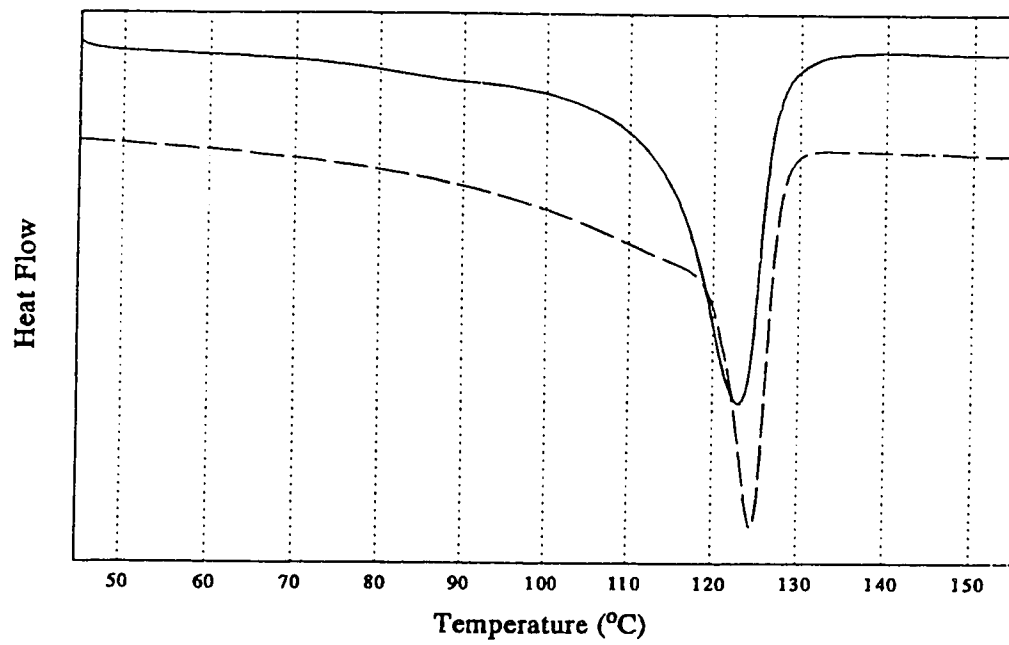
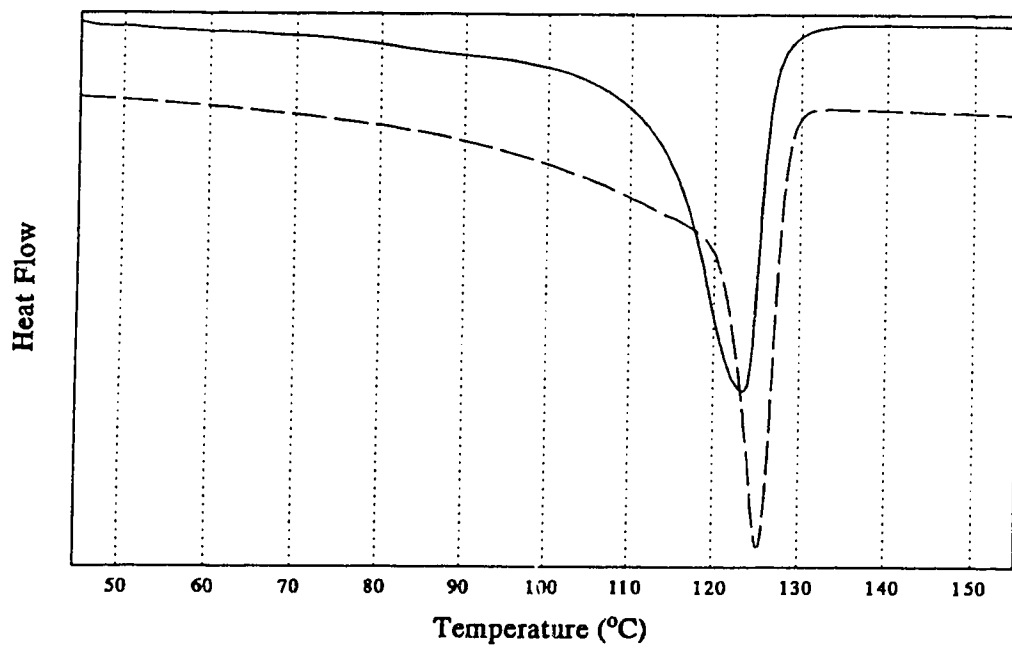


Figure 7.9 Endotherms (offset for clarity) of samples examined in Section 7.3: (a) 0 psi H₂ (Run 23); (b) 10 psi H₂ (Run 34); (c) 60 psi H₂ (Run 38); and (d) 100 psi H₂. Solid line: powder; dashed line: resin.

(c)



(d)



In Section 5.2, it was proposed that the extent of copolymerization is related to the time-dependent reduction of Ti^{+4} by the cocatalyst, and that copolymerization precedes homopolymerization. If this supposition is correct, linear polyethylene molecules are formed around branched polyethylene molecules. In the solid phase these two types of molecules cannot aggregate into phase-separated domains during polymerization and are thus *kinetically* miscible at the molecular level as required by the surface reaction kinetics. Such kinetic miscibility is metastable, for it is irreversibly destroyed upon melting as molecules are given sufficient thermal energy to overcome the solid crystal constraints. Upon cooling, linear molecules crystallize before branched molecules and the immiscible blends are formed.

8. CHARACTERIZATION OF POLYETHYLENE

Part 3: DSC Fraction of Linear-Low Density Polyethylene

Although temperature rising elution fractionation, when used in conjunction with GPC, has achieved a status as the consummate technique for molecular characterization of LLDPE, the process has several undesirable features. First, the entire process, which involves dissolution, crystallization, and elution, is time-consuming; second, it is labour-intensive without automation; and third, it involves hazardous solvents, most commonly the derivatives of benzene. Logistics aside, the theoretical aspects of the separation or the experimental limitation of the technique have yet to be investigated in detail (Wild, 1991). Advances in the thermodynamics of polymer-solvent interaction, the rheology of dilute polymer solution, and the physics of crystallization have not been considered *in toto* to address the basic issues such as the selection of solvent, the optimal concentration of the solution, the impact of stirring on the conformation of polymer coils, the driving force for chain-folding, etc.

A new technique (Monrabal, 1994), known as crystallization analysis fractionation, or CRYSTAF, addresses the concerns of time and automation by directly monitoring the polymer solution concentration during the cooling cycle. No column packing is required in CRYSTAF, for the elution cycle has been completely dispensed with. There are also several alternatives which have been explored lately to reduce the use of solvent. In one of the revisions (Mara and Menard, 1994), LLDPE solutions were crystallized inside DSC pans, which were subsequently scanned to generate endotherms which were in excellent agreement with TREF profiles in terms of the relative amount of branched and linear molecules. Another revision (Keating and McCord, 1994; Chiu et al., 1995) avoided the use of solvent all together; polymer melts were isothermally crystallized in descending 5 or 10°C steps inside the DSC pans from above T_m to room temperature. As linear molecules were annealed into thicker and stabler

lamella at higher temperatures relative to branched molecules, LLDPE was segregated into domains of varying equilibrium thickness. Fractionation was poor and possibly incomplete when larger temperature steps (20-30°C) and shorter time intervals (2 hours) were used (Balbontin et al., 1994).

The novelty of the last revision (hereafter designated as fractional DSC, or FDSC) notwithstanding, an impetus to further investigate this technique is the potential to represent the molecular composition of LLDPE in bulk in much the same way as TREF or CRYSTAF in dilute solution. Quantitative comparison between fractional DSC and analytical TREF will be presented here as an initial step towards the stated objective, for published studies on this technique, with the exception of the work by Balbontin et al. (1994), did not make any direct comparison with TREF results.

For the present study, samples with varying degrees of branching frequency (Runs 48, 49, 40, 50, and 47) were crimped in nonhermetic type aluminium DSC pans and subjected to the thermal treatment shown in Table 8.1. At the completion of the annealing process, samples were heated at 10°C/min to generate the endotherms shown in Figure 8.1.

Table 8.1 Temperature programme used for DSC fractionation

Temperature (°C)	Duration (hr) ¹
145	20
135, 125, 115	6
105, 95, 85	5
75, 60	4
45, 30	3

¹Durations were chosen in accordance with the guideline of Keating and McCord (1994).

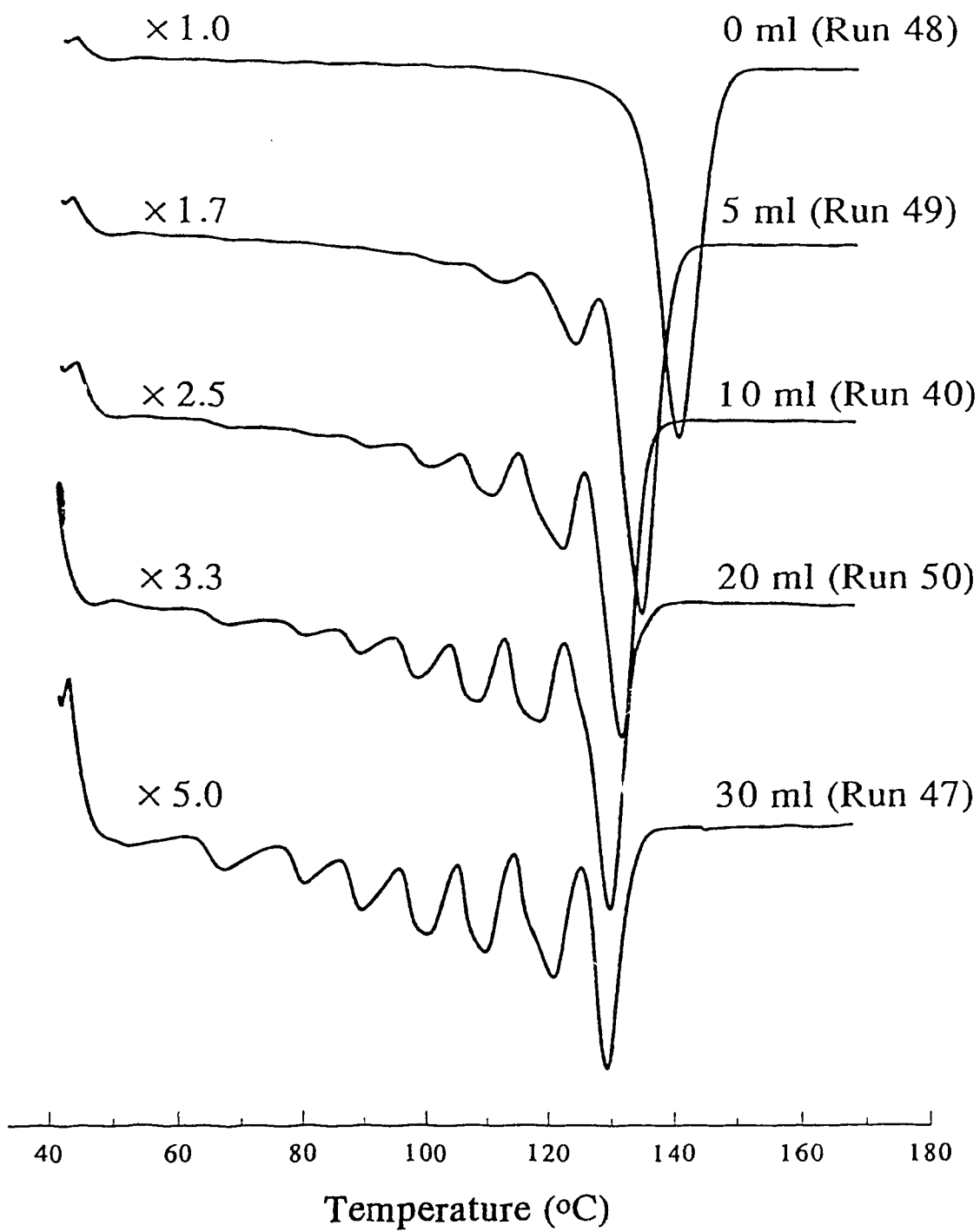


Figure 8.1 Endotherms of thermally fractionated LLDPE.

The effect of branching on the shape of the F-DSC endotherm was clearly indicated in Figure 8.1. It was observed that the valleys of each endotherm corresponded to the pre-set annealing temperatures. For an ethylene homopolymer, the heat trace was a single peak with a minor tail on the lower temperature side, for the majority of the linear molecules were able to crystallize in one temperature step. Successive increases in the branching frequency produced a greater number of clearly defined peaks in the individual endotherms.

Endotherms in Figure 8.1 were deconvoluted into individual Gaussian peaks through Peakfit™, and the areas corresponding to each annealing temperature are plotted in Figure 8.2. It is noted that only molecules free of side branches were able to form the most stable crystals at the highest annealing temperature (135°C). This feature had a resemblant counterpart in TREF, as it has been pointed out in Section 5.4 that the elution temperature for a homopolymer was about 6°C higher than that for the linear fraction of a copolymer. Such observation indicated that molecules eluted in the "linear" fraction may have sufficient side branches to shift the elution temperature downwards by several degrees in TREF and lower the maximum annealing temperature by one step in F-DSC. Among the copolymers, it was observed that the increased comonomer incorporation was met with increasing lower temperature fractions, as expected. Through integration, Figure 8.2 was transformed to Figure 8.3, a plot of mass fraction x as a function of annealing temperature T_A . With a properly chosen cut-off temperature, the relative composition of linear and branched molecules can be estimated in the same manner described in Section 5.4.

In Figure 8.4, the TREF elution temperatures (T_E) corresponding to the mass fractions of the annealing temperatures $x=f(T_A)$ were plotted against T_A , i.e. $T_E(x(T_A))$ versus T_A . The remarkable correlation between T_A and T_E again indicated that estimation of the branching frequency based on analytical TREF can be made probably just as well with F-DSC. Such excellent correlation raised one question, however. It is known that DSC endotherms should register, in principle at least, the melting of crystalline domains in the specimen. (Note in Figure 8.1

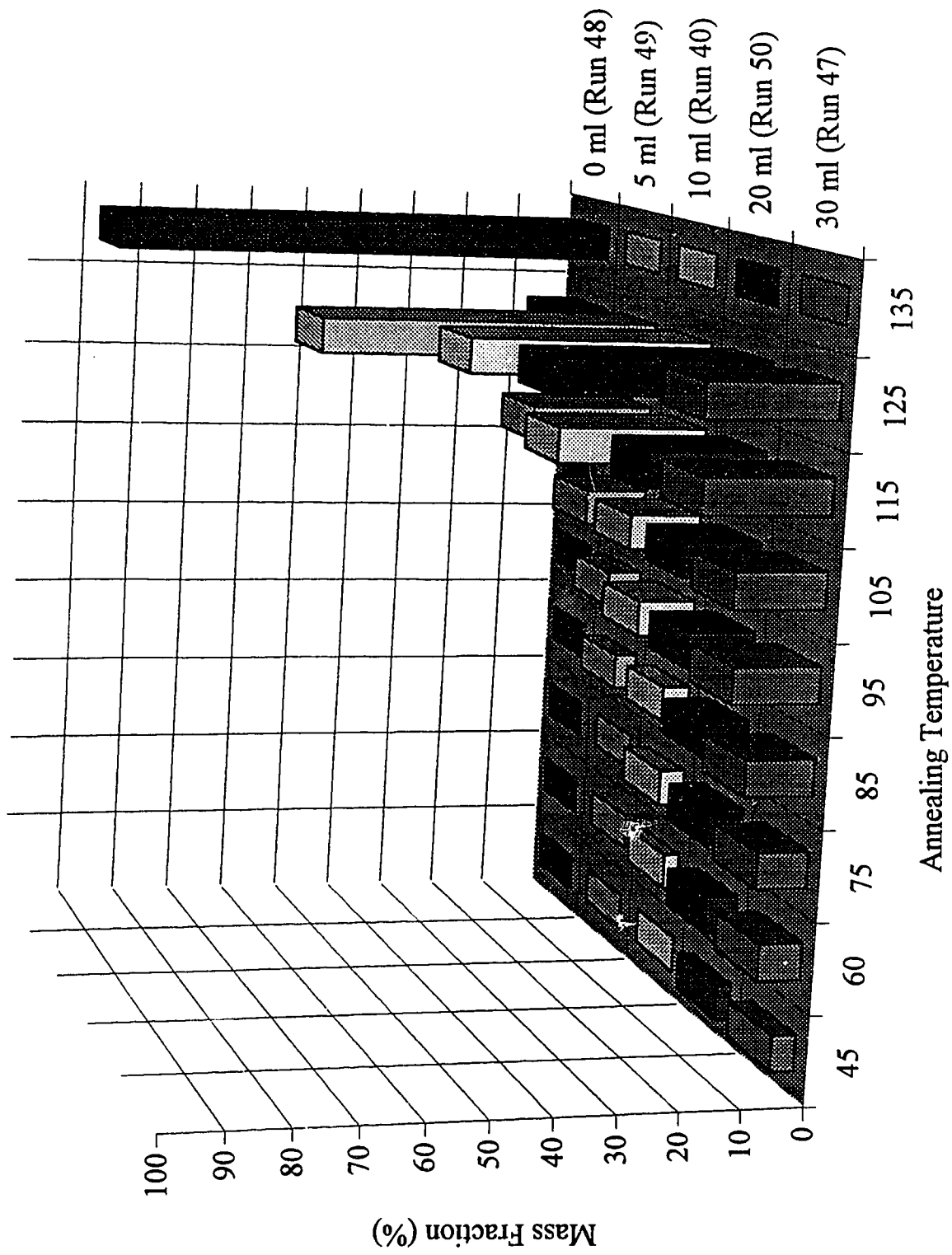


Figure 8.2 Percentage of fractionated molecules versus temperature

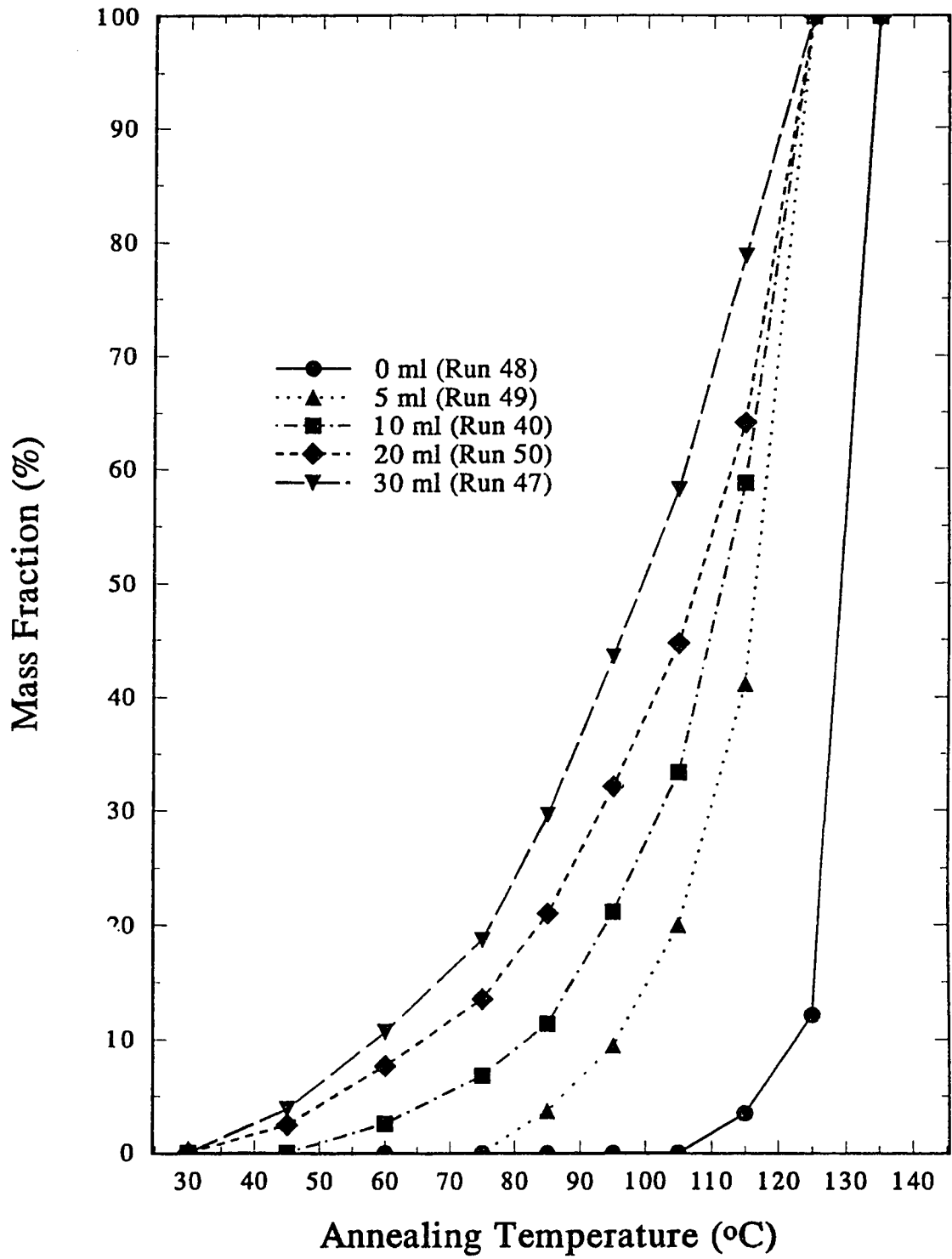


Figure 8.3 Integrated F-DSC profiles

$$T_E = -30.9 + 0.956 T_A, R^2=0.982$$

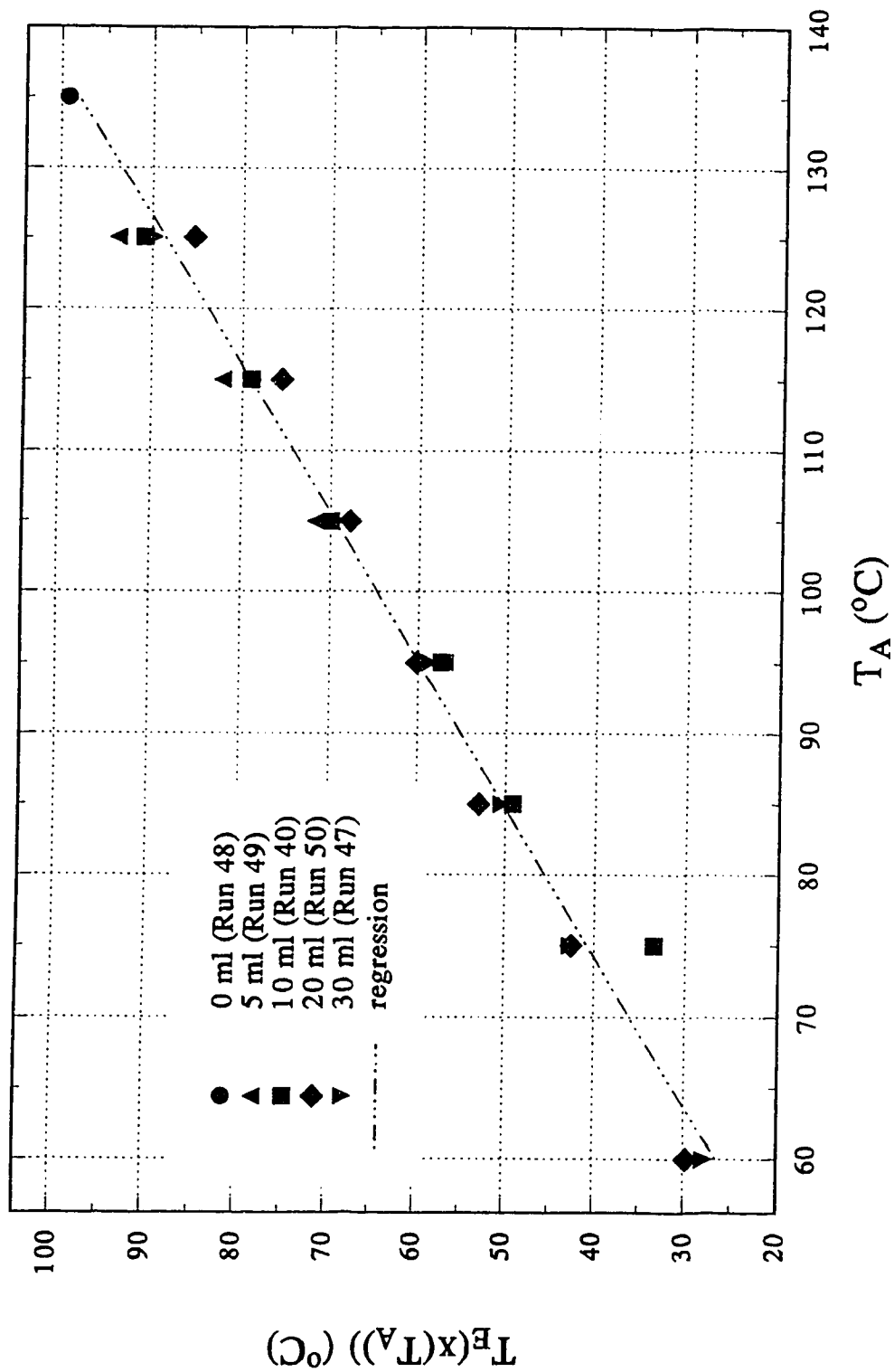


Figure 8.4 Elution temperature versus annealing temperature

that the increase of branching was accompanied by a decrease in the signal intensity.) TREF on the other hand is generally thought to achieve complete recovery of the molecules, crystalline as well as amorphous, by the end of the cooling period. Since the measured objects were different, it was not understood as to why the outcomes from these two techniques would neatly mirror each other. Further studies in this area are needed to resolve this quandry.

9. CONSIDERATIONS FOR FUTURE STUDIES

Conclusions made at the end of each section will not be reiterated other than to serve as background information for the proposed studies in the kinetics of propagation (Section 9.1) and termination (Section 9.2), characterization techniques such as GPC (Section 9.3), DSC (Section 9.4), TREF (Section 9.5) and MALDI-MS (Section 9.6), modelling of dilute-solution crystallization (Section 9.7), and blending of polyolefins (Section 9.8).

9.1 Kinetics of Comonomer Incorporation

In Chapter 5, it was suggested that due to the continued reduction of titanium valence by the cocatalyst, the extent of copolymerization should decrease with time. According to this supposition, the logical consequence becomes that branching distributions of LLDPE produced at different time intervals would vary, for the majority of the branched polyethylene are produced prior to the formation of a significant amount of linear polyethylene. (Unfortunately, sampling of reactor product at different stages of reaction is difficult under the present set-up; the only recourse to a study of branching distribution as a function of time would require several runs under the identical experimental conditions but for different time durations.)

If copolymerization of ethylene and 1-butene indeed precedes homopolymerization of ethylene, the initial TREF profile would have a large peak at the lower temperature range for the branched polyethylene and a small one for the linear. As time progresses, the relative sizes of these two peaks will change; the longer the experiment, the smaller the ethylene/1-butene copolymer peak. These TREF profiles can be normalized according to the reactor yields, and overlapping these individual profiles would indicate the changing composition

of LLDPE as a function of time. Representing the series of TREF profiles by a contour plot can be equally informative about the kinetic behaviour of the catalyst.

Nevertheless, it is important to remember that the stress created by polyethylene formed on the surface causes the friable catalyst particles to fracture; newer active sites are susceptible to polymerization upon valence reduction. Catalyst particles continue to fracture until no further disintegration is possible, and if this process is complete before the majority of Ti^{+3} sites are converted to Ti^{+2} , the time-temperature-concentration contour plot described above would be affected little. On the other hand, a prolonged period of particle disintegration would not confine the comonomer incorporation to the initial stages of the reaction, and the series of TREF profiles would be time-insensitive. To minimize the period of catalyst disintegration, it is possible to operate the reactor at a higher overall pressure such that polyethylene molecules rapidly fill the pores and shatter the catalyst particles.

While the diffusional limitation of ethylene or 1-butene to the active sites has been demonstrated to be almost nonexistent, there is no dispute regarding the very real hinderance experienced by bulky aluminium alkyl molecules to the catalyst surface. As the access of the cocatalyst depends on the morphology of the catalyst particles and of the nascent polyethylene powders, active sites are more vulnerable to overreduction initially than would be a short while later. If the linear peak is dominant at first and gradually diminishes with respect to the branched peak, it is likely to be caused by the overreduction of catalyst.

The wealth of information that can be afforded potentially by the time-temperature-concentration plots deserves serious investigation. Currently all the three-dimensional plots available in open literature are MMD-temperature-concentration, a lamentable fact given that TREF is not an analytical tool merely capable of characterizing commercial resins. The ability of TREF to fractionate molecules according to the branching frequency should be better utilized to generate insights which would enhance the understanding of the dynamic behaviour of Ziegler-Natta polymerization kinetics.

9.2 Kinetics of Termination by Hydrogen

In Chapter 6, number-average molar mass was plotted against hydrogen pressure to determine the termination rate order. It was suggested that copolymer sites are terminated via first-order kinetics whereas homopolymer sites terminate via half-order. This hypothesis can be verified if the samples produced in Section 9.1 are carefully analyzed.

It is possible, however, that over a wide range of hydrogen pressure, the termination rate order can be affected by surface coverage: at low surface coverage, hydrogen molecules are dissociately adsorbed onto two different sites and terminate the growing chains via half-order kinetics, whereas at high surface coverage, hydrogen molecules can only react directly with the propagation centres to terminate the chains. To verify this hypothesis, it is suggested that polymerization experiments be carried out under various hydrogen pressures at several different temperatures. (As the activation energy for chain termination is greater than for propagation, a sample prepared at a lower temperature would have a higher molar mass under the same amount of hydrogen pressure, and vice versa. In other words, samples prepared at low temperature with scant amount of hydrogen would have molar masses too high for GPC¹, whereas those prepared at high temperature with substantial amount of the chain transfer agent would be too low².)

¹The upper limit of GPC measurement is dictated by the pore size of the packing material. Complete exclusion occurs when the diameter of a molecule's hydrodynamic volume is greater than the largest openings of the porous gel. No separation takes place under such circumstance.

²The lower limit of GPC is governed by the rheology of dilute polymer solution in addition to the pore size distribution. Smaller molecules may require a different set of Mark-Houwink parameters to account for the extra hydrodynamic volumes occupied by the non-spherical random-coils. These molecules may also completely permeate the pores such that no chromatography is possible.

With experiments carried out at high temperature covering the low- P_{H_2} range and those at low temperature, high- P_{H_2} , it is possible to assemble sets of molar mass data measured reliably by GPC. If the slope of $\log(M_n)$ versus $\log(P_{H_2})$ is a constant for samples prepared at each isotherm, termination rate order is independent of surface coverage. On the other hand if the slopes remain functions of hydrogen pressure, termination rate order can be stated with certainty to be dependent on the surface coverage of hydrogen.

9.3 Gel Permeation Chromatography

Accurate determination of molar mass distribution is pivotal to the validity of kinetic arguments presented in Chapter 6. While the operation of GPC for MMD determination has become routine, the calibration of elution time versus molar mass is not. The lack of narrowly-distributed polyethylene standards requires the use of universal calibration curves to relate the hydrodynamic volume (HDV) of polystyrene standards to the elution time. Further conversion of HDV_{PS} to HDV_{PE} would depend on accurately determined Mark-Houwink parameters (K ; α) for both polymers, yet values for K and α reported in the open literature often vary considerably. Another serious defect of the Mark-Houwink relationship is its limited range of applicability: molar masses for molecules with extreme sizes are known to deviate significantly from the predicted values.

In the absence of narrowly-distributed polyethylene samples for calibration, it is recommended that a recent revision (Sanayei et al., 1993) to the Mark-Houwink relationship be implemented, for it has been shown to better predict the intrinsic viscosity of polymer solution over a wider range of molar mass. Alternatively, one would bypass the universal calibration curve by establishing a reliable correlation between retention time and molar mass of narrowly-distributed polyethylene samples whose MMDs are precisely determined by matrix-assisted laser ionization desorption (MALDI) mass spectroscopy, which is discussed in Section 9.6.

9.4 Differential Scanning Calorimetry

The integrity of crystallinity studies presented in Chapter 7 rests in the proper determination of fusion enthalpy. Due to the difference in heat capacity for solid and melt, endotherms do not return to the same baseline after the melting process. For the present study, the effect of heat capacity variation was repressed by intensifying the enthalpy signal through a high heating rate of 10°C/min. For future investigations, it is recommended that Modulated DSCTM (MDSC), a technique in which a sinusoidal temperature fluctuation is superimposed upon a linear heating rate, be implemented to clearly isolate the actual melting of crystals from the heating of amorphous materials. Such investment is warranted by the future understanding in the structural properties of both powders and resins and the crystallization behaviour both during polymerization and from melt which is not available otherwise.

9.5 Temperature Rising Elution Fractionation

The slow cooling step in TREF is a process of complex interaction between the thermodynamics of precipitation and the kinetics of crystallization. It is well known that at any given temperature T , macromolecules would rather interact with themselves than with solutions and precipitate from the solution if $T < \theta_f$, conform to unswollen random coils if $T = \theta_f$, or expand into larger random coils if $T > \theta_f$. (θ is the theta temperature for the polymer molecule.) It is also understood that the spacing between successive branch points known as the methylene sequence length affects the kinetics of crystallization. However, it remains to be addressed as to how the thermodynamically controlled precipitation is connected to the kinetically controlled chain-folding. A sizable difference between precipitation temperature and crystallization temperature would suggest that not all polymer molecules have been crystallized by the end of the cooling process.

If a complete recovery of the highly branched molecules from solution is not feasible, off-column crystallization technique deserves review and the analytical TREF profiles or TREF-GPC contour plots should be interpreted with caution and skepticism.

9.6 Matrix-Assisted Laser Desorption Ionization Mass Spectroscopy

Unlike gel permeation chromatography, determination of molar mass distribution of large molecules by mass spectroscopy (MS) does not require any calibration, the source of various complications in GPC. Although MS is immensely popular for characterizing large biomolecules such as proteins and peptides and in recent years for several synthetic polymers such as polymethylmethacrylate or polystyrene, it is not suited for characterizing various polyolefins due to the absence of any free electrons needed for ionization.

However, at least two routes exist to attach functional groups to polyethylene. Firstly, one would obtain functionalized polyethylene by terminating the polymerization with Br_2 or H_2O_2 on metallocene-type catalysts to form $\text{CH}_3-(\text{CH}_2)_n-\text{Br}$ or $\text{CH}_3-(\text{CH}_2)_n-\text{OH}$ (Bercaw, 1995), both of which have lone electron pairs ready for ionization by Li^+ , Na^+ , or K^+ . Alternatively, noting that polyethylene produced over chromium oxide catalyst are predominately terminated via β -elimination, it is possible that the resulting terminal double bonds in these molecules be functionalized by the adding bromine or hydrogen peroxide into some dilute polymer solution to form the same functionalized PEs.

Rather than attaching functional groups to all PE molecules for MMD characterization, it is recommended that narrowly-distributed fractions of these samples³ with the potential of being functionalized be used as GPC standards.

³Polymers produced over metallocene catalysts have very narrow MMD; furthermore, at low temperature, living polymerization can be achieved to afford monodisperse functionalized PE. Those produced over CrO_3 generally have very broad MMDs; repeated preparative GPC is necessary.

This would enable one to relate the retention times to the molar masses as determined precisely by matrix-assisted laser desorption ionization mass spectroscopy (MALDI-MS).

9.7 Modelling of Crystallization in Dilute Solution

The notion that a diffusional barrier not only exists but has several different types (Ray, 1991) has led to a tremendous amount of modelling work on kinetics of Ziegler-Natta polymerization and the molar mass distribution of the products. However, there is ruefully little published work on the modelling of comonomer incorporation. While there are few studies directed toward deducing fundamental kinetic parameters from TREF profiles *a posteriori*, the level of mathematical sophistication is rudimentary by comparison. Quite likely this absence of modelling studies is the lack of reliable experimental verifications from the unstandardized technique of TREF, which in turn lacks a unified approach to generate reproducible profiles. The purpose of the remainder of this section is to lay a framework for predicting the distribution of comonomer incorporation (i.e. TREF profiles) based on a few kinetic parameters.

In a highly dilute polymer solution where molecules are separated by a distance greater than the averaged end-to-end distance⁴, the only factor which would govern the ability of an individual molecule to chain-fold from random-

⁴It is known that the end-to-end distance is related to intrinsic viscosity as

$$[\eta] = \Phi \frac{(\overline{r^2})^{3/2}}{M}$$

(Flory and Fox, 1951). Since the intrinsic viscosity can be estimated by the Mark-Houwink relationship ($[\eta]=KM^a$), the above equation can be rewritten as

$$\overline{r^2} = \left(\frac{KM^{a+1}}{\Phi} \right)^{2/3}$$

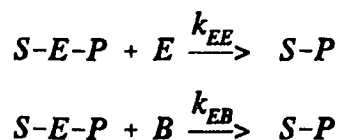
where Φ is around $2.4 \pm 0.3 \times 10^{21}$ dl/mol·cm³ (Brandrup and Immergut, 1989).

coil conformation becomes the spans between the successive branch points called methylene sequence length (MSL). MSL is equivalent to twice the kinetic parameter r_1 , or the ratio of k_{EE} to k_{EB} ⁵. There is a possibility where MSL is a constant within a molecule such that all ethyl branches are located at the junctures of chain-folds. Yet a realistic LLDPE molecule would have an MSL distribution (MSLD), which is a vector of MSLs describing the pattern of the intramolecular branching distribution.

While an LLDPE molecule is comprised of segments of different methylene sequence length, it does not crystallize in isolated segments at different temperatures corresponding to individual MSLs. Hence there exists a characteristic MSL (cMSL) which corresponds to the temperature at which a given polyethylene molecule chain-folds. It can be envisaged that if a given segment's MSL is smaller than cMSL of the molecule under the prevailing conditions, both ethyl endgroups and all methylene units in between will be excluded from the folded array, and the entire segment will not crystallize. On the other hand, if the segment's MSL is larger than the cMSL of the molecule, only the portion equal to cMSL or its multiple will be accommodated by the crystal lattice, with the excess methylene units residing in the amorphous domain.

In the very unlikely scenario where all MSLs in an LLDPE molecule have the same value, evaluation of cMSL is a trivial task as MSLD is a delta function. For more realistic molecules, it is necessary to establish a routine procedure for generating a value of significance to crystallization from any MSLD. Similar to the ratios of successive moments used extensively in the field of polymer science for characterizing the statistical natures of key properties, the number-average

⁵These two parameters are defined as follows:



where E, B, S, and P represent ethylene, 1-butene, the active site, and the propagating polymer chain, respectively.

MSL (MSL_n) and weight-average MSL (MSL_w) for MSLD can be defined analogously. It is quite possible that MSL_w would better approximate the onset of chain-folding as MSL_n is unable to discriminate a molecule with evenly spaced branches from another with blocky structure.

The problem that remains is to generate myriads of computational LLDPE molecules and for each molecule calculate its cMSL and elution temperature.⁵ The process of building fictitious molecules with rules such as time, branching frequency, and molar mass distribution falls into the realm of Monte Carlo simulation. Simple statistical models such as Bernoulli or Poisson are fundamentally flawed, for fractionation of *molecules* is not based on the individual segments of methylene sequence.

9.8 Polyethylene Blends

The purpose for polymer blending is to obtain a new type of material which would retain the desirable physical and rheological properties of the constituents. Adding HDPE to LLDPE which is multimodal in branching frequency distribution can be viewed as adjusting the fraction of linear molecules in LLDPEs. The very fact that linear-low density polyethylene is comprised of linear and branched molecules was not widely known to the polymer blends community until very recently. Various reports on the cocrystallization of LLDPE with HDPE have yet to acknowledge that LLDPE itself is a blend of polyethylene molecules with

⁵Once cMSL is determined for an LLDPE molecule, the elution temperature of the molecule can be predicted according to the following expression which is valid up to the onset of chain-folding:

$$\frac{1}{T} = \frac{1}{T_0} + C \frac{\ln cMSL}{cMSL}$$

(Bonner et al., 1993). T_0 and C are parameters, specific to the solvent system used, to be determined through the calibration of linear paraffins.

varying degree of branching; blends of HDPE with LLDPE's linear molecules crystallizing together is only intuitive.

Whether the desired mixture of linear and branched polyethylene molecules can be achieved directly through polymer reaction engineering is of great interest, as the process of blending different grades of polyethylenes might thereby be eliminated. While experimental studies in polyethylene blends have become popular, definite conclusions are difficult to draw, for rarely the starting materials are characterized fully by analytical techniques available. Systematic studies on the rheological and physical properties of the products generated in the proposed experiments outlined in Sections 9.1 and 9.2 may provide the much needed information on the structure-property relationships of polyethylene blends, especially when the results are analyzed in conjunction with reliable MMD and TREF characterization. Ultimately the purpose would be to collect comprehensive sets of thermodynamic data for the preparation of phase diagrams and the development of equations of state which would provide information on the phase transition behaviour along with detailed thermal, mechanical, rheological, optical, morphological, and processing characteristics at various molar mass distribution, branching frequency and type, and ratio of linear to branched molecules, all of which are related to the reactor operating conditions to guide the future design of catalysts.

10. REFERENCES

- Al-Hillo, Malik R. Y., Robert N. Haward, and Ian W. Parsons, "A Comparison Between Alkylgallium and Alkylmagnesium Reduced Vanadium-based Ziegler-Natta Catalysts: Gallium versus Magnesium Chloride as Support for Vanadium," *Polymer*, 31:949 (1990).
- Balbontin, Giulio, Isabella Camurati, Tiziano Dall'Occo, Anita Finotti, Rocco Franzese, and Giancarlo Vecellio, "Determination of 1-Butene Distribution in LLDPE by DSC Analysis After Thermal Fractionated Crystallization," *Die Angewandte Makromolekulare Chemie*, 219:139 (1994).
- Barlow, A., L. Wild, and R. Ranganath, "Gel Permeation Chromatography of Polyethylene. I. Calibration," *Journal of Applied Polymer Science*, 21:3319, (1977).
- Bercaw, John E., Department of Chemistry, California Institute of Technology, private communication, 1995.
- Brandrup, J., and E. H. Immergut, eds., *Polymer Handbook*, 3rd ed., Wiley-Interscience, New York, 1989, Chapter VII.
- Bonner, J. G., C. J. Frye, and G. Capaccio, "A Novel Calibration for The Characterization of Polyethylene Copolymers by Temperature Rising Elution Fractionation," *Polymer*, 34:3532 (1993).
- Boor, John, *Ziegler-Natta Catalysts and Polymerizations*, Academic Press, New York, 1979, Chapter 10.
- Bremner, T., A. Rudin, and D. G. Cook, "Melt Flow Index and Molecular Weight Distributions of Commercial Thermoplastics," *Journal of Applied Polymer Science*, 41:1617 (1990).
- Bremner, T., D. G. Cook, and A. Rudin, "Further Comments on the Relations between Melt Flow Index Values and Molecular Weight Distributions of Commercial Plastics," *Journal of Applied Polymer Science*, 43:1773 (1991).
- Bu, N., D. T. Lynch, and S. E. Wanke, "Kinetics of Catalytic Gas-Phase Homopolymerization of Ethylene over SiO₂/MgCl₂ - Supported TiCl₄ Catalysts," *Polymer Reaction Engineering*, 3:1 (1995).
- Busico, Vincenzo, Paolo Corradini, Luigi De Martino, Antonio Proto, Vito Savino, and Enrico Albizzati, "Polymerization of Propene in the Presence of MgCl₂-

Supported Ziegler-Natta Catalysts, 1. The Role of Ethyl Benzoate as 'Internal' and 'External' Base," *Die Makromolekulare Chemie*, 186:1279 (1985).

Busico, Vincenzo, Paolo Corradini, Luigi De Martino, and Antonio Proto, "Polymerization of Propene in the Presence of $MgCl_2$ -supported Ziegler-Natta Catalysts, 2. Effects of the Co-catalyst Composition," *Die Makromolekulare Chemie*, 187:1115 (1986).

Calabro, D. C., and F. Y. Lo, "A Comparison of the Reaction Kinetics for the Homo- and Copolymerization of Ethylene and Hexene with a Heterogeneous Ziegler Catalyst" in *Transition Metal Catalyzed Polymerisations, Alkenes and Dienes*, Roderic P. Quirk Ed., MMI Press Symposium Series, Hardwood, New York, 1981, p. 729.

Chen, Christopher Ming-Po, *Gas Phase Olefin Copolymerization with Ziegler-Natta Catalysts*, PhD thesis, Department of Chemical Engineering, University of Wisconsin, Madison, Wisconsin, USA, 1993.

Chien, James C. W., Chi-I Kuo, and Tsunle Ang, "Magnesium Chloride Supported High-Mileage Catalysts for Olefin Polymerizations. VI. Definitive Evidence Against Diffusion Limitation," *Journal of Polymer Science: Part A: Polymer Chemistry*, 23:723 (1985).

Chien, James C. W., and Phillippe L. Bres, "Magnesium Chloride Supported High-Mileage Catalysts for Olefin Polymerizations. XII. Polymerization of Ethylene," *Journal of Polymer Science: Part A: Polymer Chemistry*, 24:2483 (1986).

Chien, J. C. W., "Polymerization of Olefins with Magnesium Chloride-Supported Catalysts" in *Advances in Polyolefins — The World's Most Widely Used Polymers*, Raymond B. Seymour and Tai Cheng Eds., Plenum Press, New York, 1987, p. 255.

Chien, James C. W., and Youliang Hu, "Magnesium Chloride Supported High-Mileage Catalysts for Olefin Polymerizations. XVIII. Effect of Hydrogen and Lewis Bases," *Journal of Polymer Science: Part A: Polymer Chemistry*, 25:2881 (1987).

Chien, James C. W., and Chi-I Kuo, "Magnesium Chloride Supported High-Mileage Catalysts for Olefin Polymerization. XVIII. Effect of Hydrogen and Lewis Bases," *Journal of Polymer Science: Part A: Polymer Chemistry*, 24:1779 (1986).

Chien, James C. W., Siegfried Weber, and Youliang Hu, "Magnesium Chloride Supported Catalysts for Olefin Polymerization. XIX. Titanium Oxidation States, Catalyst Deactivation, and Active Site Structure," *Journal of Polymer Science: Part A: Polymer Chemistry*, 27:1499 (1989).

Chien, James C. W., and Takashi Nozaki, "Ethylene-Hexene Copolymerization by Heterogeneous and Homogeneous Ziegler-Natta Catalysts and the

'Comonomer' Effect," *Journal of Polymer Science: Part A: Polymer Chemistry*, 31:227 (1993).

Chiu, Fang-Chyou, M. Y. Keating, and Stephen Z. D. Cheng, "Molecular Segmental Segregation Effect on the Melting Behaviours and Morphology of Linear Low-Density Polyethylene," *Proceedings of the Society of Plastics Engineers Annual Technical Conference - ANTEC*, 53:1503 (1995).

Chung, Jin Suk, In Kyu Song, Wha Young Lee, and Hong Man Park, "Morphology Control of a $MgCl_2$ -supported Ziegler-Natta Catalyst by the Recrystallization Method," *Macromolecular Chemistry and Physics*, 196:1205 (1995).

Defoor, F., G. Groenickx, P. Schouterden, and B. Van der Heijden, "Molecular, Thermal, and Morphological Characterization of Narrowly Branched Fractions of 1-Octene Linear Low-Density Polyethylene: 1. Molecular and Thermal characterization," *Polymer*, 33:3878 (1992).

de Santa Maria, Luiz Claudio, Kazuo Soga, and Takeshi Shiono, "Polymerization of Olefins with the $TiCl_4/SiO_2$ Catalyst System Modified with $MgCl_2$," *Macromolecular Chemistry and Physics*, 195:2591 (1994).

Dumoulin, M. M., P. J. Carreau, and L. A. Utracki, "Rheological Properties of Linear Low-Density Polyethylene/Polypropylene Blends. Part 2: Solid State Behaviour," *Polymer Engineering and Science*, 27:1627 (1987).

Dusseault, John J. A., *The Gas-Phase Polymerization Kinetics of Ethylene over $MgCl_2$ Supported Ziegler-Natta Catalyst*, PhD thesis, Department of Chemical Engineering, Queen's University, Kingston, Ontario, Canada, 1991.

Dusseault, John J. A., and Cheng C. Hsu, " $MgCl_2$ -Supported Ziegler-Natta Catalysts for Olefin Polymerization: Basic Structure, Mechanism, and Kinetic Behavior," *Journal of Macromolecular Science — Review in Macromolecular Chemistry and Physics*, C33(2):103 (1993).

Flory, P. J., and T. G. Fox, "Treatment of Intrinsic Viscosities," *Journal of the American Chemical Society*, 73:1904 (1951).

Flory, Paul J., *Principles of Polymer Chemistry*, Cornell University Press, Ithaca, NY, 1953.

Floyd, S., Tomi Heiskanen, T. W. Taylor, G. E. Mann, and W. H. Ray, "Polymerization of Olefins Through Heterogeneous Catalysis. VI. Effect of Particle Heat and Mass Transfer on Polymerization Behavior and Polymer Properties," *Journal of Applied Polymer Science*, 33:1021 (1987).

Foreman, Jonathon A., and Roger L. Blaine, "Optimization of the Modulated DSC Technique for Plastics," *Proceedings of the Society of Plastics Engineers Annual Technical Conference - ANTEC*, 53:2499 (1995).

Galimberti, M., Piemontesi, F., Giannini, U., and Albizzati, E., "Transition-Metal Organometallic Compounds as Cocatalysts in Olefin Polymerization with $MgCl_2$ -Supported Catalysts," *Macromolecules*, 26:6771 (1993).

Gates, Bruce C., James R. Katzer, and G. C. A. Schuit, *Chemistry of Catalytic Processes*, McGraw-Hill, New York, 1979, p. 127.

Ghosh, Tamal A., Jim C. Huang, and Michael C. Williams, "Melt Index for Molecular Weight Quality Control," submitted to *Polymer Engineering and Science*, (1995).

Greenspun, V., K. F. O'Driscoll, and A. Rudin, "High Temperature Size Exclusion Chromatography," *ACS Symposium Series*, 245:273 (1984).

Harrison, Ian R., Department of Materials Science, Penn State University, private communication (1995).

Hellmuth, E., and B. Wunderlich, "Superheating of Linear High-Polymer Polyethylene Crystals," *Journal of Applied Physics*, 36:3039 (1965).

Hill, Mary J., "Liquid-Liquid Phase Separation in Binary Blends of A Branched Polyethylene with Linear Polyethylenes of Different Molecular Weight," *Polymer*, 35:1991 (1994).

Hill, Mary J., and Peter J. Barham, "Liquid-Liquid Phase Separation in Melts of Blends of Linear with Branched Polyethylenes: Morphological Exploration of the Phase Diagram," *Polymer*, 33:4099 (1992a).

Hill, Mary J., and Peter J. Barham, "Diffusion Effects in Blends of Linear and Branched Polyethylenes," *Polymer*, 33:4891 (1992b).

Hill, Mary J., and P. J. Barham, "Interpretation of Phase Behaviour of Blends Containing Linear Low-Density Polyethylenes Using A Ternary Phase Diagram," *Polymer*, 35:1802 (1994).

Hill, Mary J., and P. J. Barham, "Absence of Phase Separation Effects in Blends of Linear Polyethylene Fractions of Differing Molecular Weight," *Polymer*, 36:1523 (1995).

Hill, M. J., P. J. Barham, and J. van Ruiten, "Liquid-Liquid Phase Segregation in Blends of a Linear Polyethylene with A Series of Octene Copolymers of Different Branch Content," *Polymer*, 35:2975 (1993).

Hill, M. J., L. Oiarzabal, and J. S. Higgins, "Preliminary Studies of Polypropylene/Linear Low Density Polyethylene Blends by Transmission Electron Microscopy," *Polymer*, 35:3332 (1994).

Hosoda, S., K. Kojima, and M. Furuta, "Morphological Study of Melt-Crystallized Linear Low-Density Polyethylene by Transmission Electron Microscopy," *Die Makromolekulare Chemie*, 187:1501 (1986).

Hosoda, Satoru, "Structural Distribution of Linear Low-Density Polyethylenes," *Polymer Journal*, 20:383 (1988).

Hsieh, H. L., "Olefin Polymerization Catalysis Technology," *Catalysis Review — Science and Engineering*, 26:631 (1984).

Hu, Shi-Ru, Thein Kyu, and Richard S. Stein, "Characterization and Properties of Polyethylene Blends. I. Linear Low-Density Polyethylene with High-Density Polyethylene," *Journal of Polymer Science: Part B: Polymer Physics*, 25:71 (1987).

Jaber, Isam A., Klaus Hauschild, and Gerhard Fink, "TiCl₄/MgH₂-supported Ziegler-type Catalyst System, 2: Effect of Ti Concentration, Ti Content and Surface Area of TiCl₄/MgH₂ Catalyst on the Concentration of Active Sites in Ethylene Polymerization," *Die Makromolekulare Chemie*, 191:2067 (1990).

Jaber, Isam A., and W. Harmon Ray, "Polymerization of Olefins through Heterogeneous Catalysis. XII. The Influence of Hydrogen in the Solution Copolymerization of Ethylene," *Journal of Applied Polymer Science*, 49:1695 (1993).

Janzen, Jay, "Elastic Moduli of Semicrystalline Polyethylenes Compared with Theoretical Micromechanical Models for Composites," *Polymer Engineering and Science*, 32:1242 (1992).

Jejelowo, M. O., D. T. Lynch, and S. E. Wanke, "Comparison of Ethylene Polymerization in Gas-Phase and Slurry Reactors," *Macromolecules*, 24:1755 (1991).

Joskowicz, Pablo L., Alberto Muñoz, Julio Barrera, and Alejandro J. Müller, "Calorimetric Study of Blends of Low Density Polyethylene (LDPE) and Linear Low Density Polyethylene (LLDPE) Temperature Rising Elution Fractionation (TREF) Fractions," *Macromolecular Chemistry and Physics*, 196:385 (1995).

Kakugo, Masahiro, Tatsuya Miyatake, and Kooji Mizunuma, "Chemical Composition Distribution of Ethylene—1-Hexene Copolymer Prepared with TiCl₃-Al(C₂H₅)₂Cl Catalyst," *Macromolecules*, 24:1469 (1991).

Karbashewski, Elizabeth, A. Rudin, L. Kale, W. J. Tchir, and H. P. Schreiber, "Effects of Polymer Structure on the Onset of Processing Defects in Linear Low Density Polyethylenes," *Polymer Engineering and Science*, 31:1581 (1991).

Karbashewski, Elizabeth, L. Kale, A. Rudin, W. J. Tchir, D. G. Cook, and J. O. Pronovost, "Characterization of Linear Low Density Polyethylene by Temperature Rising Elution Fractionation and by Differential Scanning Calorimetry," *Journal of Applied Polymer Science*, 44:425 (1992).

Karol, Frederick J., "Studies with High Activity Catalysts for Olefin Polymerization," *Catalysis Review — Science and Engineering*, 24:557 (1984).

Karol, F. J., B. E. Wagner, I. J. Levine, G. L. Goeke, and A. Noshay, "New Catalysis and Processes for Ethylene Polymerization" in *Advances in Polyolefins*, Raymond B. Seymour and Tai Cheng Eds., Plenum Press, New York, 1987, pp. 337-354.

Karol, Frederick J., Sun-Chueh Kao, and Kevin J. Cann, "Comonomer Effects with High-Activity Titanium- and Vanadium-Based Catalysts for Ethylene Polymerization," *Journal of Polymer Science: Part A: Polymer Chemistry*, 31:2541 (1993).

Karol, Frederick J., "Catalysis and the UNIPOL Process in the 1990s," *Macromolecular Symposia*, 89:563 (1995).

Keating, M. Y., and E. F. McCord, "Evaluation of the Comonomer Distribution in Ethylene Copolymers Using DSC Fractionation," *Thermochimica Acta*, 243:129 (1994).

Keii, Tominaga, Yoshiharu Doi, Eiichi Suzuki, Masanori Tamura, Masahide Murata, and Kazuo Soga, "Propene Polymerization with a Magnesium Chloride-Supported Ziegler Catalyst, 2: Molecular Weight Distribution," *Die Makromolekulare Chemie*, 185:1537 (1984).

Keii, Tominaga, "Mechanistic Studies on Ziegler-Natta Catalysis" in *Catalytic Polymerization of Olefins*, T. Keii and K. Soga Eds., Studies in Surface Science and Catalysis, Elsevier, Amsterdam, 1987, 25:1.

Kelusky, Eric C., Clay T. Elston, and Ron E. Murray, "Characterization Polyethylene-Based Blends with Temperature Rising Elution Fractionation (TREF) Techniques," *Polymer Engineering and Science*, 27:1562 (1987).

Kim, I., M. C. Chung, H. K. Choi, J. H. Kim, and S. I. Woo, "Olefin Polymerization with $\text{TiCl}_4/\text{THF}/\text{MgCl}_2$ Catalyst" in *Catalytic Olefin Polymerizations*, T. Keii and K. Soga Eds., Studies in Surface Science and Catalysis, Elsevier, Amsterdam, 1990, p. 56:323.

Kinkelin, Eberhard, Gerhard Fink, and Borislav Bogdanovic, " MgH_2 — A new Support for Ziegler-catalysts," *Die Makromolekulare Chemie — Rapid Communications*, 7:85 (1986).

Kissin, Y. V., *Isospecific Polymerization of Olefins with Heterogeneous Ziegler-Natta Catalysts*, Springer-Verlag, New York, 1985, Chapter IV

Kissin, Y. V., "Molecular Weight Distributions of Linear Polymers: Detailed Analysis from GPC Data," *Journal of Polymer Science: Part A: Polymer Chemistry*, 33:227 (1995).

Koivumäki, Jari, and Jukka V. Seppälä, "Observations on the Rate Enhancement Effect with $\text{MgCl}_2/\text{TiCl}_4$ and Cp_2ZrCl_2 Catalyst Systems upon 1-Hexene Addition," *Macromolecules*, 26:5535 (1993).

Kyu, Thein, Shi-Ru Hu, and Richard S. Stein, "Characterization and Properties of Polyethylene Blends. II. Linear Low-Density with Conventional Low-Density Polyethylene," *Journal of Polymer Science: Part B: Polymer Physics*, 25:89 (1987).

Lacombe, Yves, *TREF and SEC Characterization of Ethylene—1-Butene Copolymers Produced at Various 1-Butene and Hydrogen Pressures*, M.Sc. Thesis, Department of Chemical Engineering, University of Alberta, 1995.

Lu, Honglan, and Shijing Xiao, "Structure and Behaviour of $\text{SiO}_2/\text{MgCl}_2$ Bisupported Ziegler-Natta Catalysts for Olefin Polymerization," *Die Makromolekulare Chemie*, 194:421 (1993).

Lynch, David T., M. Olukayode Jejelowo, and Sieghard E. Wanke, "The Influence of Aluminum Alkyls on the Polymerization of Ethylene with $\text{SiO}_2/\text{MgCl}_2$ -Supported TiCl_4 Catalysts," *Canadian Journal of Chemical Engineering*, 69:657 (1991).

Lynch, David T., and Sieghard E. Wanke, "Reactor Design and Operation for Gas Phase Ethylene Polymerization Using Ziegler-Natta Catalysts," *Canadian Journal of Chemical Engineering*, 69:332 (1991).

Mara, J. J., and K. P. Menard, "Characterization of Linear Low Density Polyethylene by Temperature Rising Elution Fraction and by Differential Scanning Calorimetry," *Acta Polymer*, 45:378 (1994).

Marques, Maria M. V., Clemente Pedro Nunes, Peter J. T. Tait, and Alberto Ramao Dias, "Polymerization of Ethylene Using a High-Activity Ziegler-Natta Catalyst. I. Kinetic Studies," *Journal of Polymer Science: Part A: Polymer Chemistry*, 31:209 (1993).

Marques, Maria M. V., Clemente Pedro Nunes, Peter J. T. Tait, and Alberto Ramao Dias, "Polymerization of Ethylene Using a High-Activity Ziegler-Natta Catalyst. II. Molecular Weight Regulation," *Journal of Polymer Science: Part A: Polymer Chemistry*, 31:219 (1993).

Monrabal, Benjamin, "Crystallization Analysis Fractionation: A New Technique for the Analysis of Branching Distribution in Polyolefins," *Journal of Applied Polymer Science*, 52:491-499 (1994).

Mirabella, Francis M., and Emory A. Flord, "Characterization of Linear Low-Density Polyethylene: Cross-Fractionation According to Copolymer Composition and Molecular Weight," *Journal of Polymer Science: Part B: Polymer Physics*, 25:777 (1987).

Muñoz-Escalona, A., H. Garcia, and A. Albornoz, "Homo- and Copolymerization of Ethylene with Highly Active Catalysts Based on $TiCl_4$ and Grignard Compounds," *Journal of Applied Polymer Science*, 34:977 (1987).

Muñoz-Escalona, A., A. Fuentes, J. Liscano, and A. Albornoz "High Active Ziegler-Natta Catalysts for Homo- and Copolymerization of Ethylene by Supporting a Grignard Compound and $TiCl_4$ and SiO_2 " in *Catalytic Olefin Polymerization*, T. Keii and K. Soga Eds., Studies in Surface Science and Catalysis, Elsevier, Amsterdam, 1990, 56:377.

Nooijen, G. A. H., "On the Importance of Diffusion of Cocatalyst Molecules Through Heterogeneous Ziegler/Natta Catalysts," *European Polymer Journal*, 30:11-15 (1994).

Nowlin, T. E., Y. V. Kissin, and K. P. Wagner, High Activity Ziegler-Natta Catalysts for the Preparation of Ethylene Copolymers, *Journal of Polymer Science: Part A: Polymer Chemistry*, 26:755 (1988).

Ottani, Stefano, and Roger S. Porter, "A Calorimetric Investigation on High Molecular Weight Polyethylene Reactor Powders," *Journal of Polymer Science: Part B: Polymer Physics*, 29:1179 (1991).

Parsons, I. W., A. D. Caunt, R. N. Haward, J. A. Licchelli, and M. R. Y. Al-Hillo, "Highly Active Ethene Polymerization Catalysts Based on Titanium and Vanadium" in *Transition Metal Catalyzed Polymerisations, Alkenes and Dienes*, Roderic P. Quirk Ed., MMI Press Symposium Series, Hardwood, New York, 1981, p. 299.

Pasquet, Véronique, and Roger Spitz, "Molecular Weight Control of Linear Polyethylenes Prepared in Gas Phase with Ziegler Catalysts," *Die Makromolekulare Chemie*, 192:1509 (1991).

Pasquet, Véronique, and Roger Spitz, "Irreversible Activation Effects in Ethylene Polymerization," *Die Makromolekulare Chemie*, 194:451 (1993).

Peña, Begoña, Juan A. Delgado, Antonio Bello, and Ernesto Pérez, "Polymerization of 1-Decene with MgCl₂-supported Ziegler-Natta Catalyst Systems. Effect of Lewis Bases," *Die Makromolekulare Chemie — Rapid Communications*, 12:353 (1991).

Pino, P., P. Cioni, J. Wei, B. Rotzinger, and S. Arizzi, "Recent Developments in Basic Research on the Stereospecific Polymerization of α -Olefins" in *Transition Metal Catalyzed Polymerizations — Ziegler-Natta and Metathesis Polymerization*, Roderic P. Quirk Ed., Cambridge University Press, Cambridge, 1988a, p. 1.

Puig, C. C., M. J. Hill, and P. J. Barham, "Liquid Liquid Phase Separation in Polypropylene Homopolymer/Polypropylene Copolymer Melts," *Polymer*, 34:3117 (1993).

Puig, Cristian C., Jeffrey A. Odell, Mary J. Hill, Peter J. Barham, and Michael J. Folkes, "A Comparison of Blends of Linear with Branched Polyethylenes Prepared by Melt Mixing and by Solution Blending," *Polymer*, 35:2452 (1994).

Quijada, Raul, and Ana Maria Ramos Wanderley, "The Copolymerization of Ethylene and α -Olefins" in *Catalytic Polymerization of Olefins*, T. Keii and K. Soga Eds., Studies in Surface Science and Catalysis, Elsevier, Amsterdam, 1987, 25:419.

Ree, Moonhor, Thein Kyu, and Richard S. Stein, "Quantitative Small-Angle Light-Scattering Studies of the Melting and Crystallization of LLDPE/LDPE Blends," *Journal of Polymer Science: Part B: Polymer Physics*, 25:105 (1987).

Sailors, H. R., and J. P. Hogan, "History of Polyolefins" in *History of Polymer Science and Technology*, Raymond B. Seymour Ed., Marcel Dekker, New York, 1982, pp. 313-338.

Sanayei, R. Amin, S. Pang, and A. Rudin, "A New Approach to Establishing Universal Calibration Curves for Size Exclusion Chromatography," *Polymer*, 34:2320 (1993).

Sehanobish, K., R. M. Patel, B. A. Croft, S. P. Chum, and C. I. Kao, "Effect of Chain Microstructure on Modulus of Ethylene- α -Olefin Copolymers," *Journal of Applied Polymer Science*, 51:887 (1994).

Soga, Kazuo, Tsuneji Sano, and Rikuo Ohnishi, "Copolymerization of Ethylene with Propylene over the Thermally-Reduced γ -Al₂O₃-Supported TiCl₄ Catalyst," *Polymer Bulletin*, 4:157 (1981).

Soga, Kazuo, Shian-Ing Chen, and Rikuo Ohnishi, "Correlation Between the Oxidation States of Titanium and the Polymerization Activities for higher α -Olefins and Diene Compounds," *Polymer Bulletin*, 8:473 (1982).

Soga, Kazuo, Shian-Ing Chen, Y. Doi, and T. Shiono, "Highly Active Chromium Catalysts for Ethylene Polymerization" in *Advances in Polyolefins — The World's Most Widely Used Polymers*, Raymond B. Seymour and Tai Cheng Eds., Plenum Press, New York, 1987, p. 143.

Soga, Kazuo, Takeshi Shiono, and Yoshiharu Doi, "Influence of Internal and External Donors on Activity and Stereospecificity of Ziegler-Natta Catalysts," *Die Makromolekulare Chemie*, 189:1531 (1988).

Soga, Kazuo, Hisayoshi Yanagihara, and Dong-ho Lee, "Effect of Monomer Diffusion in the Polymerization of Olefins over Ziegler-Natta Catalysts," *Die Makromolekulare Chemie*, 190:995 (1989).

Soga, Kazuo, Masaaki Ohgizawa, Takeshi Shiono, and Dong-ho Lee, "Possibility of Mass-Transfer Resistance in Ethylene Polymerization with $MgCl_2$ -Supported Catalysts," *Macromolecules*, 24:1699 (1991).

Spitz, R., L. Duranel, P. Masson, M. F. Darricades-Llauro, and A. Guyot, "Difference in Reactivity between Ethylene and Propene with Supported Ziegler-Natta Catalysts" in *Transition Metal Catalyzed Polymerizations — Ziegler-Natta and Metathesis Polymerization*, Roderic P. Quirk Ed., Cambridge University Press, Cambridge, 1988a, p. 719.

Spitz, Roger, Patrick Masson, Charles Bobichon, and Alain Guyot, "Propene Polymerization with $MgCl_2$ Supported Ziegler Catalysts: Activation by Hydrogen and Ethylene," *Die Makromolekulare Chemie*, 189:1043 (1988b).

Spitz, Roger, Patrick Masson, Charles Bobichon, and Alain Guyot, "Activation of Propene Polymerization by Hydrogen for Improved $MgCl_2$ -supported Ziegler-Natta Catalysts," *Die Makromolekulare Chemie*, 190:717 (1989).

Spitz, R., C. Brun, and J. P. Joly, "Control of the Catalyst and Polymer Properties of Linear Polyethylenes" in *Catalytic Olefin Polymerization*, T. Keii and K. Soga Eds., Studies in Surface Science and Catalysis, Elsevier, Amsterdam, 1990, 56:117.

Stevens, Malcolm P., *Polymer Chemistry*, 2nd ed., Oxford University Press, New York, 1990, Chapter 6.

Sun, L., C. C. Hsu, and D. W. Bacon, "Polymer-Supported Ziegler-Natta Catalysts. I. A Preliminary Study of Catalyst Synthesis," *Journal of Polymer Science: Part A: Polymer Chemistry*, 32:2127 (1994).

Suzuki, Eiichi, Masanori Tamura, Yoshiharu Doi, and Tominaga Keii, "Molecular Weight during Polymerization of Propene with the Supported Catalyst System $TiCl_4/MgCl_2/C_6H_5COOC_2H_5/Al(C_2H_5)_3$," *Die Makromolekulare Chemie*, 180:2235 (1979).

Tait, P. J. T., "Kinetic Studies on Ziegler-Natta Polymerization - An Interpretation of Results" in *Catalytic Polymerization of Olefins*, T. Keii and K. Soga Eds., Studies in Surface Science and Catalysis, Elsevier, Amsterdam, 1987, 25:305.

Tait, P. J. T., G. W. Downs, and A. A. Akinbami, "Copolymerization of Ethylene and α -Olefins: A Kinetic Consideration" in *Transition Metal Catalyzed Polymerizations — Ziegler-Natta and Metathesis Polymerization*, Roderic P. Quirk Ed., Cambridge University Press, Cambridge, 1988, p. 834.

Takaoka, Tooru, Shigeru Ikai, Masanori Tamura, and Takefumi Yano, "Copolymerization of Ethylene with α -Olefins at High Temperature and Characterization of Copolymers," *Journal of Macromolecular Science - Pure and Applied Chemistry*, A32:83 (1995).

Tashiro, K., "Thermodynamic and Kinetic Aspects of Cocrystallization and Phase Segregation Phenomena of Polyethylene Blends between the D and H species as Viewed from DSC, FTIR, and Synchrotron X-ray Scattering," *Acta Polymer*, 110-113 (1995).

Tashiro, Kohji, Richard S. Stein and Shaw L. Hsu, "Cocrystallization and Phase Segregation of Polyethylene Blends. 1. Thermal and Vibrational Spectroscopic Study by Utilizing the Deuteration Technique," *Macromolecules*, 25:1801 (1992a).

Tashiro, Kohji, Michael M. Satkowski, Richard S. Stein, Yingjie Li, Benjamin Chu, and Shaw L. Hsu, "Cocrystallization and Phase Segregation of Polyethylene Blends. 2. Synchrotron-Sourced X-ray Scattering and Small-Angle light Scattering Study of the Blends between the D and H Species," *Macromolecules*, 25:1809 (1992b).

Tashiro, Kohji, Masaaki Izuchi, Masamichi Kobayashi, and Richard S. Stein, "Cocrystallization and Phase Segregation of Polyethylene Blends between the D and H Species. 3. Blend Content Dependence of the Crystallization Behavior," *Macromolecules*, 27:1221 (1994a).

Tashiro, Kohji, Masaaki Izuchi, Masamichi Kobayashi, and Richard S. Stein, "Cocrystallization and Phase Segregation of Polyethylene Blends between the D and H Species. 4. The Crystallization Behaviour As Viewed from the Infrared Spectral Changes," *Macromolecules*, 27:1221 (1994b).

Tashiro, Kohji, Masaaki Izuchi, Masamichi Kobayashi, and Richard S. Stein, "Cocrystallization and Phase Segregation of Polyethylene Blends between the D and H Species. 5. Structural Studies of the Blends as Viewed from Different Levels of Unit Cell to Spherulite," *Macromolecules*, 27:1221 (1994c).

Tashiro, Kohji, Masaaki Izuchi, Masamichi Kobayashi, and Richard S. Stein, "Cocrystallization and Phase Segregation of Polyethylene Blends between the D

and H Species. 6. Time-Resolved FTIR Measurements for Studying the Crystallization Kinetics of the Blends under Isothermal Conditions," *Macromolecules*, 27:1221 (1994d).

Terano, Minoru, and Kazuhiro Ishii, "A Study on the Active Sites of a Primary Type of MgCl_2 -Supported Catalyst by Ethylene-Propylene Copolymerization," in *Catalytic Olefin Polymerization*, T. Keii and K. Soga Eds., Studies in Surface Science and Catalysis, Elsevier, Amsterdam, 1990, 56:277.

Usami, T., Y. Gotoh, and S. Takayama, "Generation Mechanism of Short-Chain Branching Distribution of Linear Low-Density Polyethylenes," *Macromolecules*, 19:2726 (1986).

Wang, Ge, and Ian R. Harrison, "Polymer Melting: Thermal Resistance Effects in a DSC," *Thermochimica Acta*, 230:309 (1993).

Wang, Jianguo, Deren Pang, and Baotong Huang, "On the Intermolecular and Intramolecular Branching Distribution in Ethylene/ α -olefin Copolymers," *Polymer Bulletin*, 23:127 (1990).

Wang, Jian-Guo, De-Ren Pang, Xiao-Tan Cheng, and Bao-Tong Huang, "Factors Affecting the Role of SiO_2 in MgCl_2 -supported Ziegler-Natta Copolymerization Catalysts," *Die Makromolekulare Chemie*, 194:211 (1993).

Wardhaugh, Leigh T., and Michael C. Williams, "Blockiness of Olefin Copolymers and Possible Microphase Separation in the Melt," *Polymer Engineering and Science*, 35:18 (1995).

Wild, L., T. R. Ryle, and D. C. Knobloch, "Branching Distribution in LLDPEs," *ACS Polymer Preprints*, 23(2):133 (1982a).

Wild, L., "Temperature Rising Elution Fractionation," *Advances in Polymer Science*, 98:1 (1991).

Wunderlich, Bernhard, *Macromolecular Physics*, vol. 3, Academic Press, New York, 1980.

Xiao, Shijing, and Honglan Lu, "Behaviour of Ethylene Homopolymerization and Ethylene-1-Butene Copolymerization with $\text{SiO}_2/\text{MgCl}_2$ Bisupported Titanium Catalyst," *Journal of Molecular Catalysis*, 76:195 (1992).

Xie, Tuyu, Kim B. McAuley, James C. C. Hsu, and David W. Bacon, "Gas Phase Ethylene Polymerization: Production Processes, Polymer Properties, and Reactor Modeling," *Industrial and Engineering Chemistry Research*, 33:449 (1994).

Zhou, Xiao-Qi, and J. N. Hay, "Fractionation and Structural Properties of Linear Low-Density Polyethylene," *European Polymer Journal*, 29:291 (1993).

Zlotinkov, L. M., Ye. L. Ponomareva, S. Ya. Khaikin, S. I. Korotkov, V. A. Grigor'ev, V. P. Budtov, and S. S. Ivanchev, "Determination of the Concentration of Active Centres and the Propagation Reaction Rate Constants of the Macrochain on Polymerization of Ethylene on Highly Active Catalysts," *Polymer Science U.S.S.R.*, 30:16 (1988).

Zhou, Xiao-Qi, and J. N. Hay, "Fractionation and Structural Properties of Linear Low Density Polyethylene," *European Polymer Journal*, 29:291 (1993).

Zucchini, Umberta, and Guiliano Cecchin, "Control of Molecular-Weight Distribution in Polyolefins Synthesized with Ziegler-Natta Catalytic Systems," *Advances in Polymer Science*, 51:101 (1983).

Appendix: Annotated Summary of All Experimental Runs

Run	Catalyst (mg)	Cocatalyst (ml)		Ethylene (psi)	Hydrogen (psi)	1-Butene (pchg. ml)	Temp. set pt. (°C)	Time (hr)	Yield (g)	Comments
		type	cleaning							
1	224	TEAL	1	100	0	0	70	2.6	13.3	support: 200 gm glassbeads; catalyst suspended in decane until Run 23
2	224	TEAL	1	100	0	30	70	1.5	12.6	sticky layer of polymer at bottom
3	224	TEAL	1	100	0	0	70	1.9	29	support: 150 gm salt
4	224	TEAL	1	100	0	0	70	2.2	66.2	support: 200 gm PE
5	224	TEAL	1	100	0	0	70	2	63.5	support: 200 gm PE
6	224	TEAL	1	100	0	0	70	2.2	65.6	support: 200 gm PE
7	224	TNHAL	1	100	0	0	70	3	278	support: 200 gm PE
8	224	TNHAL	1	100	0	0	70	n/a	n/a	reactor contamination; aborted
9	112	TNHAL	1	100	0	0	70	2.1	62.5	support: 200 gm glassbeads; temperature fluctuated throughout the run
10	56	TNHAL	1	100	0	0	70	3.3	85.3	support: 100 gm PE
11	56	TNHAL	1	100	0	0	70	0.5	nil	support: 100 gm PE; no activity for 30 minutes; problem not identified
12	112	TNHAL	1	100	0	0	70	2	113	support: 200 gm salt; a repeat of Run 9
13	112	TNHAL	1	100	0	0	70	1.9	141	support: 200 gm salt; no further change in seedbed
14	56	TNHAL	1	100	0	0	70	3.5	61.4	intermittent 1-butene feed; erratic GC spec
15	56	TNHAL	1	150	0	30	70	2	14.2	intermittent 1-butene feed; erratic GC spec
16	56	TNHAL	1	200	0	0	70	2.9	155	intermittent 1-butene feed; erratic GC spec
17	56	TNHAL	1	200	0	0	70	2	137	intermittent 1-butene feed; erratic GC spec
18	56	TNHAL	1	200	0	0	70	2	130	intermittent 1-butene feed; no cocatalyst was added into the reactor other than the initial 1.0 ml used as moisture scavenger; thermal runaway; erratic GC spec
19	56	TNHAL	1	200	0	0	70	2	150	intermittent 1-butene feed; initial thermal runaway; erratic GC spec
20	28	TNHAL	1	200	0	0	70	2	34.1	intermittent 1-butene feed; erratic GC spec

Appendix: Annotated Summary of All Experimental Runs (continued)

Run	Catalyst (mg)	Cocatalyst (ml)		Ethylene (psi)	Hydrogen (psi)	1-Butene (pchg, ml)	Temp. set pt.(°C)	Time (hr)	Yield (g)	Comments
		type	cleaning reaction							
21	28	TNHAL	1	0	200	0	70	2	29.6	intermittent 1-butene feed; erratic GC spec
22	28	TNHAL	1	0	200	0	70	2	81.3	intermittent 1-butene feed; erratic GC spec
23	30	TNHAL	1	0	200	0	70	2	67.5	catalyst suspended in heptane between Runs 23 and 124; fair run
24	30	TNHAL	1	0	200	0	70	2	76.9	1-butene feed not under control; poor run
25	30	TNHAL	1	0	200	20	70	2	49.7	hydrogen pressure control problem; fair run
26	30	TNHAL	1	0	200	40	70	2	1.48	catalyst injected into hydrogen; poor run
27	30	TNHAL	1	0	200	40	70	2	30.3	catalyst injected into ethylene; fair run
28	30	TNHAL	1	0	200	10	70	2	26.7	hydrogen pressure control problem; fair run
29	30	TNHAL	1	0	200	10	70	2	40.6	hydrogen pressure control problem; fair run
30	30	TNHAL	1	0	200	20	70	2	36.7	hydrogen pressure control problem; fair run
31	30	TNHAL	1	0	200	30	70	2	37	fair run
32	30	TNHAL	1	0	200	10	70	2	45	large temperature overshoot; poor run
33	30	TNHAL	1	0	200	10	70	2	40.9	fair run
34	30	TNHAL	1	0	200	10	70	2	66.2	fair run
35	30	TNHAL	0	1	200	20	70	2	48	fair run
36	30	TNHAL	0	1	200	20	70	2	41.7	fair run
37	30	TNHAL	0	1	200	20	70	2	53.8	fair run
38	30	TNHAL	0	1	200	60	70	2	50.9	good run
39	30	TNHAL	0	1	200	80	70	2	38.2	good run
40	30	TNHAL	0	1	200	100	70	2	40.6	good run
41	30	TNHAL	0	1	200	40	70	2	56.3	fair run; temperature overshoot
42	30	TNHAL	0	1	200	200	70	2	trace	poorly operated run
43	60	TNHAL	0	1	200	200	70	2	32.3	good run
44	60	TNHAL	0	1	200	300	70	2	3.88	poor run
45	60	TNHAL	0	1	200	150	70	2	48.5	fair run
46	60	TNHAL	0	1	150	250	70	2	20.9	fair run
47	60	TNHAL	0	1	200	100	70	2	49.3	good run

Appendix: Annotated Summary of All Experimental Runs (continued)

Run	Catalyst (mg)	Cocatalyst (ml)		Ethylene (psi)	Hydrogen (psi)	1-Butene (pchg. ml)	Temp. set pt. (°C)	Time (hr)	Yield (g)	Comments
		type	cleaning reaction							
48	60	TNHAL	0	200	100	0	70	2	69.7	fair run
49	60	TNHAL	0	200	100	5	70	2	55.1	fair run
50	60	TNHAL	0	200	100	20	70	2	68.5	fair run
51	60	TNHAL	0	200	100	10	70	2	36.3	fair run
52	150	TNHAL	0	200	0	0	50	n/a	n/a	thermal runaway
53	60	TNHAL	0	200	100	10	50	1.3	n/a	thermal runaway after 15 minute prepolymerization
54	60	TNHAL	0	200	100	3	50	3.5	n/a	another failed attempt at prepolymerization
55	60	TNHAL	0	200	300	10	70	n/a	n/a	pressure regulator leaked after 40 min; aborted
56	60	TNHAL	0	200	300	10	70	2	n/a	excess 1-butene fed during reaction; sticky polymer powders were not separated from seedbed
57	60	TNHAL	0	200	300	10	70	2	7.5	excess 1-butene fed
58	60	TNHAL	0	varied	100	0	50	n/a	n/a	thermal runaway
59	60	TNHAL	0	200	100	0	50	2	78.6	1-butene not precharged but fed
60	60	TNHAL	0	200	100	10	50	n/a	n/a	thermal runaway
61	60	TNHAL	0	200	100	10	50	2	5.89	sudden jump in ethylene flowrate unaccounted for
62	60	TNHAL	0	200	100	0	50	2	32.2	good run
63	60	TNHAL	0	200	100	0	50	2	32.2	repeat of previous run with different reactor pretreatment
64	60	TNHAL	0	200	100	10	50	2	58.8	large temperature overshoot; poor run
65	60	TNHAL	0	200	100	0	50	2	32.7	repeat of Run 65
66	60	TNHAL	0	200	100	15	50	2	65.7	fair run
67	60	TNHAL	0	200	300	10	50	2	8.82	fair run
68	60	TNHAL	0	200	300	0	50	2	15.9	ethylene supply dropped below set pressure; poor run
69	60	TNHAL	0	200	200	0	50	2	23.8	ethylene supply dropped below set pressure; poor run

Appendix: Annotated Summary of All Experimental Runs (continued)

Run	Catalyst (mg)	Cocatalyst (ml)		Ethylene (psi)	Hydrogen (psi)	1-Butene (pchg, ml)	Temp. set pt.(°C)	Time (hr)	Yield (g)	Comments
		type	cleaning							
70	60	TNHAL	0	1	200	0	50	2	28.4	good run
71	60	TNHAL	0	1	200	0	50	2	33.6	good run
72	60	TNHAL	0	1	200	0	50	2	51.5	good run
73	60	TNHAL	0	1	200	0	50	2	7.26	good run
74	60	TNHAL	0	1	200	0	50	2	28.2	good run
75	60	TNHAL	0	1	200	0	50	2	31.7	good run
76	60	TNHAL	0	1	200	0	50	2	54.1	ethylene pressure dropped to 188 psi by the end of the experiment
77	60	TNHAL	0	1	200	0	50	2	31	intermittent 1-butene feed
78	60	TNHAL	0	1	200	10	50	2	22	variation of 1-butene feed pattern; fair run
79	60	TNHAL	0	1	200	10	50	2	44.4	variation of 1-butene feed pattern; large temperature overshoot
80	60	TNHAL	0	1	200	n/a	50	2	n/a	problem with 1-butene precharge; reaction aborted
81	60	TNHAL	0	1	200	10	50	2	50.6	variation of 1-butene feed pattern; large temperature overshoot
82	60	TNHAL	0	1	200	10	50	2	50	variation of 1-butene feed pattern; temperature overshoot
83	60	TNHAL	0	1	200	10	50	2	68.3	variation of 1-butene feed pattern; large temperature overshoot
84	60	TNHAL	0	1	200	10	50	2	53.3	variation of 1-butene feed pattern; fair run
85	60	TNHAL	0	1	200	10	50	2	66.5	variation of 1-butene feed pattern; fair run
86	60	TNHAL	0	1	200	10	50	2	57.7	variation of 1-butene feed pattern; fair run
87	60	TNHAL	0	1	200	10	50	2	73	variation of 1-butene feed pattern; large temperature overshoot
88	60	TEAL	0	1	200	10	50	2	28.2	variation of 1-butene feed; fair run
89	60	TNHAL	0	1	200	0	50	2	20.9	fair run
90	60	TNHAL	0	1	200	0	50	2	38.4	fair run

Appendix: Annotated Summary of All Experimental Runs (continued)

Run	Catalyst		Cocatalyst (ml)		Ethylene		Hydrogen		1-Butene		Temp. set pt.(°C)	Time (hr)	Yield (g)	Comments
	(mg)	type	cleaning	reaction	(psi)	(psi)	(psig. ml)	(psig. ml)	(psig. ml)	(psig. ml)				
91	60	TEAL	0	0.2	200	100	10	10	50	2	14.4	2	14.4	fair run
92	60	TEAL	0	0.2	200	100	10	10	50	0.4	8.91	0.4	8.91	fair run
93	60	TNHAL	0	0.4	200	100	10	10	50	0.4	n/a	0.4	n/a	problem for low activity unidentified
94	60	TNHAL	0	0.5	200	100	10	10	50	2	44.2	2	44.2	variation of 1-butene feed pattern; fair run
95	60	TNHAL	3	0.5	200	100	10	10	50	0.3	n/a	0.3	n/a	reactor pretreated with 3 ml TEAL
96	60	TNHAL	0	1	200	100	10	10	50	2	52.1	2	52.1	0.5 ml silicon tetrachloride added
97	60	TEAL	0	0.5	200	100	10	10	50	2	12.6	2	12.6	0.5 ml silicon tetrachloride added
98	60	TEAL	0	1.5	200	100	10	10	50	2	27.8	2	27.8	0.5 ml silicon tetrachloride added
99	60	TEAL	0	1	200	100	15	15	50	2	58.1	2	58.1	0.5 ml silicon tetrachloride added
100	60	TEAL	0	1	200	100	15	15	50	2	66.7	2	66.7	large temperature overshoot, low rate
101	60	TEAL	0	1	200	100	20	20	50	n/a	n/a	n/a	n/a	exceeded meter range; poor run
102	60	TNHAL	0	1	200	100	15	15	50	2	90.8	2	90.8	vacuum pump malfunctioned; aborted
103	60	TEAL	0	1	200	100	15	15	50	1.5	8.31	1.5	8.31	0.5 ml silicon tetrachloride added; severe thermal runaway
104	30	TEAL	0	1.5	200	100	15	15	50	2	22.4	2	22.4	fair run
105	60	TEAL	0	1	200	100	15	15	50	2	17.2	2	17.2	temperature fluctuated throughout; fair run
106	60	TEAL	0	0.5	200	100	15	15	50	2	16.9	2	16.9	fair run
107	60	TEAL	0	1	200	100	0	0	70	2	19	2	19	fair run
108	60	TEAL	0	1	200	100	0	0	70	2	9.51	2	9.51	catalyst injected into 50 psi ethylene; good run
109	60	TEAL	0	1	200	100	0	0	70	2	1.72	2	1.72	catalyst injected into 25 psi ethylene and 25 psi nitrogen; erratic ethylene flow; fair run
110	60	TEAL	0	1	200	100	0	0	70	2	14.1	2	14.1	catalyst injected into pure nitrogen; startup delayed 15 min; fair run
111	60	TEAL	0	1	200	100	0	0	70	2	11.6	2	11.6	catalyst injected into pure ethylene; startup delayed 15 minutes
														catalyst injected into 25 psi ethylene and 25 psi nitrogen; startup delayed 15 minutes; fair run

Appendix: Annotated Summary of All Experimental Runs (continued)

Run	Catalyst		Cocatalyst (ml)		Ethylene (psi)	Hydrogen (psi)	1-Butene (pchg. ml)	Temp. set pt.(°C)	Time (hr)	Yield (g)	Comments
	(mg)	type	cleaning	reaction							
112	60	TEAL			varied	varied	varied	70	n/a	n/a	poorly operated run
113	60	TEAL	3 (1 M)	1	200	100	0	70	2	28.7	good run
114	60	TEAL	3 (1 M)	1	200	100	0	70	5	58.5	good run; activity for the initial 2 hours doubled from previous run
115	60	TEAL	3 (1 M)	0.5	200	100	0	70	2	39.7	good run
116	60	TEAL	3 (1 M)	0	200	100	0	70	20	407	good run; activity for the initial 2 hours doubled from previous run
117	40	TEAL	3 (1 M)	0	200	100	0	70	n/a	n/a	thermal runaway
118	40	TEAL	3 (1 M)	0	200	100	0	70	2	64.2	repeat of Run 116; activity comparable to its first two hours
119	40	TEAL	1 (1 M)	0	200	100	0	70	n/a	n/a	small quantities of TEAL added in search of optimal Al/Ti
120	40	TEAL	2 (1 M)	0	200	100	0	70	n/a	n/a	poorly operated run; reaction aborted
121	40	TEAL	2 (1 M)	1 (1 M)	varied	varied	0	70	n/a	n/a	pressure manipulated throughout
122	40	TEAL	2 (1 M)	1 (1 M)	varied	varied	0	70	n/a	n/a	small quantities of TEAL added in search of optimal Al/Ti
123	40	TEAL	3 (1 M)	varied	varied	varied	0	70	n/a	n/a	small quantities of TEAL added in search of optimal Al/Ti
124	30	TEAL	3 (1 M)	0	200	100	0	70	n/a	n/a	pressure control problem; aborted
125	30	TEAL	3 (1 M)	0	200	100	0	70	2	44.9	catalyst suspended in hexadecane; good run
126	30	TEAL	3 (1 M)	0	200	100	0	70	n/a	n/a	reactor contamination; aborted
127	30	TEAL	3 (1 M)	0	200	100	0	70	2	57.4	catalyst suspended in decane; poor stirring; catalyst suspended in decane for all subsequent runs.
128	30	TEAL	3 (1 M)	0	200	100	0	70	n/a	nil	testing baking method; catalyst displayed no activity without additional cocatalyst
129	30	TEAL	3 (1 M)	0	200	100	0	70	2	53.9	catalyst suspended in decane; poor stirring

Appendix: Annotated Summary of All Experimental Runs (continued)

Run	Catalyst		Cocatalyst (ml)		Ethylene (psi)	Hydrogen (psi)	1-Butene (pchg. ml)	Temp. set pt. (°C)	Time (hr)	Yield (g)	Comments
	(mg)	type	cleaning	reaction							
130	30	TEAL	3 (1 M)	0	200	100	0	70	3.5	56.1	repeat of previous run
131	30	TEAL	3 (1 M)	varied	varied	0	0	70	n/a	n/a	small quantities of TEAL added in search of optimal Al/Ti
132	30	TEAL	3 (1 M)	varied	varied	0	0	70	n/a	n/a	small quantities of TEAL added in search of optimal Al/Ti
133	30	TEAL	3 (1 M)	varied	varied	0	0	70	n/a	n/a	small quantities of TEAL added in search of optimal Al/Ti
134	30	TEAL	3 (1 M)	1 (0.2 M)	200	100	0	70	2	88.8	catalyst and cocatalyst injected from the same syringe; highest yield with TEAL ever
135	30	TEAL	3 (1 M)	varied	varied	0	0	70	n/a	n/a	small quantities of TEAL added in search of optimal Al/Ti
136	30	TEAL	3 (1 M)	1 (0.6 M)	200	100	0	70	2	55.5	poor stirring; MagneDrive serviced